BORON-NEUTRON-CAPTURE RADIATION TREATMENT OF POLYMERS FOR APPLICATION IN LAMINATED GLASS WINDOW INTERLAYER MATERIAL

A Dissertation Presented to the Faculty of the Graduate School of the

University of Missouri – Columbia

In Partial Fulfillment of the Requirements for the Degree

Doctor of Philosophy

In

Civil and Environmental Engineering

By

JOSEPH CALEB PHILIPPS

Dr. Hani Salim, Dissertation Supervisor

May 2022

The undersigned, appointed by the Dean of the Graduate School, have examined the dissertation entitled

BORON-NEUTRON-CAPTURE RADIATION TREATMENT OF POLYMERS FOR APPLICATION IN LAMINATED GLASS WINDOW INTERLAYER MATERIAL

presented by Joseph Caleb Philipps,

a candidate for the degree of doctor of philosophy in Civil and Environmental Engineering and hereby certify that, in their opinion, it is worthy of acceptance.

_____

Dr. Hani Salim, PE

_____

Dr. John Gahl, PE

_____

Dr. Yaw Adu-Gyamfi

_____

Dr. John J. Bowders, PE

ACKNOWLEDGEMENTS

I would like to thank Dr. Hani Salim for the opportunity to work with him and his team at the University of Missouri-Columbia. You have shown a great deal of patience with me and your support is greatly appreciated. I'd like to thank Dr. John Gahl for his continued support in my research and education efforts. You have been very inspirational.

I would also like to thank Dr. John Bowders and Dr. Yaw Adu-Gyamfi for serving on my PhD dissertation defense committee. It is an honor to have such prestigious mentors as a part of my committee.

Thanks to Dr. John Brockman for his continued mentorship and assistance with projects at the University of Missouri Research Reactor (MURR). His knowledge regarding chemistry and radiation has been a major benefit to the research effort.

A very special thanks to Dr. Aaron Saucier, who has been there to support my development in research and other life endeavors. I appreciate all that you've done.

Experimental results presented in this paper were performed at MURR and the Remote Test Facility, University of Missouri-Columbia. The technical support of Rich Oberto is greatly appreciated. His wisdom is extraordinarily helpful to all the students that work with him. I would like to thank my team at the labs; Dr. Alaa Elsisi, Jonathan Knight, Brooke Dean, Hannah Truit, Dr. Mahmoud Almasri, Akshay Koppula, and Valentina O'Donnell. Testing equipment company Anton Paar has provided technical expertise that is greatly appreciated. Thanks also to Battelle Memorial Institute and the Air Force Civil Engineering Center for the project support and financial assistance to perform this research.

TABLE OF CONTENTS

ACKNOWLEDGEMENTS ii
LIST OF FIGURES v
LIST OF TABLES x
ABSTRACT xi
1. Introduction 1
1.1. Objectives 1
1.2. Evaluation Approaches 2
1.3. Dissertation Overview 3
2. Background 4
2.1. Structure Protection 4
2.2. Laminated Glass Panels under Blast Loads 5
2.3. Boron-Neutron-Capture Process 7
2.4. Material Selection 11
3. Material Characterization Methods 14
3.1. Tensile Testing 14
3.1.1. Tensile Specimen Preparation 17
3.1.2. Quasi-Static Tensile Testing 18
3.1.3. High-Strain Rate Tensile Testing 20
3.1.4. Strain Measurement for Dynamic Tensile Test 21
3.2. Hardness Testing 23
4. Neutron Flux Treatment 28
4.1. High Neutron Flux 28
4.1.1. Experimental Setup 28
4.1.2. Analysis 30
4.1.3. Results 33
4.2. Low Neutron Flux 36
4.2.1. Experimental Setup 36
4.2.2. Analysis 39
4.2.3. Results 43
5. Treatment of Custom Polymers 47
5.1. Experimental Setup 47

5.2. Analysis 50
5.3. Results and Discussion 51
6. Treatment of LG Polymer Interlayers 52
6.1. Experimental Setup 52
6.2. Analysis 57
6.3. Results 58
6.3.1. Quasi-Static Tensile Testing 58
6.3.2. High-Strain Rate Tensile Testing 63
6.3.3. Nano-indentation 66
6.3.4. Scratch Testing 68
6.3.5. Differential Scanning Calorimeter Testing 71
7. Optimal Neutron Dose for EVA Interlayer Polymer 76
7.1. Experimental Setup 77
7.2. Analysis 77
7.3. Results 77
8. Conclusions and Recommendations 80
8.1. Conclusions 80
8.2. Recommendations and Applications 82
8.2.1. Blast and Ballistic Protection 82
8.2.2. Electrical and Radio Frequency Effects 82
8.2.3. Numerical Modeling 83
8.2.4. Patterned Hardening 84
8.2.5. Applications using Pyrex Glass 84
8.2.6. Manufacturing 85
8.2.7. Additional Testing 89
9. Bibliography 90
10. Appendices 94
VITA 104

LIST OF FIGURES

Figure 1: Bomb attack on Murrah Federal Building in Oklahoma, USA, 1995 (Hidallana-Gamage, Thambiratnam, & Perera, 2015). 5

Figure 2: Laminated glass (LG); (a) schematic, (b) test specimen.....6

Figure 3: Nuclear bombardment of 10boron with neutrons, emitting an alpha particle and a 7lithium particle. 9

Figure 4: Alpha particle interacting with the Hydrogen found in adjacent polyethylene chains; ideally creating a crosslink between the adjacent chains' carbon elements..10

Figure 5: Interaction of neutron bombardment with 10boron, emitting an alpha particle and a 7lithium particle. 11

Figure 6: PVB chain structure. 12

Figure 7: EVA Chemical Structure. 13

Figure 8: Specimen Preparation; a) Static Specimen geometry, b) Dynamic Specimen geometry, c) Static cutting die, d) Dynamic cutting die, and d) Specimen stamping. 18

Figure 9: Static Testing Frames.....19

Figure 10: Static tensile specimen cut out from treated interlayer. 19

Figure 11: Tested coupons of PVB and EVA. 20

Figure 12: Drop Weight Test Set-Up; (a) Apparatus components and specimen setup, and (b) High-speed camera.....21

Figure 13: Tracking the Gauge Length Displacement using Photo Tracking Program. ...22

Figure 14: Strain at Selected Frames During Drop Weight Test.....22

Figure 15: Prepared coupons for high strain rate tensile testing. 23

Figure 16: Rockwell Hardness measuring devices in the lab.....25

Figure 17: Micro-Vickers Testing with SU-2100 coated polycarbonate. 26

Figure 18: Shore A (left) and Shore D (right) Durometers. 27

Figure 19: High flux Green samples, L to R, 60 second irradiation, 5 second irradiation, 30 second irradiation, frozen (no irradiation, frost seen). 33

Figure 20: High flux Pink samples, L to R, frozen (no irradiation, frost seen), 30 second irradiation (swelling and discoloration seen), 5 second irradiation. 34

Figure 21: High flux testing results. 34

Figure 22: Pneumatic Tube Vehicles through progressive usage (new white tube at left). 35

Figure 23: Plan view of MURR beamport floor with specific beamport labeled (Brockman, Nigg, Hawthorne, & McKibben, Spectral Performance of a Composite Single-Crystal Filtered Thermal Neutron Beam for BNCT Research at the University of Missouri, 2009). 37

Figure 24: MURR thermal beamline design detail. The axial centerline of the reactor core is on the left of the diagram as shown (Brockman, Nigg, Hawthorne, & McKibben, Spectral Performance of a Composite Single-Crystal Filtered Thermal Neutron Beam for BNCT Research at the University of Missouri, 2009). 37

Figure 25: Low flux rate test specimen. 38

Figure 26: Samples prepared for irradiation on target. 38

Figure 27: Inserting specimen into beamport position. 39

Figure 28: First Test, Graphed results of the 1705 and 5905-minute irradiations. 45

Figure 29: Second Test, Graphed results of the 1716 and 7716-minute irradiations. 46

Figure 30: Boron Nitride for custom sample preparation. 48

Figure 31: Polycarbonate discs for custom sample preparation. 48

Figure 32: Custom borated SU8-2100 Specimen within protective case. 49

Figure 33: : Custom borated SU8-2100 Specimen with high boron nitride content and no boron nitride. 50

Figure 34: Three layers of experimental setup, aluminum bottom, polymer interlayer center, boron nitride sheet top. 55

Figure 35: Three layers of experimental setup in cross-section. 55

Figure 36: Diagram showing the neutrons passing through the aluminum plate, through the polymer interlayer, and interacting with the boron nitride plate. 56

Figure 37: Static Testing of EVA-008-001,2,3-R100N specimen with aluminum-EVA-aluminum configuration, in comparison to virgin EVA material. 60

Figure 38: Static tensile test results for PVB-001-001,2,3 and comparison to virgin material. 61

Figure 39: Static tensile test results for EVA-001-001,2,3 and comparison to virgin material. 61

Figure 40: Plot of Stress vs. Strain for 40-hour irradiated Specimen EVA-012 and its comparison with the average virgin samples. This specimen included the boron surface treatment. 62

Figure 41: Dynamic results from three samples of radiated PVB-007-001,2,3. 64

Figure 42: Dynamic results of radiated PVB-007-001,2,3 in comparison to virgin PVB. 64

Figure 43: Dynamic results from three samples of radiated EVA-007-001,2,3. 65

Figure 44: Dynamic results of radiated EVA-007-001,2,3 in comparison to virgin EVA. 65

Figure 45: Hardness vs. Penetration Depth. 66

Figure 46: Elasticity vs. Penetration Depth. 67

Figure 47: Figure showing method of scratch testing provided by Anton Paar. 68

Figure 48: Scratch testing on EVA-014-001-R100B, showing penetration depth as a function of distance with a scratch rate of 4mm/min. 69

Figure 49: Scratch testing on EVA-014-001-R100B, showing penetration depth as a function of force applied with a scratch rate of 4mm/min. 69

Figure 50: Scratch testing on EVA-014-001-R100B, showing penetration depth as a function of distance at a scratch rate of 85 mm/min. Red is the treated face, blue is the untreated face. 70

Figure 51: Scratch testing on EVA-014-001-R100B, showing penetration depth as a function of force applied at a scratch rate of 20 mm/min. Red is the treated face, black is the untreated face. 71

Figure 52: DSC Testing for Virgin PVB-005-030. 72

Figure 53: DSC Testing for Radiated PVB-001-030. 73

Figure 54: DSC Testing for Old PVB. 73

Figure 55: DSC Testing for Virgin EVA-005-015. 74

Figure 56: DSC Testing for radiated EVA-001-015. 74

Figure 57: Static tensile tested specimens for dose effects on interlayer materials. 76

Figure 58: Dose effects of EVA with surface treatment. 78

Figure 59: Modeled disc with penetrator.....83

Figure 60: Facility cross section showing pre-positioning area on the left, neutron treatment area in the middle, and the storage area on the right. 85

Figure 61: Deuterium-deuterium reaction for producing neutrons (Phoenix, 2020).....86

Figure 62: Raw Graph Data from Anton Paar showing Hardness and Elasticity, EVA-001-004, Treated Face. 94

Figure 63: Raw Graph Data from Anton Paar showing Hardness and Elasticity, EVA-001-004, Untreated Face.....94

Figure 64: Scratch #1, 4mm/min, Raw Graph Data from Anton Paar showing Penetration Depth vs Force/Distance, EVA-014-001, Treated Face. 95

Figure 65: Scratch #2, 4mm/min, Raw Graph Data from Anton Paar showing Penetration Depth vs Force/Distance, EVA-014-001, Treated Face. 95

Figure 66: Scratch #3, 4mm/min,Raw Graph Data from Anton Paar showing Penetration Depth vs Force/Distance, EVA-014-001, Treated Face. 96

Figure 67: Scratch #1, 4mm/min,Raw Graph Data from Anton Paar showing Penetration Depth vs Force/Distance, EVA-014-001, Untreated Face. 96

Figure 68: Scratch #2, 4mm/min,Raw Graph Data from Anton Paar showing Penetration Depth vs Force/Distance, EVA-014-001, Untreated Face. 97

Figure 69: Scratch #3, 4mm/min,Raw Graph Data from Anton Paar showing Penetration Depth vs Force/Distance, EVA-014-001, Untreated Face. 97

Figure 70: Scratch #1, 20mm/min,Raw Graph Data from Anton Paar showing Penetration Depth vs Force/Distance, EVA-014-001, Treated Face. 98

Figure 71: Scratch #2, 20mm/min,Raw Graph Data from Anton Paar showing Penetration Depth vs Force/Distance, EVA-014-001, Treated Face. 98

Figure 72: Scratch #3, 20mm/min,Raw Graph Data from Anton Paar showing Penetration Depth vs Force/Distance, EVA-014-001, Treated Face. 99

Figure 73: Scratch #1, 20mm/min,Raw Graph Data from Anton Paar showing Penetration Depth vs Force/Distance, EVA-014-001, Untreated Face. 99

Figure 74: Scratch #2, 20mm/min,Raw Graph Data from Anton Paar showing Penetration Depth vs Force/Distance, EVA-014-001, Untreated Face. 100

Figure 75: Scratch #3, 20mm/min,Raw Graph Data from Anton Paar showing Penetration Depth vs Force/Distance, EVA-014-001, Untreated Face. 100

Figure 76: Scratch #1, 85mm/min,Raw Graph Data from Anton Paar showing Penetration Depth vs Force/Distance, EVA-014-001, Treated Face. 101

Figure 77: Scratch #2, 85mm/min,Raw Graph Data from Anton Paar showing Penetration Depth vs Force/Distance, EVA-014-001, Treated Face. 101

Figure 78: Scratch #3, 85mm/min,Raw Graph Data from Anton Paar showing Penetration Depth vs Force/Distance, EVA-014-001, Treated Face. 102

Figure 79: Scratch #1, 85mm/min,Raw Graph Data from Anton Paar showing Penetration Depth vs Force/Distance, EVA-014-001, Untreated Face. 102

Figure 80: Scratch #2, 85mm/min,Raw Graph Data from Anton Paar showing Penetration Depth vs Force/Distance, EVA-014-001, Untreated Face. 103

Figure 81: Scratch #3, 85mm/min,Raw Graph Data from Anton Paar showing Penetration Depth vs Force/Distance, EVA-014-001, Untreated Face. 103

LIST OF TABLES

Table 1: Virgin Samples from Manufacturer, Shore D Hardness Values. 30

Table 2: Five second irradiation, Shore D Hardness Values. 31

Table 3: Thirty second irradiation, Shore D Hardness Values. 32

Table 4: Sixty second irradiation, Shore D Hardness Values. 32

Table 5: Polyethylene Pneumatic Tube Vehicles, Shore D Hardness Values. 35

Table 6: First test, Front face, 1705-minute irradiation, Shore D Hardness Values. 40

Table 7: First test, Back face, 1705-minute irradiation, Shore D Hardness Values. 40

Table 8: First test, Front Face, 5905-minute irradiation, Shore D Hardness Values. 41

Table 9: First test, Back Face, 5905-minute irradiation, Shore D Hardness Values. 41

Table 10: Second test, Front face, pre-irradiation, Shore D Hardness Values. 41

Table 11: Second test, Back face, pre-irradiation, Shore D Hardness Values. 42

Table 12: Second test, Front face, 1716 - minute irradiation, Shore D Hardness Values. 42

Table 13: Second test, Back face, 1716 - minute irradiation, Shore D Hardness Values.42

Table 14: Second test, Front face, 7716 - minute irradiation, Shore D Hardness Values. 43

Table 15: Second test, Back face, 7716 - minute irradiation, Shore D Hardness Values.43

Table 16: First Test, Overall Results, Shore D Hardness, Low Flux Rate Irradiation. 44

Table 17: Second Test, Overall Results, Shore D Hardness, Low Flux Rate Irradiation.45

Table 18: Second Test, Hardness Increase, Front to Back of Sample. 45

Table 19: Vickers Hardness Testing results for borated SU8-2100 pre and post-irradiation. 51

Table 20: Test Matrix of Specimen. 58

Table 21: 63

Table 22: Material list for DSC Testing. 72

BORON-NEUTRON-CAPTURE RADIATION TREATMENT OF POLYMERS FOR APPLICATION IN LAMINATED GLASS WINDOW INTERLAYER MATERIAL

Joseph Caleb Philipps

Dr. Hani Salim, Dissertation Supervisor

ABSTRACT

Critical infrastructure that is either vulnerable to attack or that is located within a high threat area will require increased protection. United States government facilities worldwide have seen ongoing disruption and destruction due to a lack of sufficient capabilities or technology to fully resist attack. Increased efforts to strengthen the building structure, particularly with regards to the explosion-resistant window and building envelope systems, can improve the life-safety and continued operability of critical infrastructure under adverse circumstances. The exterior envelope is the most vulnerable component of a building to an exterior hazard because it is the part of the building closest to the source of the hazard. Among all the exterior envelope components, light elements such as the glass windows are critical points of vulnerability.

Polymer interlayer materials are utilized in laminated glass systems to provide increased resilience from blast incidents. The polymer chains within the interlayer material can benefit from material modifications that increase cross-linking between adjacent chains. One theorized method of targeted cross-linking is made possible through a boron-neutron-capture process. This process utilizes neutron radiation that bombards boron-containing material, thus producing emissions of highly energetic

particles into the polymer material. Those particles are the catalyst to cross-linking between polymer chains.

Previous theoretical work suggested this methods for bulk treatment of polymeric materials. This method has been experimentally utilized for bulk material processing as well as surface treatment during the course of this research. The technique was proposed to alter polymer characteristics such as hardness and elasticity. This document describes initial experiments to evaluate the validity of the technique and to suggest alternative approaches. Commercially available borated polymers have been treated and evaluated with varied neutron flux rates and with varied total neutron dose amounts to determine effective techniques for future application. Custom blended polymers were also irradiated and tested to determine the effects of varying amounts of boron inclusion.

A new surface treatment approach using the boron-neutron-capture process is described to improve additional material characteristics such as Toughness. Early results have shown promising material behavior change in tensile tests. The surface treatment process has been extensively investigated in this study to manipulate polymers commonly used as laminated glass window interlayer material. Comparison evaluation tests have been completed to show the treated material behavior change through static tensile loading, dynamic tensile loading, indentation testing, and scratch resistance testing. Results indicate the specific material behavior changes, effects on different interlayer material, and optimizations for the treatment processes.

Data resulting from these tests will expand the understanding of the material behavior changes from treatment techniques and show evidence of the expected cross-linking. This understanding will lead to quantifiable application of system capacities to

improve the future designs of the window and building systems and lead to safer, more secure, and resilient infrastructure.

1. Introduction

Laminated glass window systems are used throughout building construction, automotive manufacturing, and other industries. These systems are composed of glass panels and a polymer interlayer that will absorb significant amounts of energy during a catastrophic event. Increased performance of the polymer material can lead to higher level of protection and advancements in the polymer's role for these applications. Theoretical research into polymer modification through radiation treatment is applied to interlayer material through this research effort, in order to realize the actual benefits of new treatment techniques. Characterization of the polymer post-treatment is indicative of the benefits provided in the application to laminated glass window systems. In this chapter, the overall objectives for the research are outlined, the contributions to the state of the art of polymer science and blast resistant window systems are outlined, and an overall summary of this research document is discussed.

1.1. Objectives

The objective of this research is to apply theoretical methods of polymer treatment towards interlayer materials that are used in window systems in order for them to become more resilient. This effort utilizes the boron-neutron-capture technique to enable cross-linking and subsequent hardening of polymer materials. The research takes steps to prove the process, and then determine a path forward for the application of advanced techniques. Research efforts optimize the process by evaluating changes in the treatment process such as boron dopant percentage, dopant inclusion techniques, neutron flux rates,

and total neutron dose. The process is applied to polymer interlayer material commonly used in window systems. Candidate polymers are evaluated and then studied in depth based on their proclivity towards the technique. A variety of material characterization methods are utilized to provide data supporting the theoretical cross-linking methods hypothesized to take place within the polymer materials.

1.2. Evaluation Approaches

The research presented in this dissertation results in the following evaluation approaches:

- Evaluation of the theoretical boron-neutron-capture technique on polymer materials by treatment of boron doped polymers.
- Evaluation of efficient neutron flux rates utilizing available irradiation techniques at the University of Missouri Research Reactor (MURR).
- Evaluation of efficient neutron total dose amounts through varying duration times under neutron radiation.
- Evaluation and optimization of the effect of boron dopant percentages by testing custom samples treated under constant total neutron radiation dose.
- Evaluation of advanced treatment techniques utilizing surface applied boron material during neutron radiation treatment.
- Evaluation and optimization of total neutron dose amounts of advanced treatment technique by varying the total duration of irradiation.
- Comparison of treated specimen to control specimen by irradiation of specimen without the boron present.

- Fully characterize material behavior changes on interlayer polymer material with a variety of testing that include dynamic tensile tests, static tensile tests, hardness, and scratch evaluation.
- Evaluation of the techique for real-world application by an understanding of long-term radioactivity and possible manufacturing techniques.
- Provide a path towards polymer interlayer treatment that can be applied to window systems for external loading protection that includes blast events.

1.3. Dissertation Overview

This dissertation reviews the background behind both the laminated glass systems and polymer interlayer materials, along with a discussion on the radiation treatment techniques used. Material characterization methods are outlined to explain the different techniques available to fully understand behaviour changes, and why those methods were selected. The following sections outline experimental irradiation processes used to treat polymer materials, an analysis of the treated material, and a discussion on the results from material testing. There are several different techniques used as the process evolved into a relatively standardized interlayer treatment technique. Finally, a discussion on applications and overall conclusions provide a good summary of the usefulness of this novel treatment technique for polymer materials.

2. Background

To understand the link between laminated glass windows and radiation treatment of polymers, some additional background on these subjects is provided to include a description of the need for structural protection, laminated glass panels and their behavior under blast loads, the radiation process utilized in the work, and the interlayer material types that were evaluated.

2.1. Structure Protection

Throughout the history of building design and construction, the safety of a building has always been a critical aspect for designers to maintain the safety of the building occupants. The exterior envelope is the most vulnerable component of a building to exterior hazards. It is also a critical line of defense for protecting the occupants of a building.

A building envelope consists of walls that include windows and doors, as well as a roof system. Public buildings must be designed to resist various kinds of hazards, such as hurricanes, high winds, flying debris, forced entry, and exterior explosions. Such hazards must be accounted for in addition to the conventional extremes of snow, wind, and seismic. These exterior hazards, if unaccounted for, can cause serious injury to occupants.

Window systems have advanced to utilize a layered combination of glass and polymer interlayer materials to protect against external hazards, including the blast hazards that will be the focus of this research. The polymer interlayer material itself can vary in its composition, and its performance can be enhanced by variations in the material

strength and behavior under loading. Methods to manipulate the polymer material can help lead to increased strength and overall resilience of the window system.

2.2. Laminated Glass Panels under Blast Loads

The increase of terrorist incidents toward civilian targets has raised concerns of buildings' safety. Laminated glass is one of the most widely used structural elements in the building envelope whenever increased safety performance is required, not only for protection from exterior events, but also because a major threat of death and injuries comes from flying glass fragments. Norville et al. reported that more than 45% of the glass injuries in the Oklahoma City bombing were within 3.0m of walls with glazing. (Norville, Harvill, Conrath, Shariat, & Mallonee, 1999), Figure 1.

Figure 1: Bomb attack on Murrah Federal Building in Oklahoma, USA, 1995 (Hidallana-Gamage, Thambiratnam, & Perera, 2015).

Laminated glass panels consists of two or more layers of glass with a polymeric interlayr material between each two layers. The glass plies can be annealed float glass, heat strengthened glass, or tempered glass. The advantages of this interlayer is that it

holds the fragments of the glass when the glass cracks due to blast loads. The cracked laminated glass panel works as a continuous membrane attached to the supporting frame and dissipates a significant amount of energy. A typical laminated glass system schematic and a laminated glass specimen are shown in Figure 2 (a) and (b), respectively (Knight, 2020).

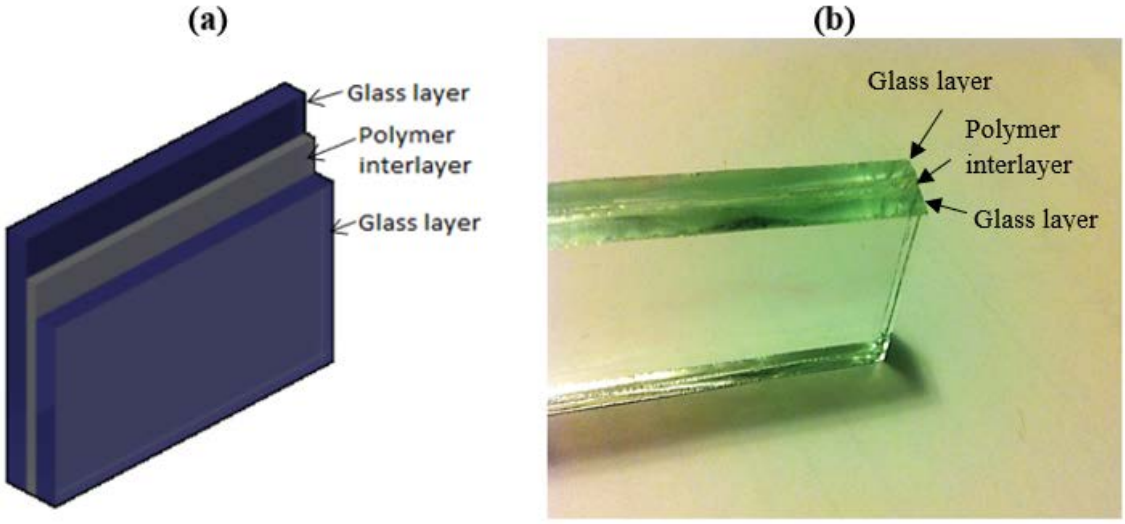

Figure 2: Laminated glass (LG); (a) schematic, (b) test specimen.

The importance of the laminated glass system was illustrated in the attack of the Murrah Federal Building in Oklahoma City, Oklahoma (Norville, Harvill, Conrath, Shariat, & Mallonee, 1999). Monolithic window glass panels were broken under air blast pressure loading, and they produced shards that flew at very high velocities, which caused significant danger to anything near the window glass panels.

Laminated glass, provides excellent protection under air blast pressure loading since laminated glass fractures as the majority of glass shards adhere to the interlayer (Norville & Conrath, Considerations for Blast-Resistant Glazing Design, 2001). The

results from research by Norville & Conrath illustrate that laminated glass windows are the most preferred system in blast-resistant glazing.

Window systems have advanced to utilize a layered combination of glass and polymer interlayer materials to protect against external hazards, including blast hazards. The polymer interlayer material itself can vary in its composition, and its performance can be enhanced by variations in the material strength. Methods to manipulate the polymer material can help lead to increased strength and overall resilience of the window system.

Laminated glass panel consists of two or more layers of glass with a polymeric material between each glass layer. The advantages of this polymeric interlayer are to hold the fragments of the glass when the glass cracks due to blast loads. The cracked laminated glass panel works as a continuous membrane attached to the supporting frame and dissipates a great amount of cracking energy, while preventing injury from projectile glass shards.

2.3. Boron-Neutron-Capture Process

Blast protection systems traditionally employ the use of polymers to increase the resilience of glass window systems. These polymers can introduce complementary properties to a traditional system through their unique material characteristics. Past research has shown that the material characteristics of polymers can be manipulated through irradiation (United States of America Patent No. US5942156, 1999) (Rej, Pickrell, & Wrobleski, Neutron-Capture-Induced Radiation Treatment of Polymeric Materials, 1996), (Calcagno, Compagnini, & Foti, 1992), (Lee & Lewis, Improved

Surface Properties of Polymer Materials by Multiple Ion Beam Treatment, 2011). Furthermore, the use of specific material doping, such as the utilization of 10boron, can create conditions that enable cross-linking of polymer chains that are exposed to a neutron field. Cross-linking is expected to produce a polymer with more rigidity, hardness, and a higher melting point than the equivalent polymer without cross-linking (Ed Vitz, 2022).

Traditional interlayer materials are composed of singular, homogenous polymer types that share their singular resistance behavior with the overall system. Addition of multiple different polymer layers can increase the overall blast resistance of a window system, but it can create concerns with clarity, adhesion, weight, and plasticizer migration. The ability to employ targeted hardening within the depths of a singular, homogenous polymer could increase the variation in resistance behaviors found within an interlayer material without additional layers, and subsequently, increase the overall resilience of the system.

The isotope 10boron has a very high neutron capture cross-section probability of roughly 3840 barns for low energy thermal neutrons, making it a good candidate for capturing the neutron radiation. Furthermore, the resultant products of the neutron capture are a stable 7lithium isotope and an alpha (helium ion) emission. The alpha emission carries an energy of 1.78 MeV, and the 7lithium isotope recoils, conserving momentum and carries an energy of 1.01 MeV (Rej, Pickrell, & Wrobleski, Neutron-Capture-Induced Radiation Treatment of Polymeric Materials, 1996). These energetic particles are subsequently used in the cross-linking mechanism for the strengthening of polymers. It is expected that hardening and increased elasticity of the material will result

from cross-linking (James E. Mark, 2005). A diagram showing this nuclear bombardment reaction is shown in Figure 3.

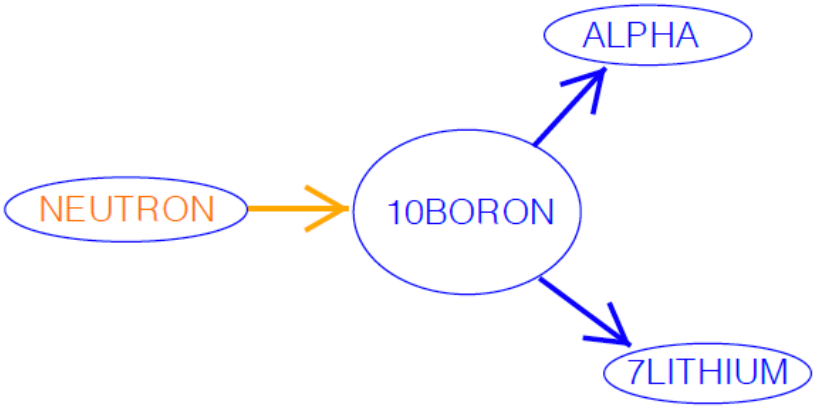

Figure 3: Nuclear bombardment of 10boron with neutrons, emitting an alpha particle and a 7lithium particle.

Polymers are formed by chains of molecules largely composed of hydrogen and carbon. If adjacent polymer chains are exposed to high energy charged particles it is possible for the hydrogen to break free, leaving the carbon available to form new bonds and cross-link, increasing the overall resilience of the material. This could take place through different mechanisms such as electron stripping from the bonded elements, where the new state will seek out a suitable bond that brings the system to its lowest energy state. This is how cross-linking is achieved in the polymer material. An example of this cross-linking mechanism can be seen in Figure 4.

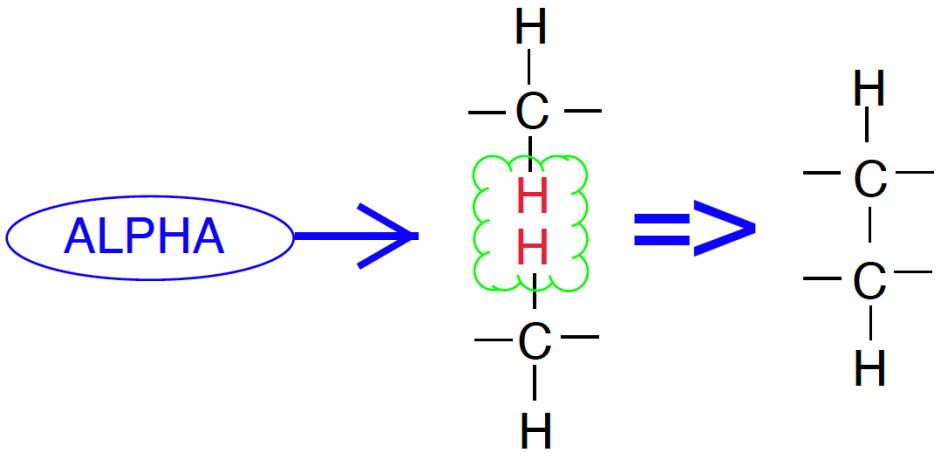

Figure 4: Alpha particle interacting with the Hydrogen found in adjacent polyethylene chains; ideally creating a crosslink between the adjacent chains' carbon elements.

Past research and industrial practice has shown that the material characteristics of polymers can be manipulated through various techniques including irradiation. Surface characteristics can be favorably altered by light-ion bombardment, the treatment area limited however to the depth of penetration of the ion beam (Calcagno, Compagnini, & Foti, 1992) (Lee & Lewis, Improved Surface Properties of Polymer Materials by Multiple Ion Beam Treatment, 2011) (Lee, Rao, Lewis, & Mansur, 1993). Rej, et al. suggested that this ion bombardment effect could be achieved throughout the bulk of a polymer by doping it with boron and irradiating the polymer with penetrating neutrons (United States of America Patent No. US5942156, 1999) (Rej, Pickrell, & Wrobleski, Neutron-Capture-Induced Radiation Treatment of Polymeric Materials, 1996).

The isotope 10boron has a large thermal neutron cross-section of approximately 3840 barns, with neutron capture resulting in alpha emission and a 7lithium nucleus. In 93% or reactions the alpha emission carries an energy of 1.46 MeV, and the 7lithium isotope recoils with an energy of 0.85 MeV. These energetic light ions can be subsequently used in the cross-linking mechanism for the strengthening of polymers (Rej,

Pickrell, & Wrobleski, Neutron-Capture-Induced Radiation Treatment of Polymeric Materials, 1996).

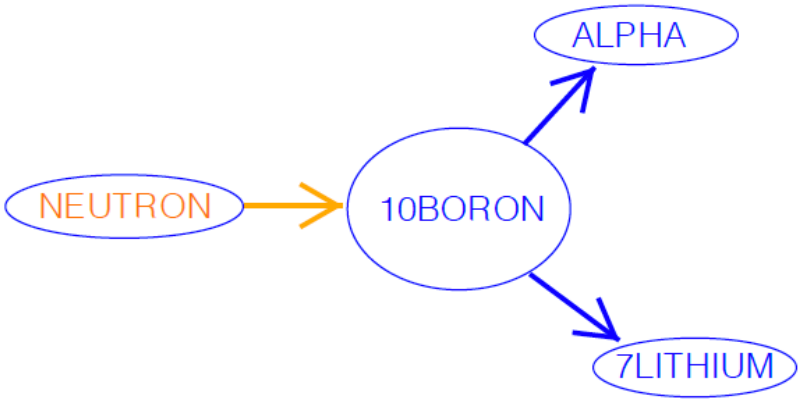

Figure 5: Interaction of neutron bombardment with 10boron, emitting an alpha particle and a 7lithium particle.

2.4. Material Selection

The polymer interlayer material selected for testing included Polyvinyl Butyral (PVB) and Ethylene Vinyl Acetate (EVA). These products are widely used and readily available in the window manufacturing industry. Tested specimens were selected from the same manufactured batch of product, eliminating inconsistencies that may result during the manufacturing process.

Polyvinyl butyral (PVB) is a solid thermoplastic resin. It has been the standard laminated glass interlayer for the last 70 years. PVB is produced from the reaction of polyvinyl alcohol with butyraldehyde (Martin, et al., 2020). The chemical structure is identical for every manufacturer and is shown in Figure 6.

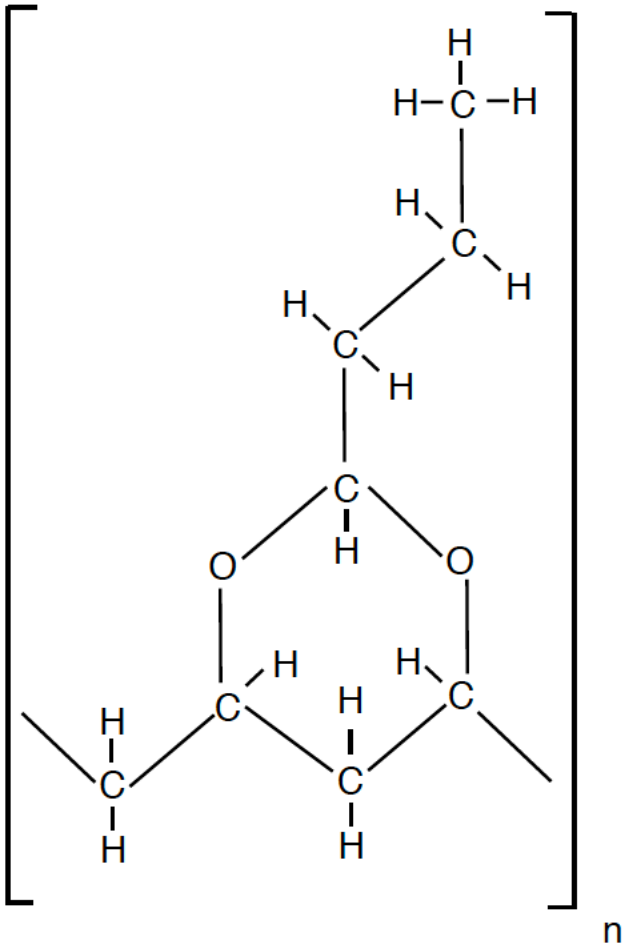

Figure 6: PVB chain structure.

Ethylene Vinyl Acetate (EVA) is also a solid thermoplastic resin produced by the co-polymerization processing of ethylene (C2H4) and a vinyl acetate monomer (C4H6O2) in a high-pressure reactor. It is often used in architectural glass panels as well as solar panels. The copolymer chemical structure can be seen in Figure 7.

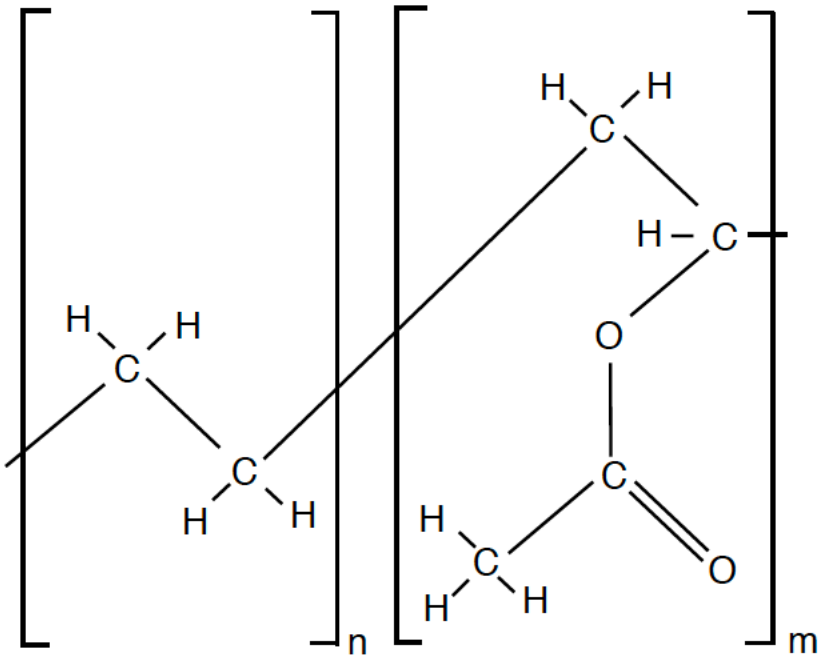

Figure 7: EVA Chemical Structure.

Both PVB and EVA show promise in their chemical structure for susceptibility towards cross-linking through their plentiful hydrogen/carbon bonds.

Borated polyethylene is commonly used as neutron shielding in various reactor related environments. Polyethylene itself reduces neutron radiation levels due to its high content of hydrogen, and the boron inclusion helps to capture neutrons due to its high neutron capture cross section. This material is commercially available and is futher discussed in Section 4.

SU8-2100 was selected for evaluation as a collaboration with other departments at the university. This material is a permanent epoxy negative photoresist that is susceptible to crosslinking under radiation (MicroChem). There was in-house experience with this material that made it a good candidate to complete a series of experiments for the project. This material is further discussed in Section 5.

3. Material Characterization Methods

To determine if the cross-linking mechanism has been successful in the interlayer materials, several methods of material evaluation were reviewed to identify clear, repeatable changes in the mechanical properties. The material characterization techniques utilized in evaluating the performance changes of the interlayer material include different tensile loading methods and hardness evaluation methods.

3.1. Tensile Testing

The introduction of the safety glass for buildings has lessened the consequences of hazards' risk on occupants dramatically. Laminated glass consists of two or more glass panes with one or more polymer layers, such as PVB or EVA, sandwiched between the glass layers. Under dynamic loading, the polymeric interlayer could experience strain rates that are high enough to alter the quasi-static material properties. Therefore, it is necessary to also understand the high strain rate properties of laminated glass, which is controlled by the polymer interlayer.

Two tensile testing techniques were applied for the polymer interlayer material. The quasi-static tensile test meets ASTM D638-14 test standards for material testing. It is a standard method of testing that pulls a specimen to failure at a low strain rate. This produces a stress/strain curve characteristic to the material. The high strain rate tensile test method is used to identify tensile loading characteristics that would be seen under blast conditions and is oftentimes referred to as a dynamic tensile test. This method pulls the specimen to failure in a very short amount of time. This also produces a stress/strain curve characteristic to the material.

Several works focus on the mechanical properties of the interlayer material under the static and dynamic strain rates (Centelles, Martin, Sole, Castro, & Cabeza, 2020) (Zhang, et al., 2020) (Lopez-Aenlle, Noriega, & Pelayo, 2019) (Zhao, Yang, Wang, & Azim, 2019) (Osnes, Holmen, Hopperstad, & Borvik, 2019) (Biolzi L. , Cattaneo, Orlando, Piscitelli, & Spinelli, 2020) (Biolzi L. , Cattaneo, Orlando, Piscitelli, & Spinelli, 2018) (El-Shami, Norville, & Ibrahim, 2012) (Hidallana-Gamage, Thambiratnam, & Perera, 2015) (Liu, et al., 2020) (Samieian, et al., 2019). The most common polymer material used in safety laminated glass is PVB. Pressure and heat are used in an autoclave to exclude air and to bond the PVB sheets to the glass panes. After breakage, the glass shards mostly adhere to the PVB membrane, retaining the fragments in place. This behaviour led to laminated glass being considered as safety glass and used for blast resistant glazing.

PVB mechanical response is highly time-dependent, and it can elongate to several times of its initial length. PVB, cured, and uncured, mechanical properties were investigated over a wide range of strain magnitudes and strain rates (Morison, 2010) (Iwasaki, Sato, Latailladeand, & Philippe, 2007) (Hooper, Blackman, & Dear, 2011). Bennison et al. suggested new formulations of PVB polymeric interlayer for blast resistance (Bennison, Sloan, Kristunas, & Buehler, 2005) (Bennison, Smith, Anderson, & Sloan, 2003). After the breakage of the glass layers, the glass shards mostly adhere to the interlayer. Due to the large deformation, these glass shards can cause additional tearing and cracks in the interlayer material. Although several works investigated interlayer materials in both virgin and laminated cases before glass breakage (Morison, 2010)

(Hooper, Blackman, & Dear, 2011), no previous research studied the after-breakage effect on the interlayer.

There was a wide range of strain rates at which PVB was tested in previous works (Morison, 2010) (Hooper, Blackman, & Dear, 2011). However, strain rates observed in blast testing were in the range of 1/s to 10/s (Hooper P. , 2011). Also, the tearing of the 0.76mm interlayer was observed at a 13% strain at a strain rate of 40 s^{-1} (Hooper P. , 2011). A strain rate of 40 s^{-1} was suggested for typical blast-resistant laminated glass for PVB material at 23ºC (Morison, 2010). In addition, in this research, finite element results were analyzed to investigate the strain rates at failure for the different windows which were tested in the field using live explosives (Lopez-Aenlle, Noriega, & Pelayo, 2019). It was noticed that the strain rate was 40 s^{-1} at failure for the windows that experienced tearing and was less than 20 s^{-1} for the windows that did not fail. Therefore, a nominal strain rate with a range of 30 to 40 s^{-1} was chosen for the high strain rate testing described in this research to simulate strain rates in the polymer interlayer under typical blast loading threats.

Two tensile testing techniques were applied for polymer interlayer material. The quasi-static (static) tensile test meets ASTM test standards for material testing, and the high-strain rate (dynamic) tensile test method was used to more accurately reflect tensile loading under blast conditions. Comparing the high-strain and static results, the dynamic loading significantly affects the material response and the energy absorption characteristics of the interlayer materials, and subsequently, the blast response of laminated glass panels.

3.1.1. Tensile Specimen Preparation

In this study, the sample geometry was, according to ASTM D638 (ASTM D638-10, 2010), a standard Type IV specimen, as shown in Figure 8a. However, modified specimen geometry was used for dynamic tests. It was designed by modifying the Type I standard specimen (ASTM D638−10 2010), which is shown in Figure 8b. The modified geometry helped to increase the bonding area between the aluminum tabs and the interlayer polymer specimens to prevent the tearing of the specimens at the ends of aluminum tabs. To ensure the accuracy of the specimen dimensions, a steel cutting die was manufactured, see Figure 8c, Figure 8d, and Figure 8e. The 1-inch central gauge length, Lg, was marked with thin black lines/points using a permanent marker pen prior to testing to enable the strain to be monitored during the test using a high-speed camera. Digital calipers were used to measure the thickness and width of the test section at three locations to an accuracy of 0.0005 inches.

a) Static Coupon geometry (Dimensions, in)

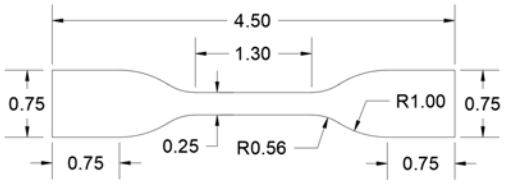

b) Dynamic Coupon geometry (Dimensions, in)

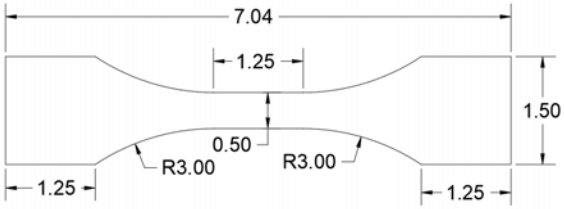

c) Dynamic Cutting die

e) Specimen stamping

d) Static Cutting die

Figure 8: Specimen Preparation; a) Static Specimen geometry, b) Dynamic Specimen geometry, c) Static cutting die, d) Dynamic cutting die, and d) Specimen stamping.

3.1.2. Quasi-Static Tensile Testing

For the quasi-static tensile test, two testing frames are available. The first one is the hydraulic tensile testing machine, shown in Figure 9a. The total travel distance for this apparatus is only 6 inches. The pneumatic testing frame is shown in Figure 9b; this device is suitable for the ductile interlayer since it has a very large travel distance of up to 18 inches. These devices can be equipped with up to 500-pound capacity load cells and a Linear Variable Differential Transformer (LVDT) to measure the total extension of the specimen. The data acquisition system is also attached to the apparatus, which transfers the test data to a specialized LabView program. In addition, the total distance between the two grips is also recorded. The deformation of the gage length of the specimen was calculated by using a high-resolution camera.

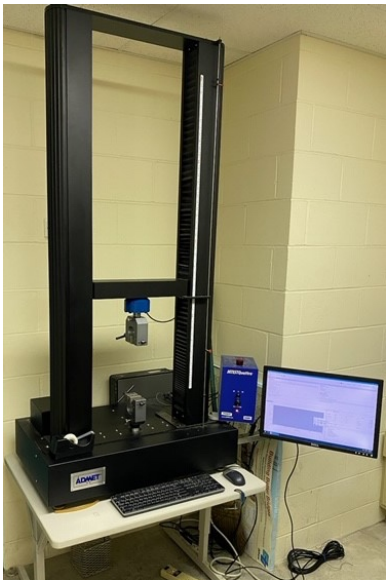

a) Mechanical Testing Frame

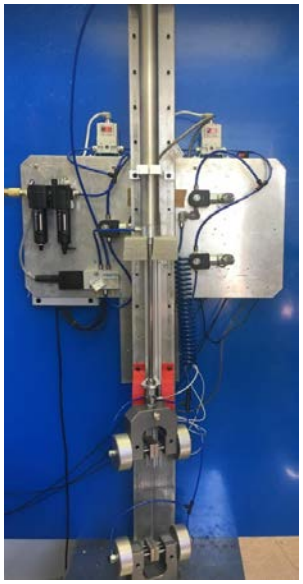

b) Pneumatic Testing Frame

Figure 9: Static Testing Frames.

Samples of tested PVB and EVA coupons can be seen in Figure 10 and Figure 11.

Figure 10: Static tensile specimen cut out from treated interlayer.

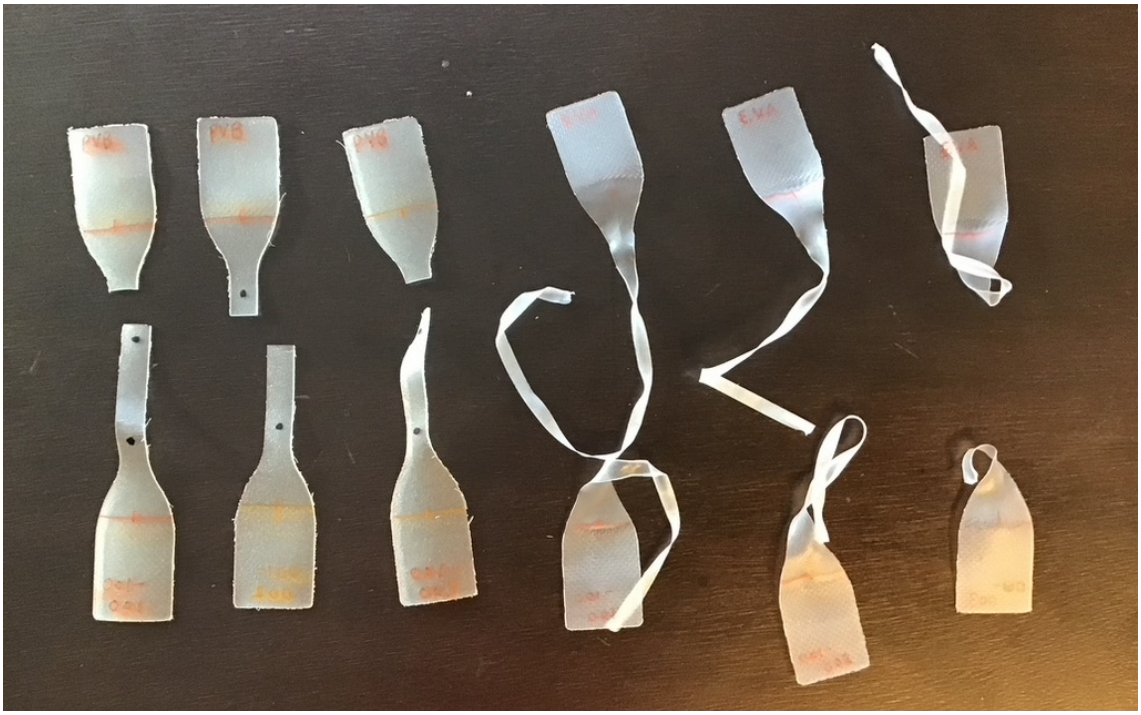

Figure 11: Tested coupons of PVB and EVA.

3.1.3. High-Strain Rate Tensile Testing

The high-strain rate tensile testing in this research was performed using a drop-weight apparatus, see

Figure 12a. The apparatus consists of a forked striker and an anvil that create an impact load to produce an extension to a tensile specimen at an acceleration above zero. A piezoelectric load-cell (Omegadyne model LC213-500) was used to measure the load and calculate the engineering stress at a rate of 3,000 data points per second. The elongation of the specimens was monitored during the test using a high-speed camera (model SC1 manufactured by Edgertronic) at a recording rate of 3,000 frames per second,

Figure 12b. The load from the piezoelectric load-cell was recorded by a National Instruments USB-6351 data acquisition system.

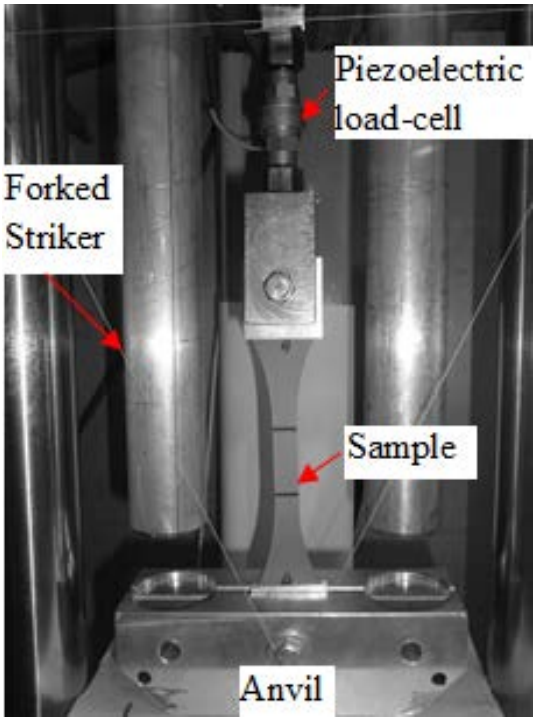

(a) Dynamic Test Setup

(b) High-Speed Camera

Figure 12: Drop Weight Test Set-Up; (a) Apparatus components and specimen setup, and (b) High-speed camera.

3.1.4. Strain Measurement for Dynamic Tensile Test

Images of the sample deformation captured by high-speed camera were post-processed to calculate the strain in the sample. Software was developed in-house, which was used to track the position of the gauge length lines during the loading event, as shown in Figure 13. The engineering strain was then calculated using the original length, determined from the frame just prior to the start of loading, and the difference in length in all subsequent frames, see Figure 14. The prepared coupons for high strain rate testing can be seen in Figure 15.

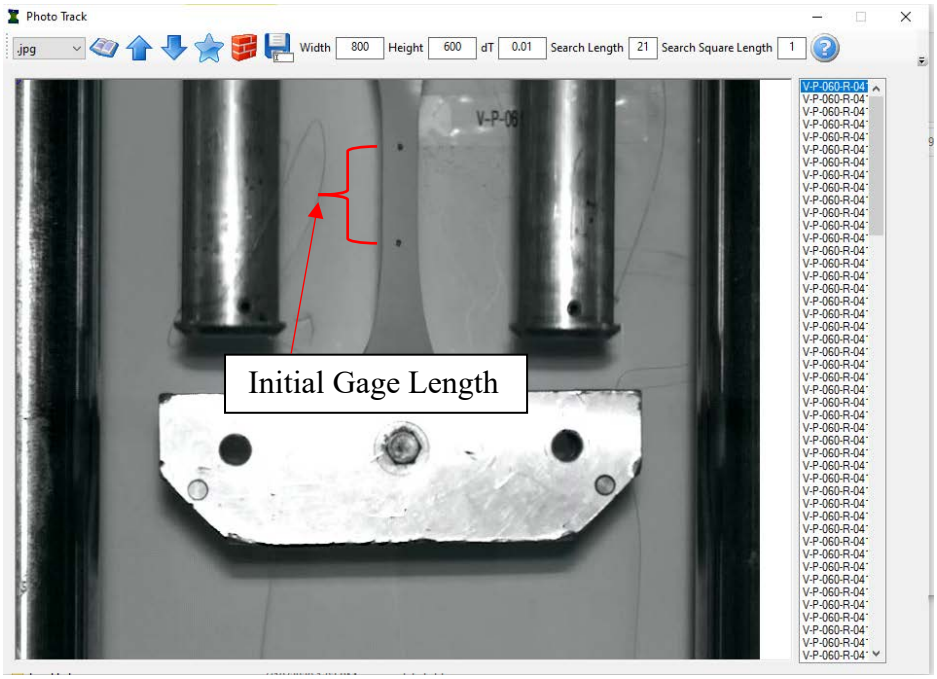

Figure 13: Tracking the Gauge Length Displacement using Photo Tracking Program.

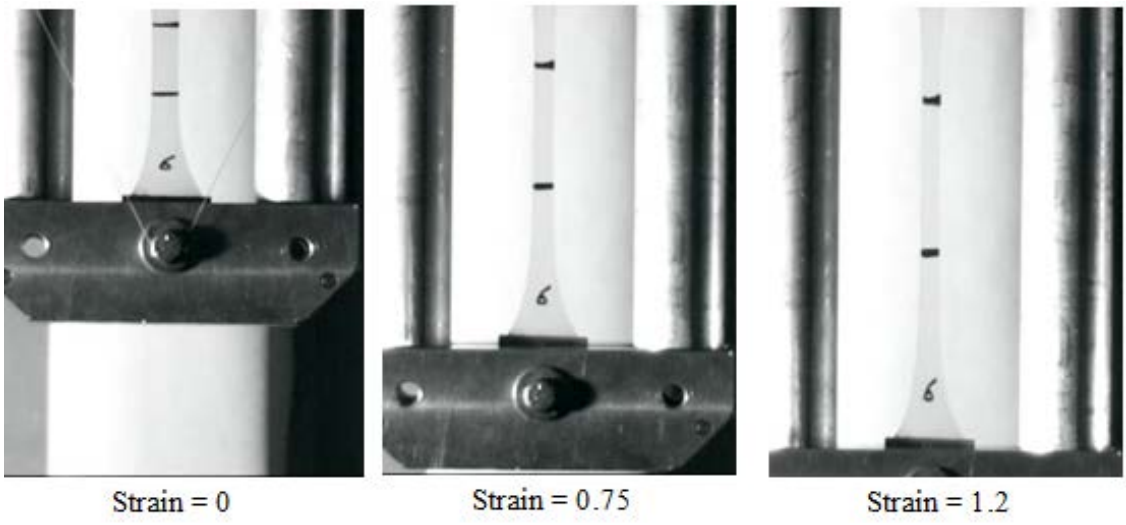

Figure 14: Strain at Selected Frames During Drop Weight Test.

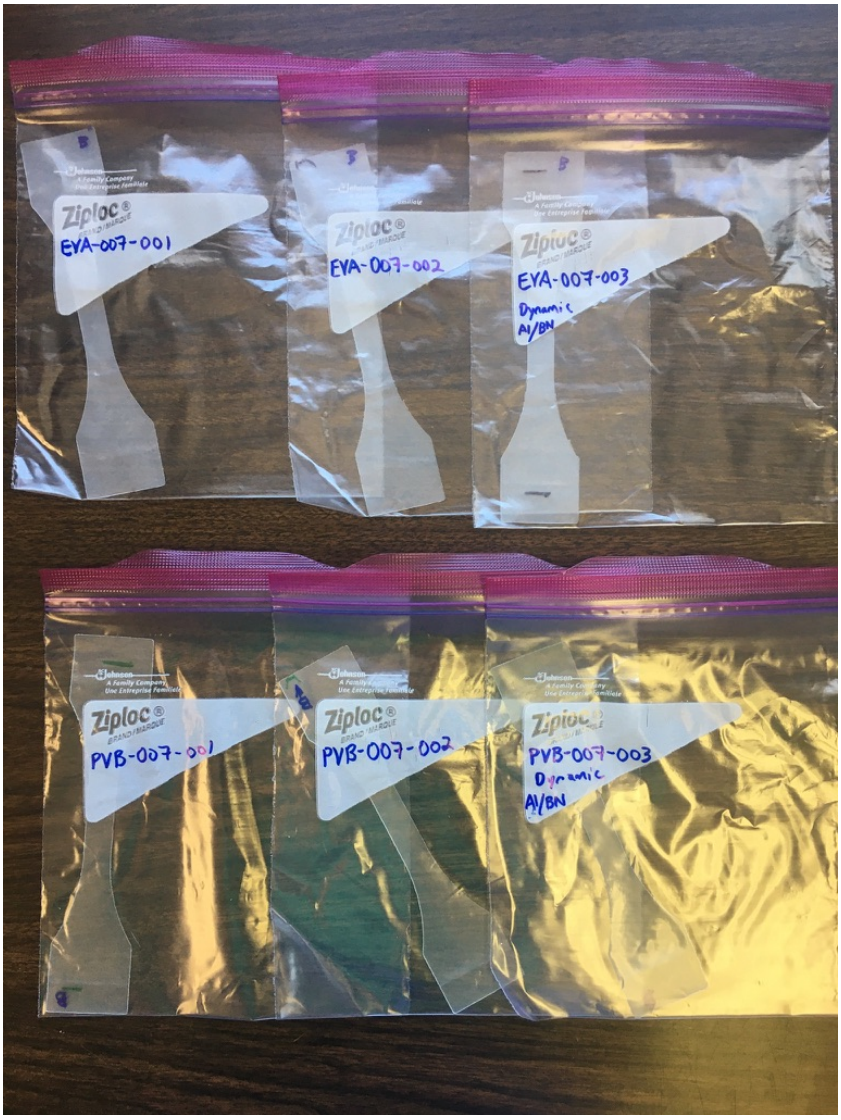

Figure 15: Prepared coupons for high strain rate tensile testing.

3.2. Hardness Testing

Hardness evaluations are commonly used throughout industry to define material properties of polymer material. This material characterization is generally quick and relatively simple to determine with the proper equipment. Furthermore, it typically results in a non-destructive evaluation of material that reduces cost and waster associated with material testing. Hardness testing is determined through specific instrumentation that can

change based on the material type and its relative softness. For instance, a Rockwell Hardness test is best suited for harder materials such as steel, whereas a Shore-A Durometer is used on softer materials such as rubber.

The technique used to evaluate hardness varied depending on the type of material, the thickness of material, and the conditions under which testing occurred. The types of hardness testing utilized with these interlayer materials included Rockwell, Shore-A, Shore-D, Micro-Vickers, nano-indentation, and scratch testing.

A Rockwell Hardness Test (ASTM E18-20, 2020) was initially used to on polycarbonate discs to determine the adequacy of this testing method. The equipment was readily available in several lab spaces, and was put to use on a relatively hard polycarbonate polymer material that was to be used as a base material for coating applications. The Rockwell Hardness Test is typically used on harder metallic materials, and therefore proved ineffective in determining the hardness of the polycarbonate polymer. A very portable Rockwell Hardness evaluation device can be seen in Figure 16.

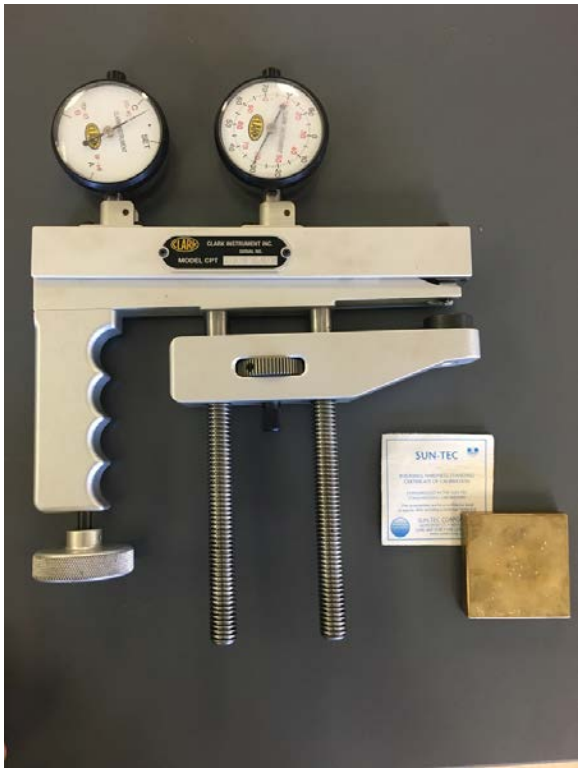

Figure 16: Rockwell Hardness measuring devices in the lab.

A Micro-Vickers Test (ASTM E384-17, 2017) was utilized next on the polycarbonate discs. This equipment was available, and portable to the radioactive material handling area so that material that was still radioactive could still be tested (See Figure 17). This equipment was capable of determining repeatable values from the polycarbonate discs, as well as polycarbonate discs with coatings, and was chosen for this specific task only.

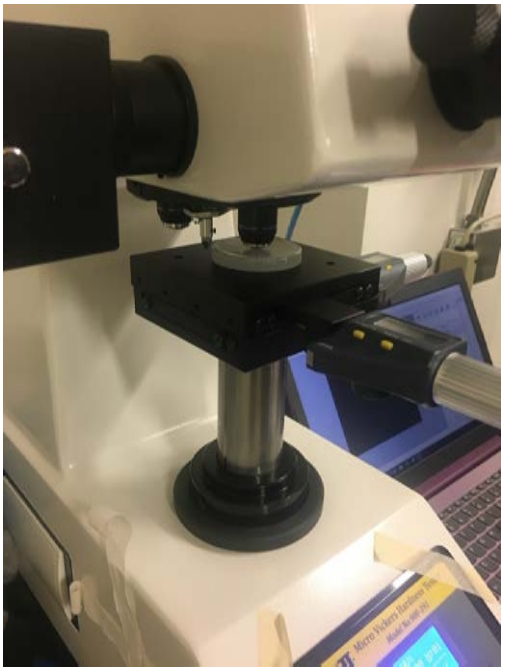

Figure 17: Micro-Vickers Testing with SU-2100 coated polycarbonate.

Shore-A and Shore-D Durometers (ASTM D2240-15, 2021) were selected for softer materials such as polyethylene. These are used as an industry standard. Hand-held durometers were procured and the Shore-D Hardness evaluation provided repeatable results from the polyethylene samples. Hardening was evaluated pre and post-irradiation. The Shore-D Durometer test method was chosen for its application to softer materials, and it's mobility within the radioactive material handling areas. It is expected that an increased amount of cross-linking will be indicated with an increase in hardness.

Figure 18: Shore A (left) and Shore D (right) Durometers.

Nano-indentation (W.C. Oliver, 1992) was used to determine Hardness and Elasticity in the thin sheet polymer interlayer materials. Anton Paar Instruments assisted the research by provided consulting services regarding this material evaluation, as well as conducting several material tests.

Scratch Testing was conducted on the material sheets to determine the resistance to scratching. Anton Paar Instruments once again assisted with this effort. These tests could also be utilized in future work to determine the adhesion of the interlayer material to the surface of the glass plies.

4. Neutron Flux Treatment

To evaluate the effects of the neutron bombardment on the boron doped polymers, initial tests were conducted with commercially available borated polymers. These materials were chosen for the early access to borated polymers with relevant properties and were used to evaluate testing processes, determine optimal neutron flux rates, and evaluate material handling. In this chapter, a description will be provided on why specific neutron flux rates were selected, how the samples were irradiated, and what the effects of those irradiaitons revealed.

4.1. High Neutron Flux

There were two primary flux positions available at the MURR facility, one of a much higher neutron flux rate than the other. The higher flux position was a near match to theoretical work, and was therefore a good selection for initial treatment. The higher flux translates to a higher rate of neutron bombardement, and could theoretically provide a quick verification of previous research through hardness evaluation.

4.1.1. Experimental Setup

Rej, et al., (Rej, Pickrell, & Wrobleski, Neutron-Capture-Induced Radiation Treatment of Polymeric Materials, 1996) had determined neutron irradiation conditions in a boron doped polymer to match the hardening results from an ion implantation experiment that had exhibited surface hardening in a polymer (Lee & Lewis, Improved Surface Properties of Polymer Materials by Multiple Ion Beam Treatment, 2011) (Lee, Rao, Lewis, & Mansur, 1993). Rej called for a 1% 10boron concentration (approximately 5% natural

boron) in a polystyrene doped polymer with a neutron flux of 10^{14} n/cm^{2}s with an irradiation time of 1.5 hr.

A series of tests were performed on samples of two commercially available 5% borated polyethylene samples. As naturally occurring boron contains approximately 20% 10boron and 80% 11boron (Baum, Ernesti, Knox, Miller, & Watson, 2010), the 5% borated polyethylene will match perfectly with the 10boron content called for by Rej. (Polyethylene and polystyrene have similar softening characteristics in response to heating). These tests exposed samples of the material to a flux rate of neutrons ($5.0x10^{13}$ N/cm^2/sec). Samples were irradiated with neutrons at the University of Missouri Research Reactor (MURR) center using a pneumatic tube irradiation position. Time within the flux zone was precisely measured at 5 seconds, 30 seconds, and 60 seconds. This experiment match closely with the irradiation Rej proposed, with the difference being a very conservative irradiation time, i.e., one minute maximum compared to 90 minutes suggest by Rej, et al. (Rej, Pickrell, & Wrobleski, Neutron-Capture-Induced Radiation Treatment of Polymeric Materials, 1996).

Samples consisted of a product from COMPANY “A” (5% Borated LDPE Sheet, pink color), and a product from COMPANY “B” (5% Borated Polyethylene, green color). Samples were small in size, roughly 5mm x 5mm x 5mm, with a mass of less than 1 gram.

Table 1: Virgin Samples from Manufacturer, Shore D Hardness Values.

Shore D Hardness Values		
Virgin Samples from Manufacturer		
Sample Type	Pink, 5%	Green, 5%
Test 1	50	67
Test 2	52	67
Test 3	51	65
Test 4	52	68
Test 5	48	68
Test 6	54	67
Test 7	54	66
Test 8	51	69
Test 9	52	68
Test 10	53	68
AVERAGE	51.7	67.3

4.1.2. Analysis

The samples were first tested at 5 seconds within the flux zone. The 5 second samples were at room temperature at the start of testing. Upon removal, gamma spectroscopy indicated significant peaks of aluminum, titanium and oxygen isotopes. These peaks indicate contamination intrinsic to the polymer. Overall radiation was low, and the samples were able to be tested using the Shore D Hardness Durometer immediately. Results under this short duration appeared to show a slight softening of the material. Samples from Company A moved from an average of 51.7 Shore D Hardness to 50 after irradiation. Samples from Company B moved from an average of 67.3 Shore D Hardness to 65.6. Results under this short duration appeared to show a slight softening of the material, as seen in Table 2.

Table 2: Five second irradiation, Shore D Hardness Values.

Shore D Hardness Values		
5 sec. irradiation, very high flux		
Sample Type	Pink, 5%	Green, 5%
Test 1	50	65
Test 2	50	67
Test 3	50	66
Test 4	50	65
Test 5	50	65
AVERAGE	50	65.6

*Neutron Flux = 5 x10^13 N/cm^2/sec

New samples were tested for a 30 second irradiation at the same flux rate. Prior to testing, the samples were cooled using liquid nitrogen (~77 degrees Kelvin). Samples showed significant additional softening. The sample from company A experienced significant discoloration around the edges and thinner portions, while also showing signs of expansion and other deformity. This made durometer measurements difficult and may have an effect on the accuracy of these readings.

Samples from Company A moved from an average of 51.7 Shore D Hardness to 29.8 after irradiation. Samples from Company B moved from an average of 67.3 Shore D Hardness to 57.8 after radiation. Hardness measurements can be seen in Table 3.

Table 3: Thirty second irradiation, Shore D Hardness Values.

Shore D Hardness Values		
30 sec. irradiation, very high flux		
Sample Type	Pink, 5%	Green, 5%
Test 1	33	52
Test 2	36	56
Test 3	25	60
Test 4	30	58
Test 5	25	63
AVERAGE	29.8	57.8

*Pink sample deformed, making it difficult to place Shore D Hardness gauge flush with material.
*Pink sample had deprived coloration around edges.
*Neutron Flux = 5 x10^13 N/cm^2/sec
*Samples cooled in Liquid Nitrogen (~77 K degrees), prior to irradiation.

A test was conducted with only the samples from Company B at 60 second irradiation. The samples were not cooled prior to irradiation. The treated samples appeared to have experienced some level of melting during this irradiation time. There were significant deformities, making the measurement of the sample very difficult, and may have an effect on the accuracy of these readings. Samples from Company B moved from an average of 67.3 Shore D Hardness to 57.8. Hardness measurements can be seen in Table 4.

Table 4: Sixty second irradiation, Shore D Hardness Values.

Shore D Hardness Values		
60 sec. irradiation, very high flux		
Sample Type	Pink, 5%	Green, 5%
Test 1		55
Test 2		60
AVERAGE		57.5

*Sample "melted." Difficult to get proper test from deformed sample.
*Neutron Flux = 5 x10^13 N/cm^2/sec

4.1.3. Results

The clear indication from these tests is that an irradiation as described in the original theoretical paper is highly unlikely to be achievable. Again, samples were melting at roughly 1% of the prescribed neutron fluence, in a material (polyethylene) with similar response to heating as that prescribed (polystyrene). It appeared that there were two options possible experimentally; either the reduction of neutron flux reducing the rate of energy deposition into the polymer, or the reduction of boron in the polymer (or both). This discovery progresses the area of research by providing evidence showing that the theoretical path may need to be adjusted in order to reach theoretical results.

Samples following treatment can be seen in Figure 19 and Figure 20.

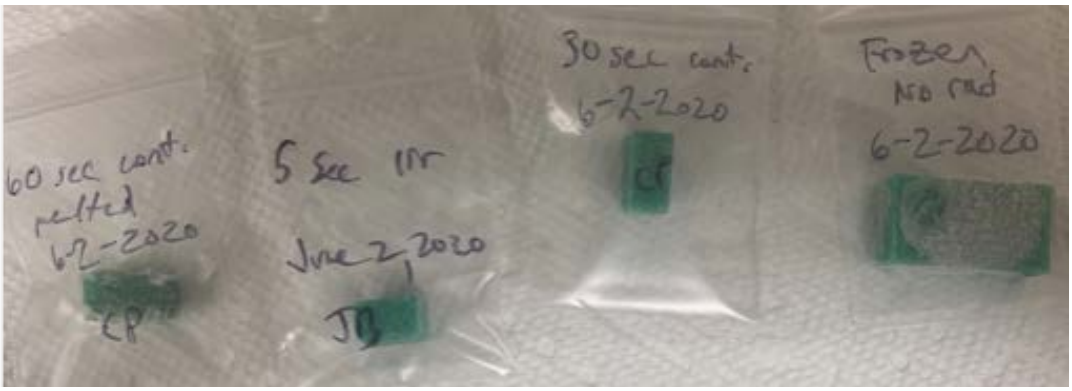

Figure 19: High flux Green samples, L to R, 60 second irradiation, 5 second irradiation, 30 second irradiation, frozen (no irradiation, frost seen).

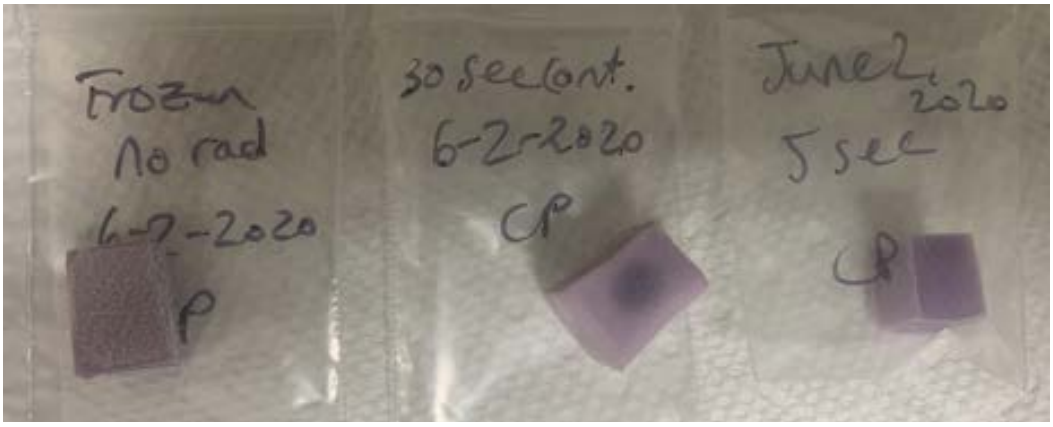

Figure 20: High flux Pink samples, L to R, frozen (no irradiation, frost seen), 30 second irradiation (swelling and discoloration seen), 5 second irradiation.

Possible causes of softening could include thermal effects of alpha decay. The inclusion of boron in the polyethylene creates a material with a much higher affinity towards neutron capture, due to the large cross-section of boron.

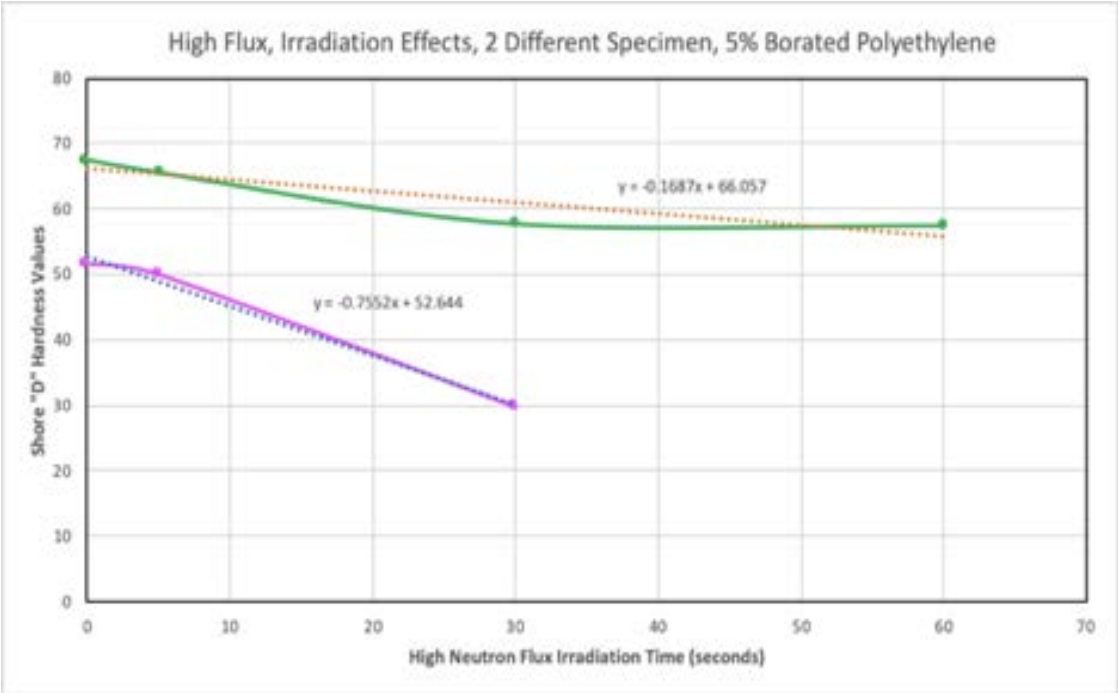

Figure 21: High flux testing results.

As an additional investigation to the test, the pneumatic tube vehicles that are made of polyethylene themselves (manufacturer differs from other samples) were tested.

Shore D Hardness tests were performed on new and used pneumatic tube vehicles to determine the irradiation effect on a non-borated polyethylene material. The Shore D results shown in Table 5 indicated an increase in hardness following irradiation (time under flux not defined). Furthermore, there is observable discoloration in the polyethylene tube vehicles following irradiation, as shown in Figure 22. Lab subject matter expert interviews have indicated that the vehicles tend to get darker following irradiation, but also lighten back up over continued usage.

Table 5: Polyethylene Pneumatic Tube Vehicles, Shore D Hardness Values.

Shore D Hardness Values		
Standard Polyethylene Tube Vehicle		
Sample Type	No RAD	Some RAD
Test 1	62	70
Test 2	62	60
Test 3	63	68
Test 4	65	70
Test 5	60	70
AVERAGE	62.4	67.6

*Neutron Flux = 5 x10^13 N/cm^2/sec

Figure 22: Pneumatic Tube Vehicles through progressive usage (new white tube at left).

4.2. Low Neutron Flux

A lower neutron flux position was available for use at the MURR facilities, and the work proceeded to utilize this second position for low neutron flux treatment. This position provided neutron bombardment at a much slower rate of $8.4x10^8$ n/cm^{2}s as compared to the high neutron flux rate of $5.0x10^{13}$ n/cm^{2}s. At this lower rate, it was expected that the heating effects of the atomic reactions would be minimized and that a more stable environment will allow for adequate process control.

4.2.1. Experimental Setup

Another series of tests were performed on samples of the two commercially available 5% borated polyethylene samples. These tests exposed samples of the material to a low flux rate of neutrons ($8.4x10^8$ n/cm^2/sec) in an external neutron beam at MURR depicted in Figure 23 and Figure 24. (Brockman, Nigg, Hawthorne, Lee, & McKibben, Characterization of a Boron Neutron Capture Therapy Beam Line at the University of Missouri Research Reactor, 2009) (Brockman, Nigg, Hawthorne, & McKibben, Spectral Performance of a Composite Single-Crystal Filtered Thermal Neutron Beam for BNCT Research at the University of Missouri, 2009) (Brockman, Nigg, & Hawthorne, Computational Characterization and Experimental Validation of the Thermal Neutron Source for Neutron Capture Therapy Research at the University of Missouri, 2013).

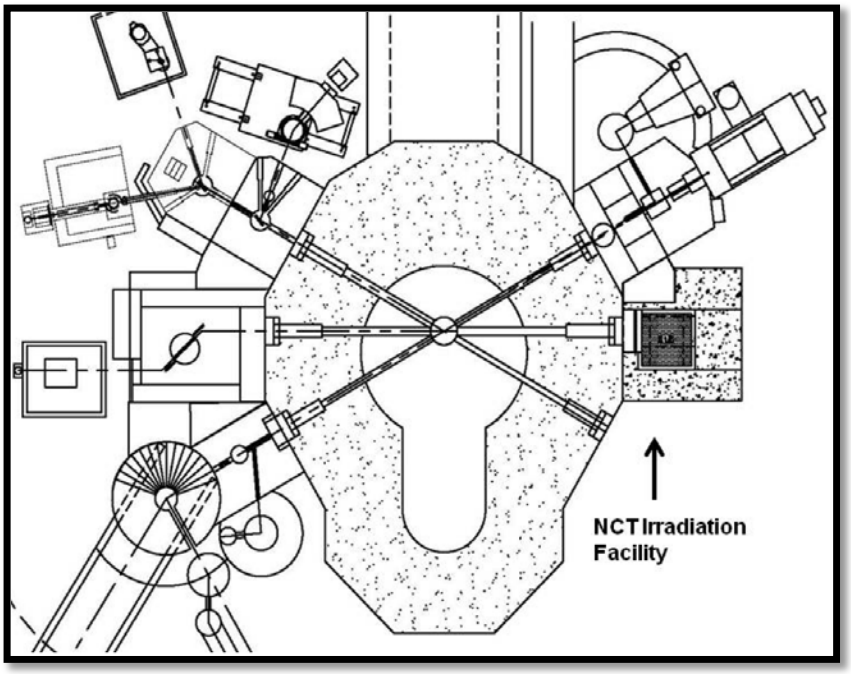

Figure 23: Plan view of MURR beamport floor with specific beamport labeled (Brockman, Nigg, Hawthorne, & McKibben, Spectral Performance of a Composite Single-Crystal Filtered Thermal Neutron Beam for BNCT Research at the University of Missouri, 2009).

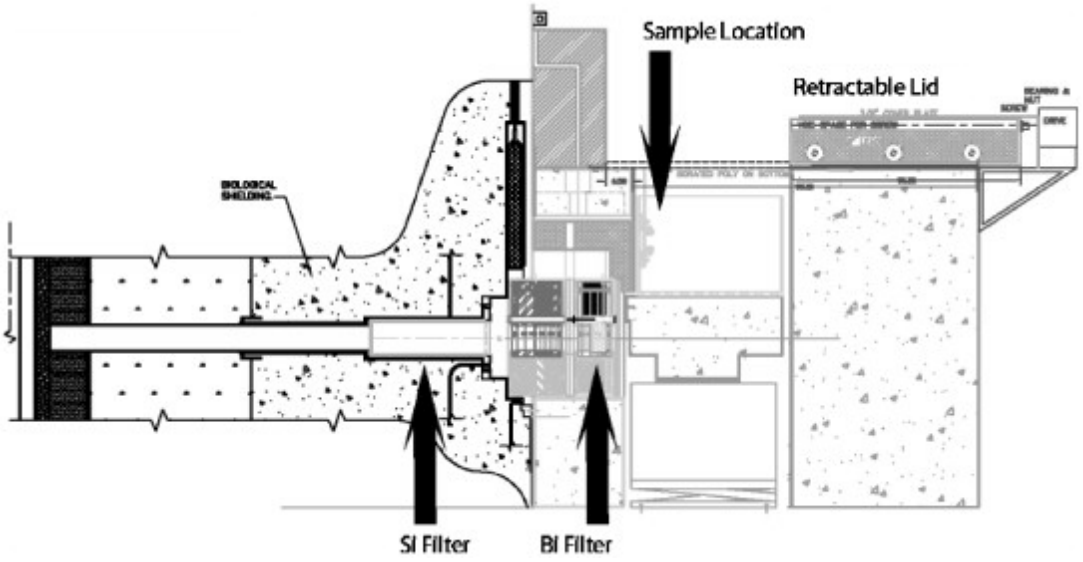

Figure 24: MURR thermal beamline design detail. The axial centerline of the reactor core is on the left of the diagram as shown (Brockman, Nigg, Hawthorne, & McKibben, Spectral Performance of a Composite Single-Crystal Filtered Thermal Neutron Beam for BNCT Research at the University of Missouri, 2009).

Samples consisted of a product from COMPANY “A” (5% Borated LDPE Sheet), and a product from COMPANY “B” (5% Borated Polyethylene). Sample sizes were roughly 10mm thickness x 20mm width x 100mm length as shown in Figure 25.

Figure 25: Low flux rate test specimen.

The samples were attached to a target, with the back labeled. The front of the target was outfitted with flux wires to confirm the expected flux rate. Test set-up can be seen in Figure 26.

Figure 26: Samples prepared for irradiation on target.

Figure 27: Inserting specimen into beamport position.

The samples were first irradiated for 28.4 hours within the flux zone, tested with a durometer, and placed back into the same flux position, and allowed to continue irradiation for 70 additional hours. The samples were at room temperature throughout testing.

Additionally, a second irradiation was performed with similar test samples. The samples were first irradiated at 28.6 hours within the flux zone, tested with the durometer, and placed back into the same flux position to continue irradiation for 100 additional hours. The samples were also at room temperature throughout testing.

4.2.2. Analysis

The samples were tested Front and Back, where front is the side that is facing the neutron irradiation beam. Samples were tested with the Shore D Hardness Durometer.

For the first test, the front-face testing results are shown in Table 6 and Table 8. The back-face results are shown in Table 7 and Table 9. For the second test, the front-

face testing results are shown in Table 10, Table 12, and Table 14. The back-face results are shown in Table 11, Table 13, and Table 15.

Table 6: First test, Front face, 1705-minute irradiation, Shore D Hardness Values.

Shore D Hardness Values, Front Face		
1705 minutes, low flux		
Sample Type	Pink, 5%	Green, 5%
Test 1	50	70
Test 2	56	69
Test 3	56	65
Test 4	57	66
Test 5	57	68
AVERAGE	55.2	67.6
STD DEV	2.9	2.1
REL STD DEV	5.34%	3.07%

Table 7: First test, Back face, 1705-minute irradiation, Shore D Hardness Values.

Shore D Hardness Values, Back Face		
1705 minutes, low flux		
Sample Type	Pink, 5%	Green, 5%
Test 1	55	65
Test 2	50	66
Test 3	58	67
Test 4	56	64
Test 5	55	67
AVERAGE	54.8	65.8
STD DEV	2.9	1.3
REL STD DEV	5.38%	1.98%

Table 8: First test, Front Face, 5905-minute irradiation, Shore D Hardness Values.

Shore D Hardness Values, Front Face		
5905 minutes, low flux		
Sample Type	Pink, 5%	Green, 5%
Test 1	58	66
Test 2	56	68
Test 3	59	68
Test 4	57	70
Test 5	57	68
AVERAGE	57.4	68
STD DEV	1.1	1.4
REL STD DEV	1.99%	2.08%

Table 9: First test, Back Face, 5905-minute irradiation, Shore D Hardness Values.

Shore D Hardness Values, Back Face		
5905 minutes, low flux		
Sample Type	Pink, 5%	Green, 5%
Test 1	57	65
Test 2	56	64
Test 3	57	65
Test 4	57	67
Test 5	57	67
AVERAGE	56.8	65.6
STD DEV	0.4	1.3
REL STD DEV	0.79%	2.05%

Table 10: Second test, Front face, pre-irradiation, Shore D Hardness Values.

Shore D Hardness Values, Front Face		
Virgin Samples from Manufacturer		
Sample Type	Pink, 5%	Green, 5%
Test 1	55	65
Test 2	57	68
Test 3	57	70
Test 4	57	69
Test 5	57	69
AVERAGE	56.6	68.2
STD DEV	0.9	1.9
REL STD DEV	1.58%	2.82%

Table 11: Second test, Back face, pre-irradiation, Shore D Hardness Values.

Shore D Hardness Values, Back Face		
Virgin Samples from Manufacturer		
Sample Type	Pink, 5%	Green, 5%
Test 1	57	70
Test 2	57	68
Test 3	55	69
Test 4	57	68
Test 5	57	69
AVERAGE	56.6	68.8
STD DEV	0.9	0.8
REL STD DEV	1.58%	1.22%

Table 12: Second test, Front face, 1716 - minute irradiation, Shore D Hardness Values.

Shore D Hardness Values, Front Face		
1716 minutes, low flux		
Sample Type	Pink, 5%	Green, 5%
Test 1	54	68
Test 2	56	69
Test 3	57	68
Test 4	56	68
Test 5	58	65
AVERAGE	56.2	67.6
STD DEV	1.5	1.5
REL STD DEV	2.64%	2.24%

Table 13: Second test, Back face, 1716 - minute irradiation, Shore D Hardness Values.

Shore D Hardness Values, Back Face		
1716 minutes, low flux		
Sample Type	Pink, 5%	Green, 5%
Test 1	53	71
Test 2	56	68
Test 3	57	68
Test 4	56	67
Test 5	57	68
AVERAGE	55.8	68.4
STD DEV	1.6	1.5
REL STD DEV	2.94%	2.22%

Table 14: Second test, Front face, 7716 - minute irradiation, Shore D Hardness Values.

Shore D Hardness Values, Front Face		
7716 minutes, low flux		
Sample Type	Pink, 5%	Green, 5%
Test 1	57	67
Test 2	57	68
Test 3	55	66
Test 4	57	70
Test 5	57	65
AVERAGE	56.6	67.2
STD DEV	0.9	1.9
REL STD DEV	1.58%	2.86%

Table 15: Second test, Back face, 7716 - minute irradiation, Shore D Hardness Values.

Shore D Hardness Values, Back Face		
7716 minutes, low flux		
Sample Type	Pink, 5%	Green, 5%
Test 1	58	70
Test 2	56	65
Test 3	55	68
Test 4	56	67
Test 5	56	68
AVERAGE	56.2	67.6
STD DEV	1.1	1.8
REL STD DEV	1.95%	2.69%

4.2.3. Results

Importantly, there were no visually observable changes to the samples following irradiation during either the first or the second test. The duration of the second test was such that total fluence was similar to the earlier, higher flux, shorter duration tests. The samples largely show results that were not statistically significant, however, low density polyethylene from Company A did show hardening during the first test with an 11% increase +/-3.66%. That hardening was most pronounced during the first 28.4 hour

irradiation period, suggesting hardening could be achieve with significantly lower neutron fluences in certain polymers.

The samples did show some mixed results from the hardness testing, but general hardening of the material was identified, summarized in Table 16, and further represented in Figure 28. Both samples indicated more hardening on the front-face, as would be expected if the polymer cross-linking was taking place.

From the first test, the pink sample showed the greatest increase of hardness, with an 11% increase +/-3.66%. The most significant hardening occurred in the first 1705-minute irradiation as discerned by the slope decrease in the 5905-minute irradiation. The green sample, while showing signs of 1% hardening on the front face, was very limited in clear results, as the average relative standard deviation of 2.57% was within the range of observed hardening. This can be seen in Table 17. However, as observed with the pink sample, the most significant hardness value increase occurred in the first 1705-minute irradiation.

Table 16: First Test, Overall Results, Shore D Hardness, Low Flux Rate Irradiation.

Hardness Increase, Front to Back		
	Pink	Green
1705 Minutes	0.40	1.80
5905 Minutes	0.20	0.60
Overall	0.60	2.40

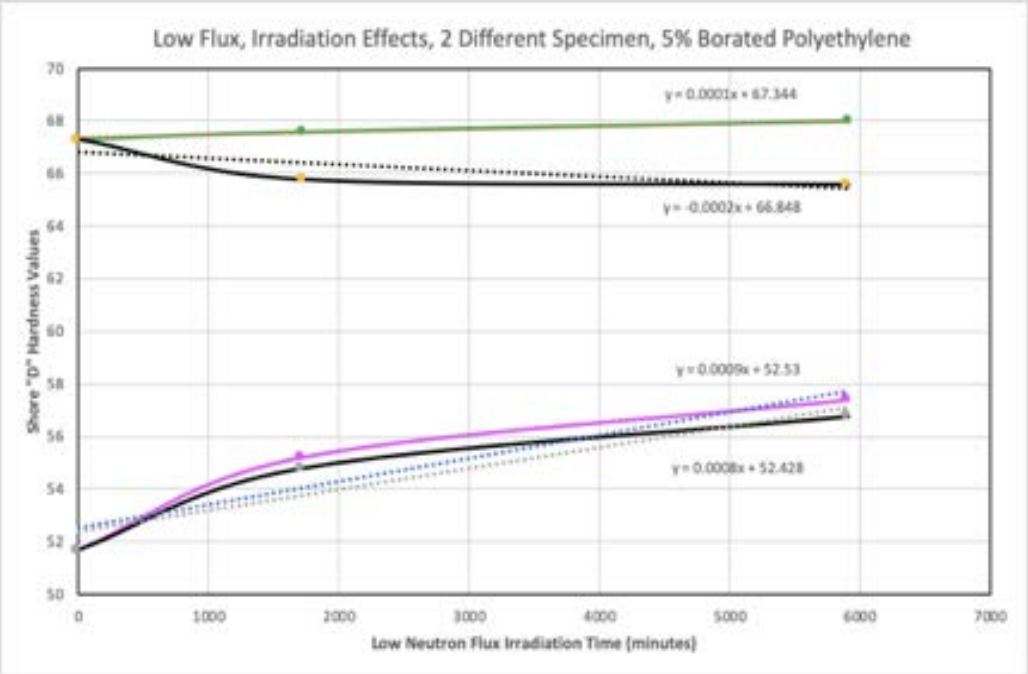

Figure 28: First Test, Graphed results of the 1705 and 5905-minute irradiations.

Table 17: Second Test, Overall Results, Shore D Hardness, Low Flux Rate Irradiation.

	Front Face		Back Face	
TIME	Pink, 5%	Green, 5%	Pink, 5%	Green, 5%
0	56.6	68.2	56.6	68.8
1716	56.2	67.6	55.8	68.4
7716	56.6	67.2	56.2	67.6
INCREASE %	0.00%	-1.47%	-0.71%	-1.74%
AVG REL STD DEV	2.11%	2.55%	2.45%	2.45%

Table 18: Second Test, Hardness Increase, Front to Back of Sample.

Hardness Increase, Front to Back		
	Pink	Green
1716 Minutes	0.40	-0.20
7716 Minutes	0.00	0.40
Overall	0.40	0.20

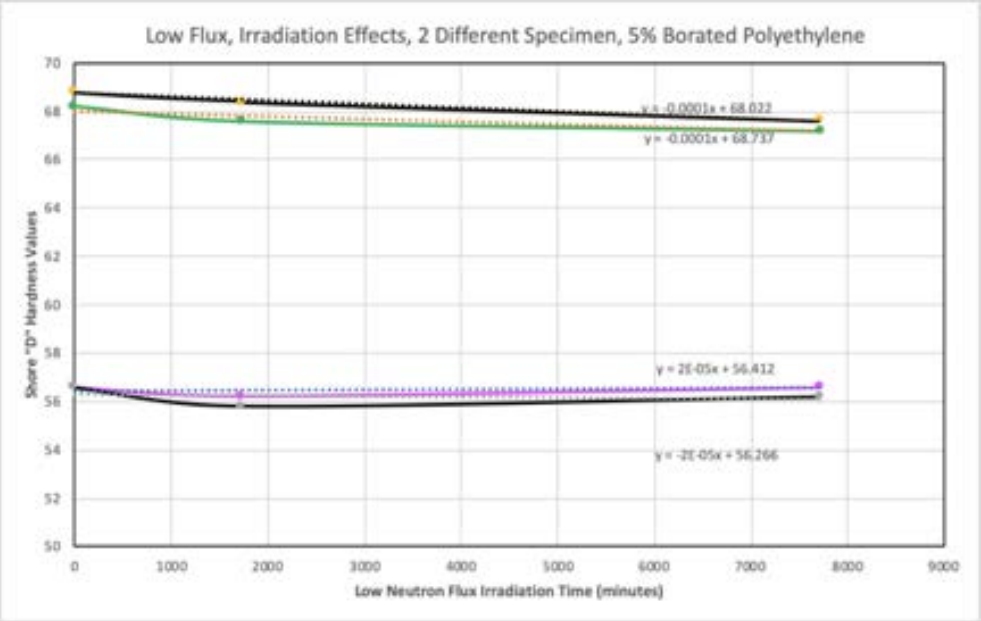

Figure 29: Second Test, Graphed results of the 1716 and 7716-minute irradiations.

It was also shown that the hardening of polymers doped with boron and exposed to substantial reactor neutron flux is likely impossible. Whether gamma heating or the energy released from the boron neutron capture reaction itself, our samples softened very quickly, in a small fraction of the calculated time required for hardening.

5. Treatment of Custom Polymers

In collaboration with a team in the Electrical Engineering Department of the University of Missouri – Columbia, polymers that included the boron material within the applied layers were produced. The polymer material that their department recommended was the SU8-2100 produced by Kayaku Advanced Materials Inc. In this chapter we will describe how boron was mixed into the polymer to produce specific mix designs. These samples were then treated through neutron irradiation to determine the mix effects, and the results of that work are provided.

5.1. Experimental Setup

This is a clear polymer that can be applied in thicknesses of 100 mm. Boron Nitride was used to introduce the boron and can be seen in Figure 30. This material was applied to the surface of 50mm polycarbonate discs, as shown in Figure 31. The result was a transparent disc, that became cloudy with additional percentages of boron added.

Figure 30: Boron Nitride for custom sample preparation.


Figure 31: Polycarbonate discs for custom sample preparation.

The amount of boron present within the material will have a significant effect on the amount of radiation that the specimen should absorb. Too little boron will create a

situation that does not produce adequate energy to develop the polymer bonding interactions, and too much boron could cause the unnecessary opacity to the material.

Figure 32: Custom borated SU8-2100 Specimen within protective case.

Figure 33: : Custom borated SU8-2100 Specimen with high boron nitride content and no boron nitride.

5.2. Analysis

The material is to be tested pre and post-irradiation with a Vickers Hardness Test to determine if there is hardening has occurred in this material. The Vickers was chosen because it has been proven to provide clear results with this material, and is capable of transport within the radioactive material handling facility. Hardening is one indication that the material has experienced cross-linking.

5.3. Results and Discussion

Results of this testing showed mixed results, as seen in Table 19. Part of this could be attributed to the non-homogenous product surface that seemed to develop as the material initially cured. Results may also indicate that the SU8-2100 material may not be a polymer that is not well suited to this particular treatment method.

Table 19: Vickers Hardness Testing results for borated SU8-2100 pre and post-irradiation.

		Pre-Irradiation	Post-Irradiation	Delta
Sample #	Description	Hardness AVG	Hardness	Hardness %
A	Polycarbonate Only	14.03	13.5	-3.78%
1	SU8-2100, No Boron	24.96	27.05	8.37%
2	SU8-2100, 5% Boron	23.48	21.54	-8.26%
9	SU8-2100, 5% Boron	21.17	22.1	4.39%
6	SU8-2100, 5% Boron	26.16	25.79	-1.41%
3	SU8-2100, 10% Boron	24.73	25.79	4.29%
7	SU8-2100, 10% Boron	26.92	25.08	-6.84%
10	SU8-2100, 10% Boron	17.405	23.31	33.93%
8	SU8-2100, 20% Boron	29.87	22.01	-26.31%
5	SU8-2100, 20% Boron	24.28	25.79	6.22%
11	SU8-2100, 2x10% Boron	24.62	21.63	-12.14%

The material maintained a level of radioactivity that prevented the material from being shared outside of the facility. This further gives reason to exclude this material for further testing and evaluation.

Due to the lack of informative data from this custom specimen experiment, the following chapters focus on the research objectives related to polymer interlayer material. This step helps to move the primary research path forward in a direction that provides real world application.

6. Treatment of LG Polymer Interlayers

Laminated glass is widely used for structural elements in buildings where safety performance is required from extreme wind gust or blast threat. Laminated glass panels consists of two or more layers of glass with a polymeric interlayer material such as Poly Vinyl Butyral (PVB) or Ethylene Vinyl Acetate (EVA) between each of the two glass panes. The advantages of the polymeric interlayer are to hold the fragments of cracked glass and also to work as a continuous structural membrane that dissipates energy from a given load.

In this chapter, the boron-neutron-capture method is applied to the polymeric interlayer material through a surface treatment technique. This method will use a boron rich material that is fixed in close proximity to a polymer interlayer to effect the outer surface of the interlayer. Effects are theoretically limited in depth of penetration, and the depth is evaluated. The polymer is characterized through various methods in order to confirm that the material properties have been successfully manipulated through the surface treatment. Neutron bombardment enables treatment of material deep within other materials that may have a lower neutron capture probability.

6.1. Experimental Setup

Polymeric sheet material EVA with a thickness of 0.381 mm was selected for initial treatment. The same low flux external neutron beam facility ($8.4x10^8$ N/cm^2/sec) was used (Brockman, Nigg, Hawthorne, & McKibben, Spectral Performance of a Composite Single-Crystal Filtered Thermal Neutron Beam for BNCT Research at the University of

Missouri, 2009) (Brockman, Nigg, Hawthorne, Lee, & McKibben, Characterization of a Boron Neutron Capture Therapy Beam Line at the University of Missouri Research Reactor, 2009) (Brockman, Nigg, & Hawthorne, Computational Characterization and Experimental Validation of the Thermal Neutron Source for Neutron Capture Therapy Research at the University of Missouri, 2013). The polymer interlayer material does not contain any boron and hence should not heat during neutron irradiation. As outlined in Rej, et al, (Rej, Pickrell, & Wrobleski, Neutron-Capture-Induced Radiation Treatment of Polymeric Materials, 1996)the boron treatment has a range of approximately 10 microns. This range, although limited, still has application on the thin interlayer material through surface treatment techniques, allowing treatment of nearly 3% of the EVA. To perform a surface treatment technique, the interlayer material was pressed between an aluminum sheet and a boron-nitride ceramic sheet. The configuration was placed such that the neutron beam first passed through the aluminum plate, then through the polymer material, and finally striking the surface of the boron rich sheet. The 6101 aluminum alloy was selected for its high aluminum content of 98%. The aluminum cross-section is low, making the aluminum plate nearly transparent to the neutrons as they pass through towards the boron rich plate. Minimal thermal neutron capture is expected within the polymer material as the neutrons continue toward the boron rich plate.

Once contacting the surface of the boron nitride sheet, many neutrons are captured due to the high cross-section of 10boron. As naturally occurring boron contains approximately 19.9% of the isotope 10boron, the neutron capture should produce ample energetic particles required for the cross-linking mechanism to occur.

Early treatment methods during this work were developed using polymeric material that had boron dispersed evenly throughout the material. This had advantages for bulk treatment at significant depth within the material. For thinner materials such as polymer interlayers (0.381-0.762 millimeters or 0.015-0.030 inches thick), a surface treatment method was developed that could affect a significant depth of the material without the additional manufacturing step of boron doping.

A series of tests were performed on samples of commonly used interlayer materials that include EVA and PVB. These tests exposed samples of the material to a low flux rate of neutrons ($8.4x10^8$ $N/cm^2/sec$). The neutron source was developed at the University of Missouri Research Reactor (MURR), and has been utilized for a variety of boron-neutron-capture research (Brockman, Nigg, Hawthorne, & McKibben, Spectral Performance of a Composite Single-Crystal Filtered Thermal Neutron Beam for BNCT Research at the University of Missouri, 2009), (Brockman, Nigg, Hawthorne, Lee, & McKibben, Characterization of a Boron Neutron Capture Therapy Beam Line at the University of Missouri Research Reactor, 2009), (Brockman, Nigg, & Hawthorne, Computational Characterization and Experimental Validation of the Thermal Neutron Source for Neutron Capture Therapy Research at the University of Missouri, 2013). The irradiation set-up consisted of a layered system to gently compress the polymer interlayer material between a boron nitride plate and an aluminum plate, as seen in Figure 34 and Figure 35. The aluminum neutron capture cross-section is low, making the aluminum plate nearly transparent to the neutrons as they pass through towards the boron rich plate. Minimal thermal neutron capture is expected within the polymer material as the neutrons continue toward the boron rich plate. Once the neutrons bombard the boron nitride plate,

the high cross-section 10boron will interact with the neutrons and emit energetic particles into the surface layer of the polymer interlayer. This can be seen in Figure 36. As naturally occurring boron contains approximately 20% of the isotope 10boron, the neutron capture should produce significant quantities of energetic particles required to develop cross-linking. The neutron bombardment technique allows for this deep treatment of material as the neutrons have little interaction with the aluminum.

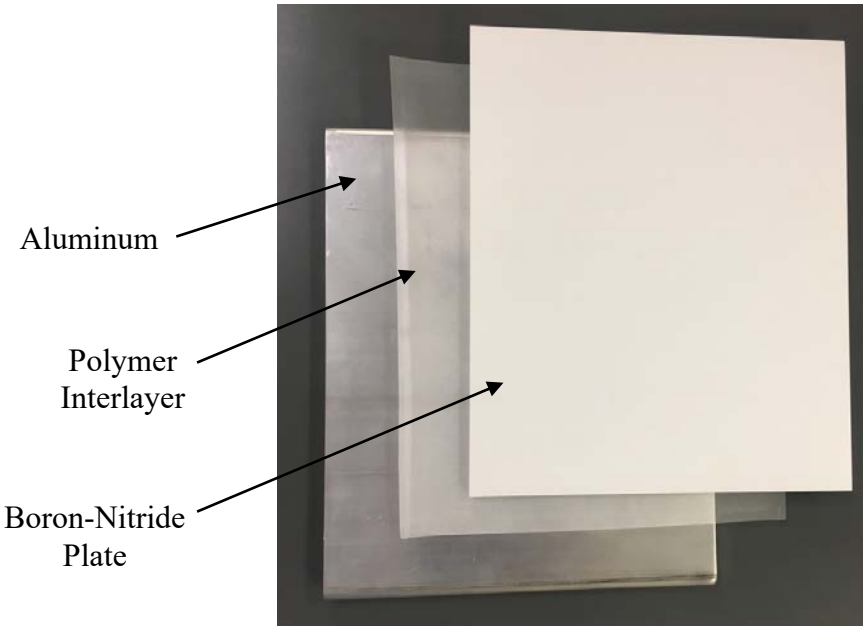

Figure 34: Three layers of experimental setup, aluminum bottom, polymer interlayer center, boron nitride sheet top.

Figure 35: Three layers of experimental setup in cross-section.

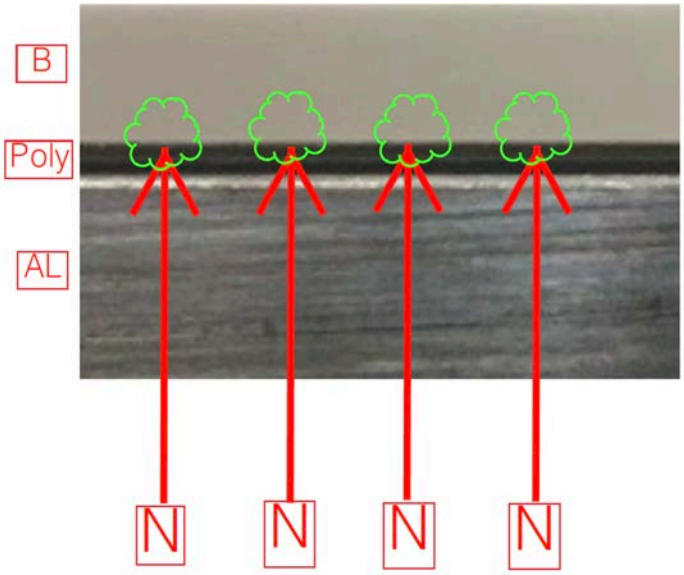

Figure 36: Diagram showing the neutrons passing through the aluminum plate, through the polymer interlayer, and interacting with the boron nitride plate.

Polymeric sheet material EVA with a thickness of 0.381 mm and PVB with a thickness of 0.762 mm were selected for initial treatment. As outlined in (Rej, Pickrell, & Wrobleski, Neutron-Capture-Induced Radiation Treatment of Polymeric Materials, 1996) the boron treatment has a range of approximately 10 microns. This range, although limited, still has application on the thin interlayer material through surface treatment techniques, allowing treatment of nearly 3% of the 0.381 mm thick EVA.

To verify that the changes in material behavior of the polymer interlayer are due to the boron surface treatment mechanism, samples of EVA and PVB were also irradiated without the boron nitride. The reason for pursuing this test was to rule out effects aside from the expected boron-neutron-capture. The absence of boron allows for observation of any effects that could be caused by gamma radiation, beta radiation, or any other unknown factor during the treatment. Aluminum plates were used on each surface and

irradiated in the same manner as the boron treated material. These samples were then tested with a quasi-static tensile test for comparison with the unirradiated control.

EVA and PVB were then irradiated with the boron nitride ceramic plate. The aluminum plate was used on the surface facing the beam. These irradiated samples were then tested with a quasi-static tensile test, high strain rate tensile test, nano-indentation test, and scratch test for comparison to the control.

Optimal neutron dose amounts were further investigated by the surface treatment method effect on EVA interlayer material. Neutron flux was 8.4×10^8 N/cm^2/sec and samples were irradiated for 0 hours, 10 hours, 20 hours, 40 hours, and 100 hours. It was hoped that the results would show an optimal change in behavior. Material was evaluated with a quasi-static tensile test.

6.2. Analysis

Both interlayer materials, EVA and PVB, were irradiated initially for a 100-hour period; however, other durations of exposure were also evaluated. Material characterization was conducted to determine changes in their properties following the treatment. A test matrix that outlines the various treatment methods and the evaluation method can be reviewed in Table 20. Test specimen are labeled to indicate the material, the specimen number in the series, the subset number in the series, radiation use, number of hours radiated, and boron use.

Table 20: Test Matrix of Specimen.

TEST MATRIX				
Material	Specimen	Subset	Treatment	Evaluation
XXX -	XXX -	XXX	Radiation Type, Duration or Virgin	Test Type
PVB -	001 -	001	Radiated at Low Flux, 100 hour, Boron Plate (R100B)	Static Tensile
PVB -	001 -	002	Radiated at Low Flux, 100 hour, Boron Plate (R100B)	Static Tensile
PVB -	001 -	003	Radiated at Low Flux, 100 hour, Boron Plate (R100B)	Static Tensile
PVB -	007 -	001	Radiated at Low Flux, 100 hour, Boron Plate (R100B)	Dynamic Tensile
PVB -	007 -	002	Radiated at Low Flux, 100 hour, Boron Plate (R100B)	Dynamic Tensile
PVB -	007 -	003	Radiated at Low Flux, 100 hour, Boron Plate (R100B)	Dynamic Tensile
EVA -	001 -	001	Radiated at Low Flux, 100 hour, Boron Plate (R100B)	Static Tensile
EVA -	001 -	002	Radiated at Low Flux, 100 hour, Boron Plate (R100B)	Static Tensile
EVA -	001 -	003	Radiated at Low Flux, 100 hour, Boron Plate (R100B)	Static Tensile
EVA -	001 -	004	Radiated at Low Flux, 100 hour, Boron Plate (R100B)	Indentation
EVA -	005 -	001	No Radiation, Virgin Material (N000N)	Indentation
EVA -	007 -	001	Radiated at Low Flux, 100 hour, Boron Plate (R100B)	Dynamic Tensile
EVA -	007 -	002	Radiated at Low Flux, 100 hour, Boron Plate (R100B)	Dynamic Tensile
EVA -	007 -	003	Radiated at Low Flux, 100 hour, Boron Plate (R100B)	Dynamic Tensile
EVA -	008 -	001	Radiated at Low Flux, 100 hour, No Boron (R100N)	Static Tensile
EVA -	008 -	002	Radiated at Low Flux, 100 hour, No Boron (R100N)	Static Tensile
EVA -	008 -	003	Radiated at Low Flux, 100 hour, No Boron (R100N)	Static Tensile
EVA -	010-	001	Radiated at Low Flux, 10 hour, Boron Plate (R010B)	Static Tensile
EVA -	010-	002	Radiated at Low Flux, 10 hour, Boron Plate (R010B)	Static Tensile
EVA -	010-	003	Radiated at Low Flux, 10 hour, Boron Plate (R010B)	Static Tensile
EVA -	012-	001	Radiated at Low Flux, 40 hour, Boron Plate (R040B)	Static Tensile
EVA -	012-	002	Radiated at Low Flux, 40 hour, Boron Plate (R040B)	Static Tensile
EVA -	012-	003	Radiated at Low Flux, 40 hour, Boron Plate (R040B)	Static Tensile
EVA -	014 -	001	Radiated at Low Flux, 100 hour, Boron Plate (R100B)	Scratch

6.3. Results

The tested sheets of interlayer were subsequently processed into individual test coupons. These coupons were then evaluated under various testing methods as outlined in the test matrix shown in Table 20. Results of individual test methods are discussed in the following sections.

6.3.1. Quasi-Static Tensile Testing

The interlayer testing was performed using a quasi-static tensile test. The quasi-static tensile test is a method of testing materials in tension under low strain rates. Quasi-static

tensile testing is generally performed at strain rates between 10^{-5} to 10^{-1} s^{-1} utilizing servo-hydraulic testing machines. Inertial and stress wave propagation effects are neglected in quasi-static testing because of the extremely low and constant rate of loading (Knight, 2020). In this research, quasi-static tensile testing of interlayer polymers was performed according to ASTM D638-10 Standard Test Method for Tensile Properties of Plastics (ASTM D638-10, 2010) utilizing a servo-hydraulic testing machine. Note that Shore-D hardness evaluation was not possible for this thin specimen, but hardness evaluation was pursued and is described in the following sections.

Review of the radiated specimens in comparison with the virgin samples shows an increase in the stress capacity under a given strain. Strain is the change in length of a sample relative to its initial length, hence strain is dimensionless, or often given as m/m. Stress has units of force over area or Pascals. The area under these curves is called Toughness and indicates how much energy per volume the polymer can absorb and is given as $MJ \times m^{-3}$.

EVA material was irradiated without boron to evaluate the effects of radiation alone on the specimen. The results from static testing can be seen in Figure 37. Static testing was performed on three samples cut from the irradiated specimen EVA-008, and then compared to a control tested on virgin EVA material.

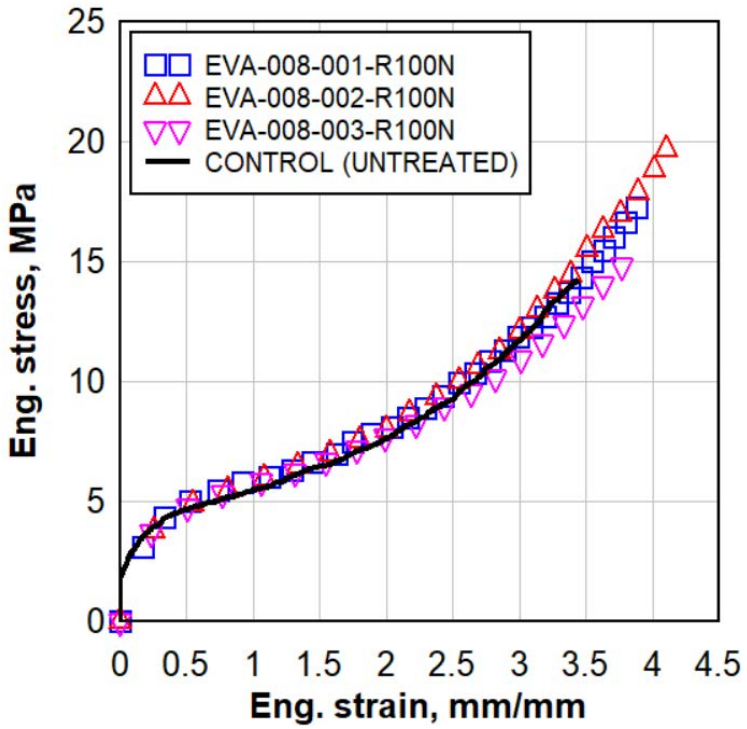

Figure 37: Static Testing of EVA-008-001,2,3-R100N specimen with aluminum-EVA-aluminum configuration, in comparison to virgin EVA material.

The results in Figure 37 show that the radiated sample without boron behaves very similar to the control EVA sample. This is a clear indication that any outside radiation effects have had very little impact on the material properties of the specimen.

EVA and PVB samples were irradiated with boron to evaluate the effects of the surface treatment technique on the specimen. In this treatment the boron plate was included, as described in Section 6.1.

Static tensile test results are shown in Figure 38 and Figure 39. These results show a comparison between virgin material that was not exposed to radiation and a series of samples tested following the previously described surface treatment technique. There were clear increases in the stress capacities at lower strains, indicating a stiffer material.

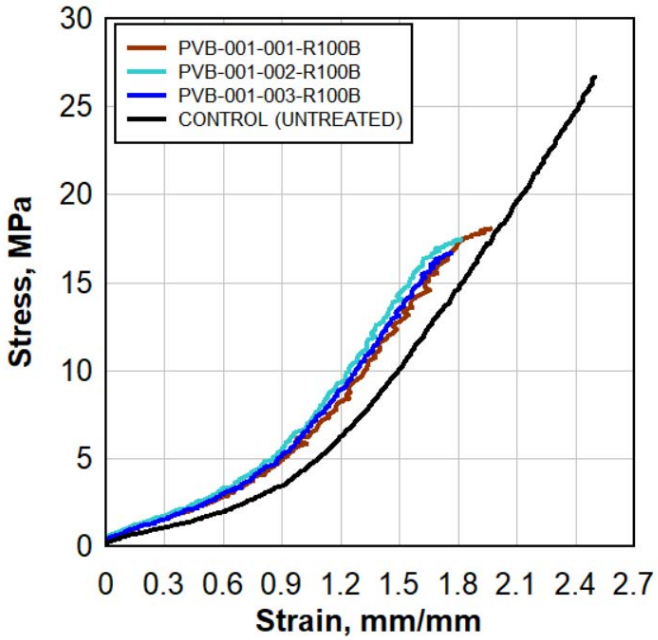

Figure 38: Static tensile test results for PVB-001-001,2,3 and comparison to virgin material.

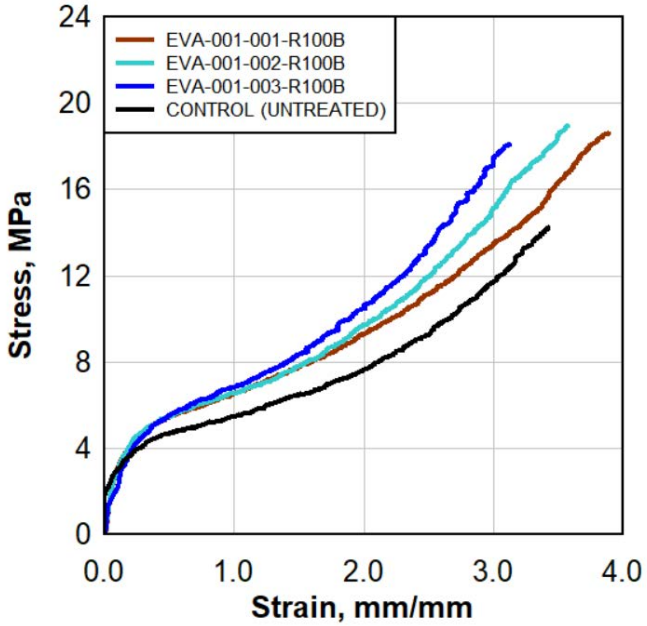

Figure 39: Static tensile test results for EVA-001-001,2,3 and comparison to virgin material.

Increases in the stress capacity contribute to overall increases in Toughness. Toughness is indicative of the amount of energy absorbed during the tensile test, and is quantified by the area under the stress-strain curve, given as $MJ*m^{-3}$.

The average of three samples cut from irradiated specimen EVA-012 are plotted with a comparison to the average virgin EVA material samples in Figure 40. These specimens were irradiated for 40 hours with the boron-nitride ceramic plate backing.

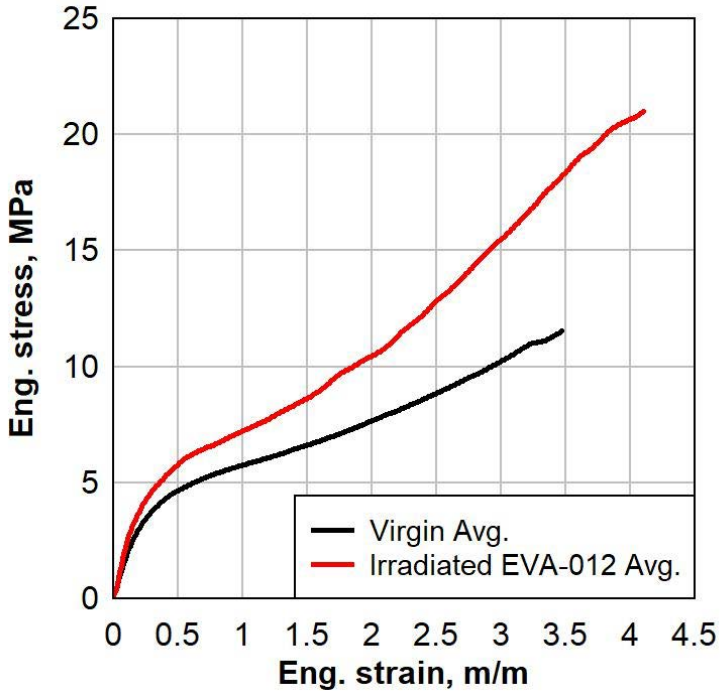

Figure 40: Plot of Stress vs. Strain for 40-hour irradiated Specimen EVA-012 and its comparison with the average virgin samples. This specimen included the boron surface treatment.

As seen in Figure 40, the stress capacity per given strain has increased in the irradiated material. The maximum strain before rupture has increased in the irradiated material as well. Overall Toughness subsequently increases due to the combined increases. A comparison between the virgin material and the irradiated material can be seen in Table 21.

Table 21:

Maximum Stress, Strain, and Toughness for Virgin EVA material in comparison to 40-hour irradiated EVA-012 material.

	Virgin	EVA-012	% Increase
Max Stress (MPa)	11.5	21.0	82.1%
Max Strain (m/m)	3.5	4.1	18.2%
Toughness ($MJ*m^{-3}$)	25.8	47.2	89.9%

6.3.2. High-Strain Rate Tensile Testing

High-strain rate (dynamic) tensile test results are shown in Figure 41, Figure 42, Figure 43, and Figure 44. These results also show a comparison between virgin material that was not exposed to radiation and a series of samples tested following the previously described surface treatment technique. Although the PVB samples did not show significant material stiffening, the EVA continued to show signs of stiffening and an implication of cross-linking occurrence from the treatment. As EVA continuously showed more pronounced results, subsequent treatments focused primarily on EVA. As seen in Figure 44, the treated specimen absorbed much greater amounts of stress in the first 3 mm/mm of strain.

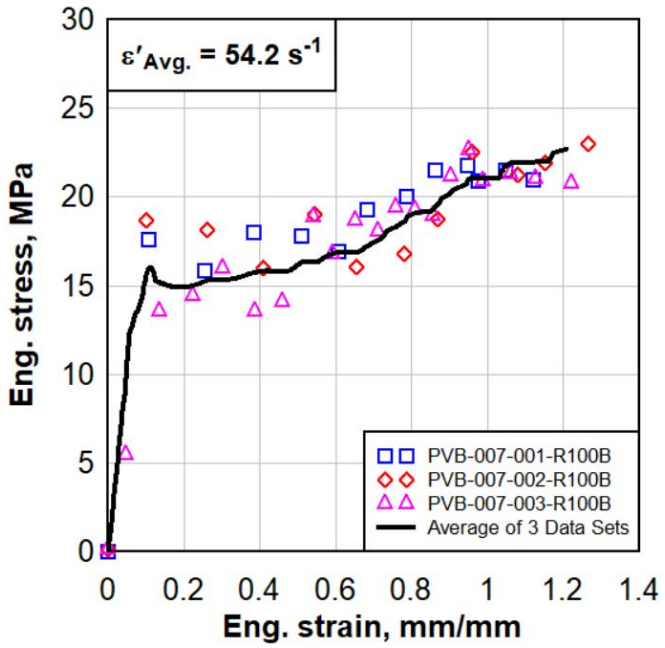

Figure 41: Dynamic results from three samples of radiated PVB-007-001,2,3.

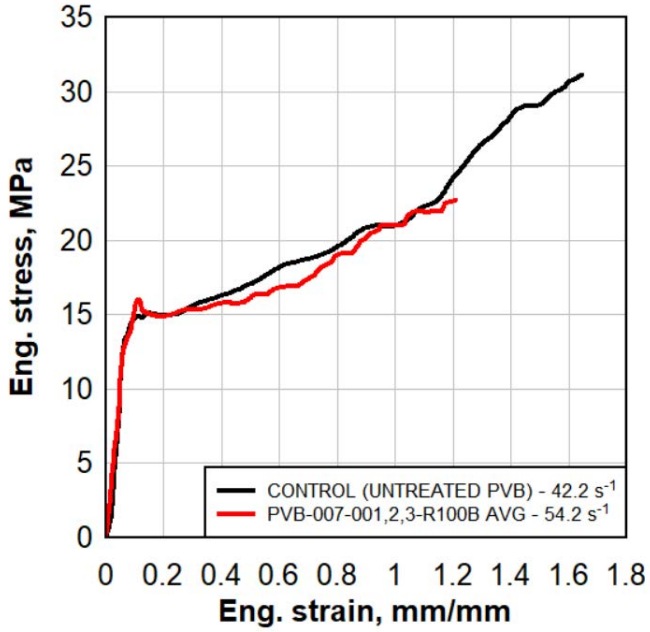

Figure 42: Dynamic results of radiated PVB-007-001,2,3 in comparison to virgin PVB.

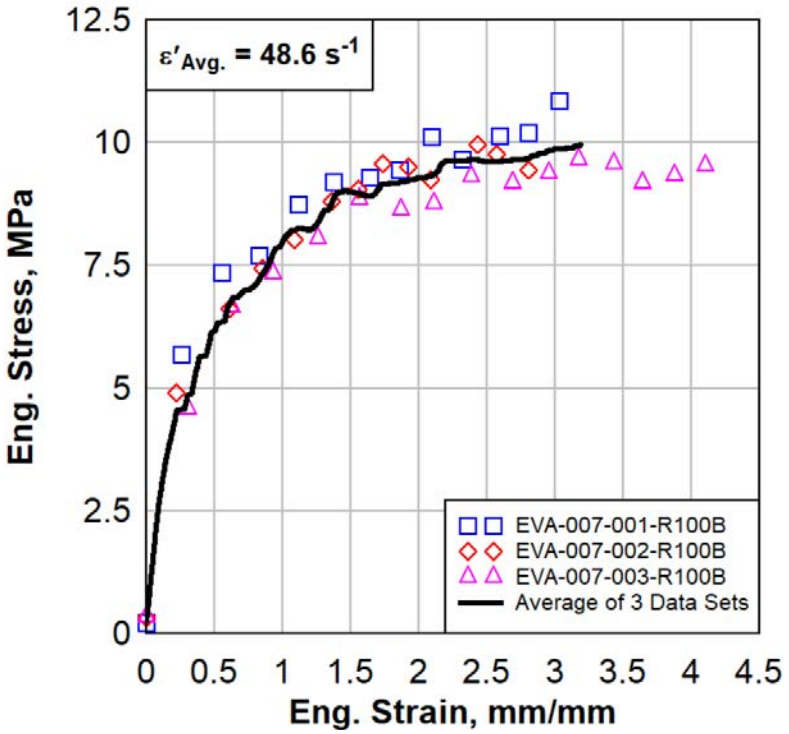

Figure 43: Dynamic results from three samples of radiated EVA-007-001,2,3.

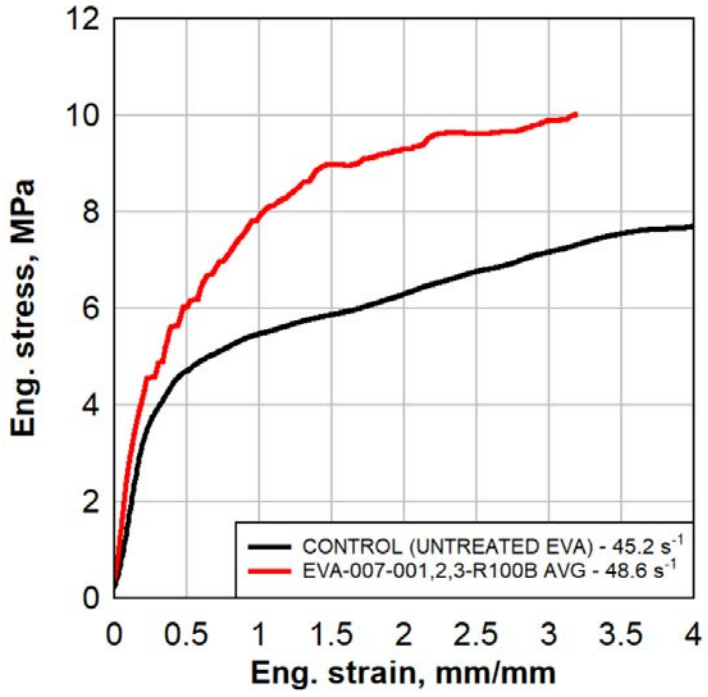

Figure 44: Dynamic results of radiated EVA-007-001,2,3 in comparison to virgin EVA.

6.3.3. Nano-indentation

Indenter testing was performed by Anton Paar. Results can be seen in Figure 45 and Figure 46. A test matrix that indicates specimen for indentation and scratch testing can be seen in Table 20, as previously noted. Furthermore, as noted in Section 6.1, the range of this treatment technique is theoretically limited to 10 microns. This range should be observable in the material behavior for the treated face.

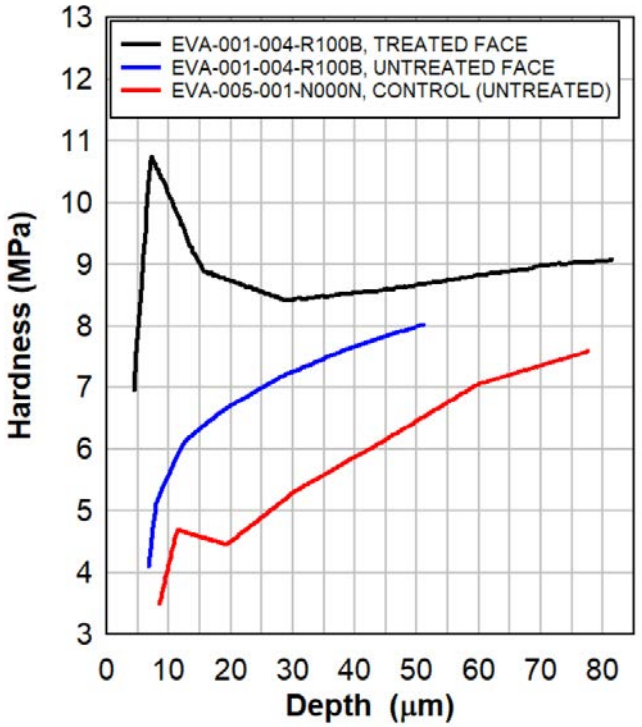

Figure 45: Hardness vs. Penetration Depth.

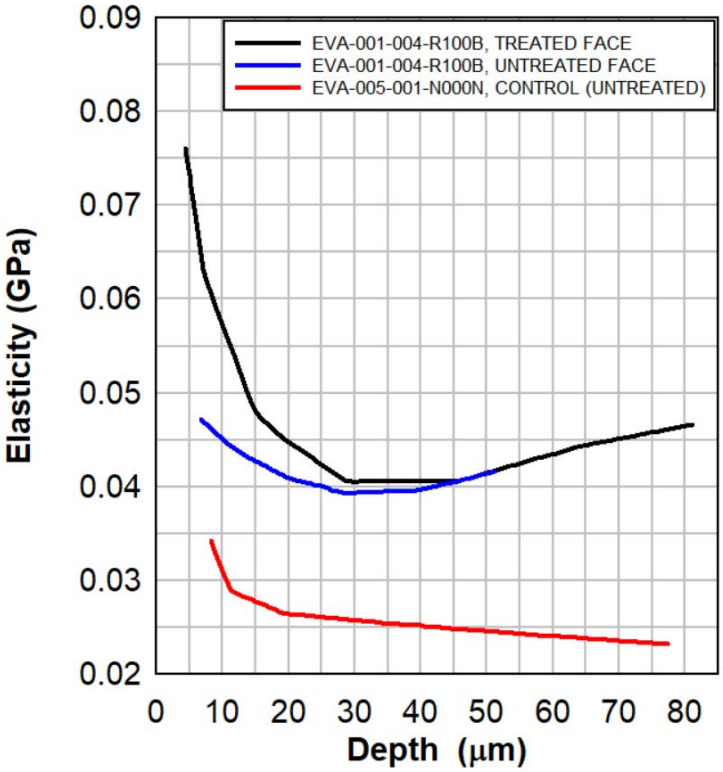

Figure 46: Elasticity vs. Penetration Depth.

As seen in the preceding figures, the theoretical range of treatment coincides with the observed increase in material performance shown through indentation testing. The hardness evaluation in the first 10 microns of the treated face in Figure 45 are roughly double the untreated face, and then trend toward parity as the testing proceeds deeper into the material cross section.

Similar results are seen in the elasticity evaluation shown in Figure 46, as the elasticity of the treated face is much higher, then trending towards parity with the untreated face as it reaches deeper into the material cross section.

Both of these evaluations exhibit very strong evidence that the theorized cross-linking mechanism through boron-neutron-capture is indeed producing the effects within the polymer material that is expected.

6.3.4. Scratch Testing

Scratch Testing was performed by Anton Paar on the treated and untreated faces of EVA specimens. This method of testing characterizes surface hardness in a manner that determines a materials resistance to scratch. The testing is conducted by dragging an indentor across the surface of the material at a set speed, applied load, and indentor size.

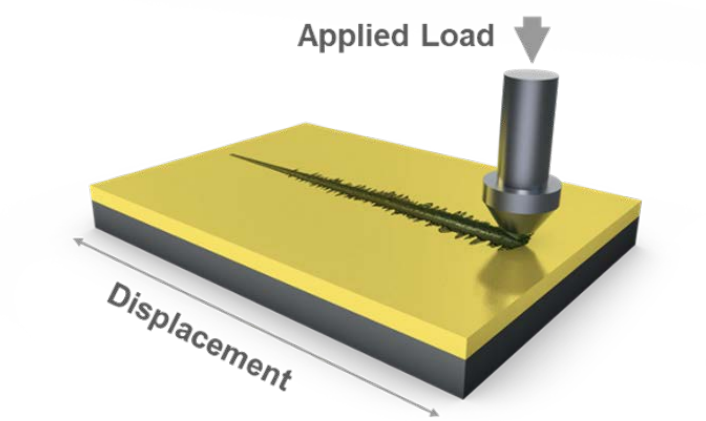

Figure 47: Figure showing method of scratch testing provided by Anton Paar.

Figure 48 shows the penetration depth as a function of scratch distance at a rate of 4 mm/min for three different scratch tests on sample EVA-014-001-R100B. The results shown in Figure 49 are for the treated face of the EVA specimen only. A close-up over the penetration depth of 10 µm is also shown in Figure 48. The applied force was increasing at a constant rate from 0.03 N to 0.50 N over a total distance of 2 mm. The penetration depth as a function of force is shown in Figure 49.

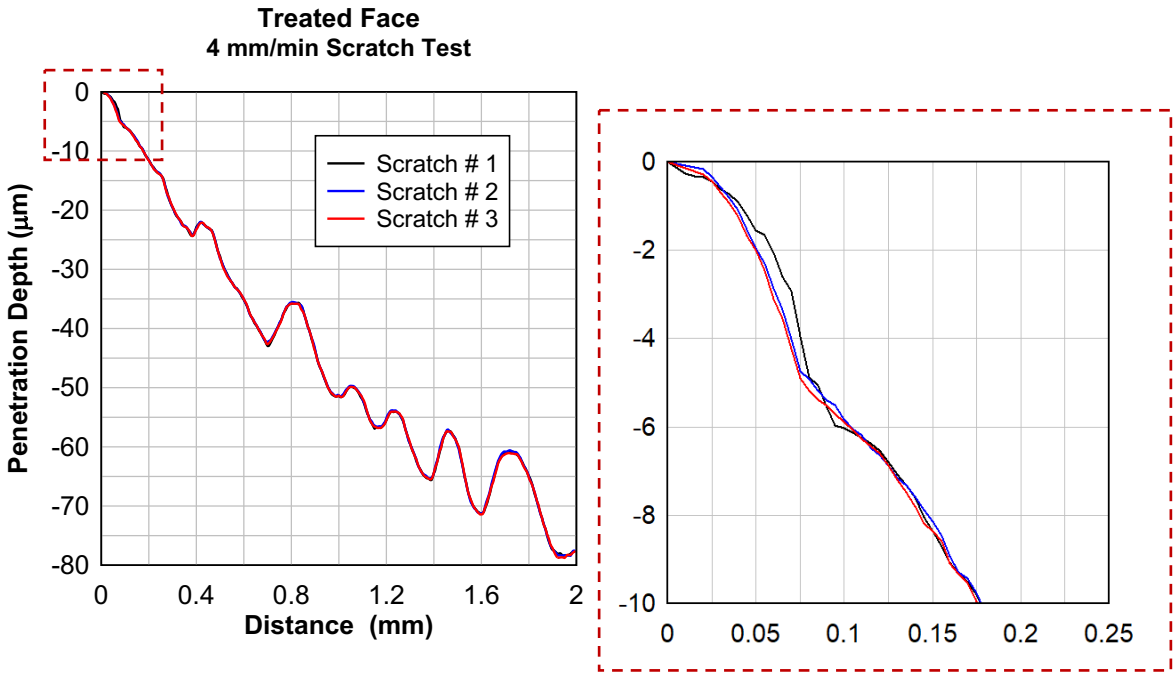

Figure 48: Scratch testing on EVA-014-001-R100B, showing penetration depth as a function of distance with a scratch rate of 4mm/min.

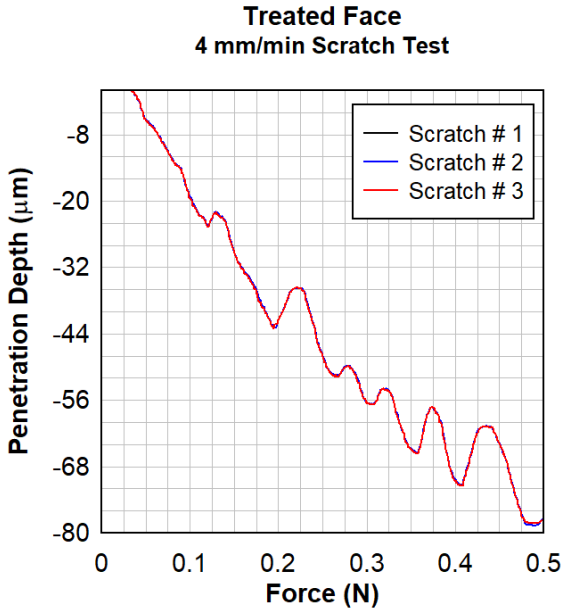

Figure 49: Scratch testing on EVA-014-001-R100B, showing penetration depth as a function of force applied with a scratch rate of 4mm/min.

The effect of the radiation treatment is shown in Figure 50, where the treated face produced a larger penetration resistance than the untreated face. Over the 10 µm depth of

the treated face, the resistance was on average 30% larger than the untreated face. This was observed at a higher rate of scratch testing of 85 mm/min. However, at slow rate of scratch testing of 20 mm/min, the difference in the force resistance was not as noticeable (Figure 51).

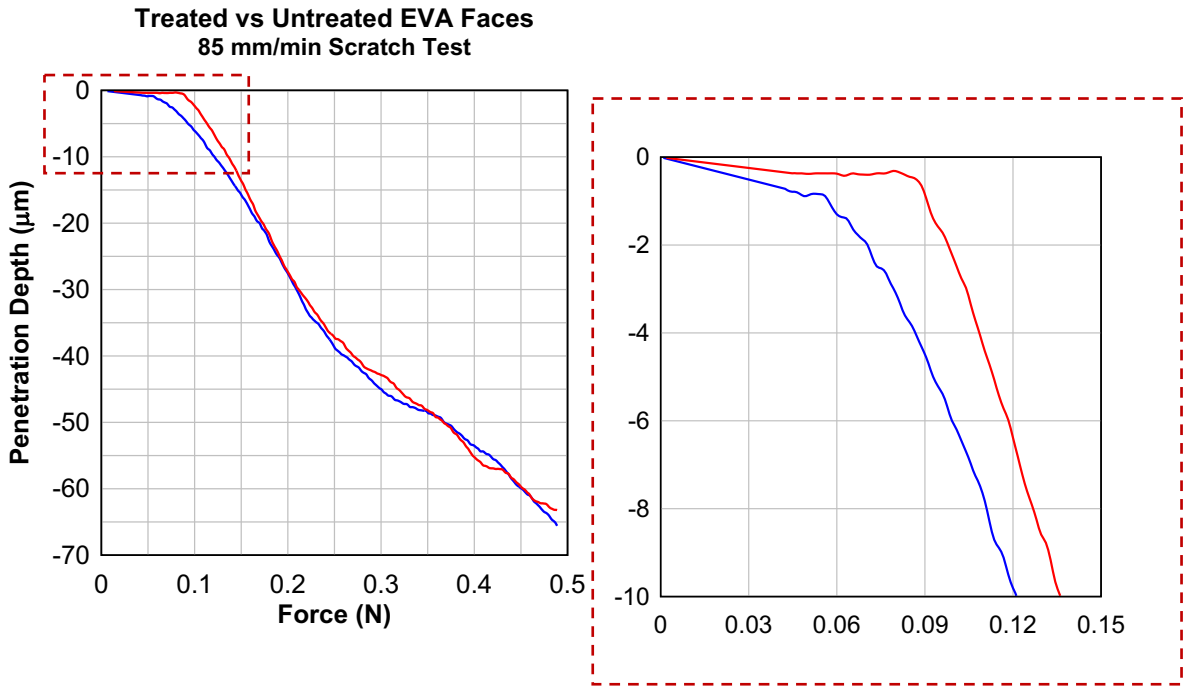

Figure 50: Scratch testing on EVA-014-001-R100B, showing penetration depth as a function of distance at a scratch rate of 85 mm/min. Red is the treated face, blue is the untreated face.

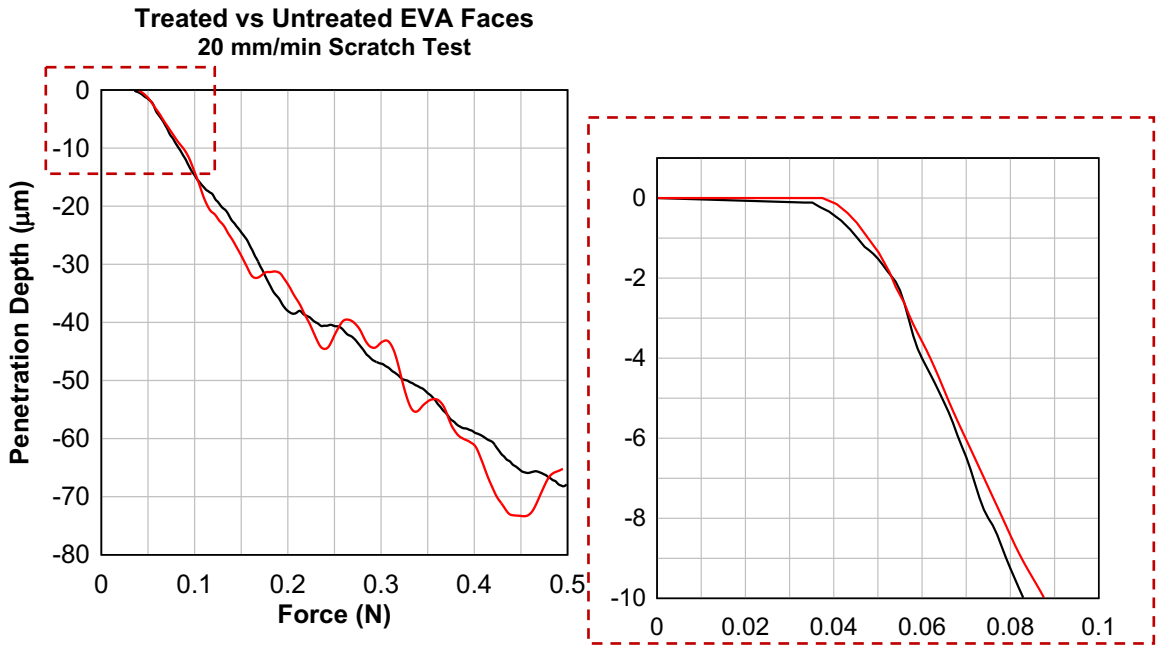

Figure 51: Scratch testing on EVA-014-001-R100B, showing penetration depth as a function of force applied at a scratch rate of 20 mm/min. Red is the treated face, black is the untreated face.

Overall, the scratch testing provided supporting material characterization data indicating that the treated surface of the EVA material was improved to provide a higher resistance to scratch. This is further indicative of a cross-linking mechanism taking place from the surface treatment process.

6.3.5. Differential Scanning Calorimeter Testing

Samples of material were shared with Battelle for testing using a Differential Scanning Calorimeter (DSC), as shown in Table 22. Results are shown in Figure 52, Figure 53, Figure 54, Figure 55, and Figure 56. Results from EVGuard and Saflex were not returned.

DSC testing is a way of determining the glass transition temperature of a material. This transition is found following heating of the material, and shows where the material

transitions from a hard glass-like material into a softer more viscous material. Changes in the glass transition temperature could show additional material behavior changes due to treatment.

Table 22: Material list for DSC Testing.

#	Polymer Type
1	EVGuard 030
2	Saflex PVB RA41 030
3	Old PVB
4	Virgin PVB 005 030
5	Radiated PVB 001 030
6	Virgin EVA 005 015
7	Radiated EVA 001 015

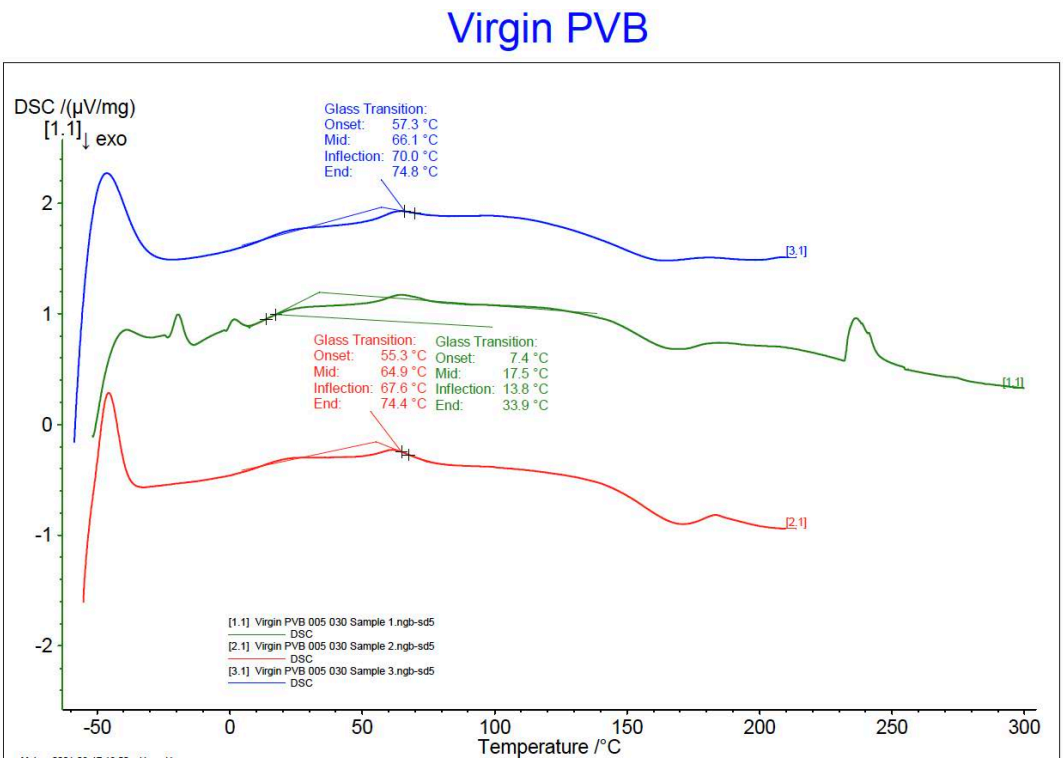

Figure 52: DSC Testing for Virgin PVB-005-030.

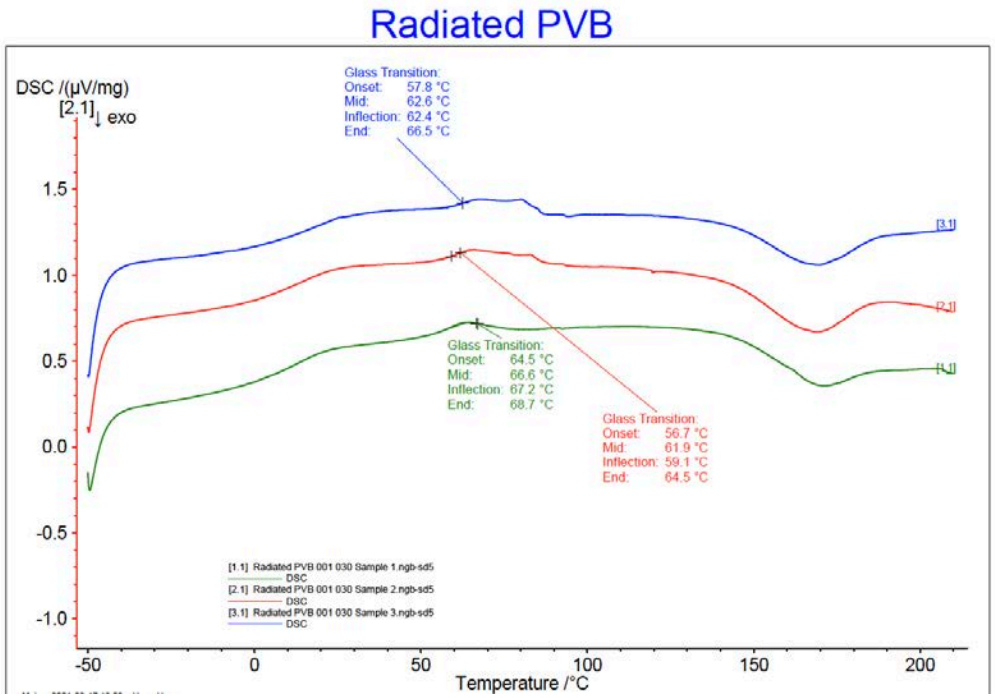

Figure 53: DSC Testing for Radiated PVB-001-030.

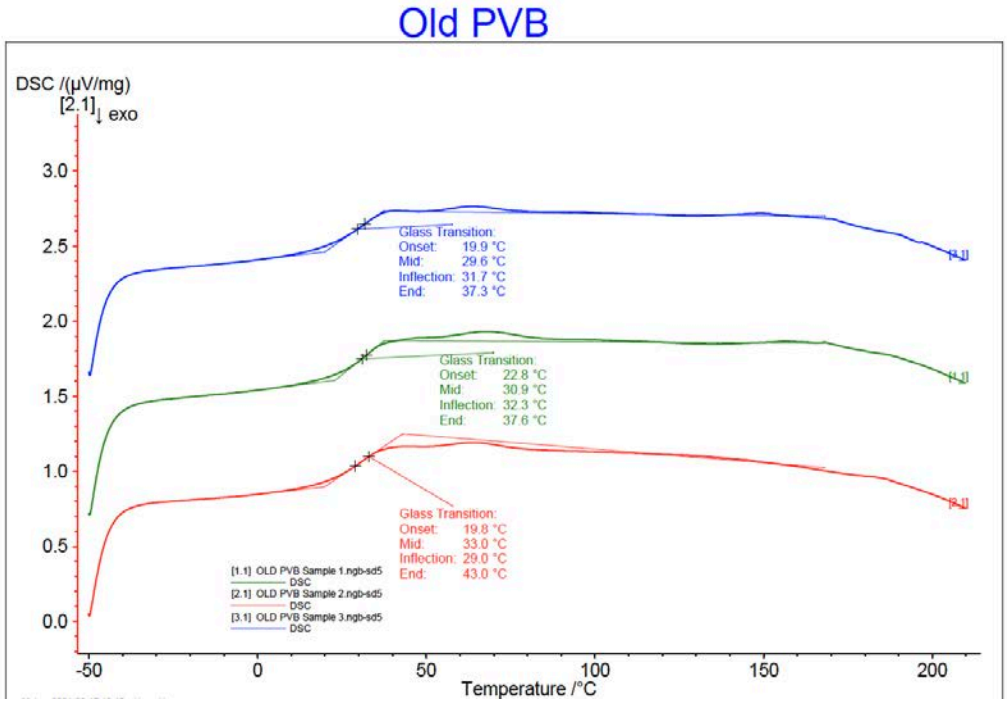

Figure 54: DSC Testing for Old PVB.

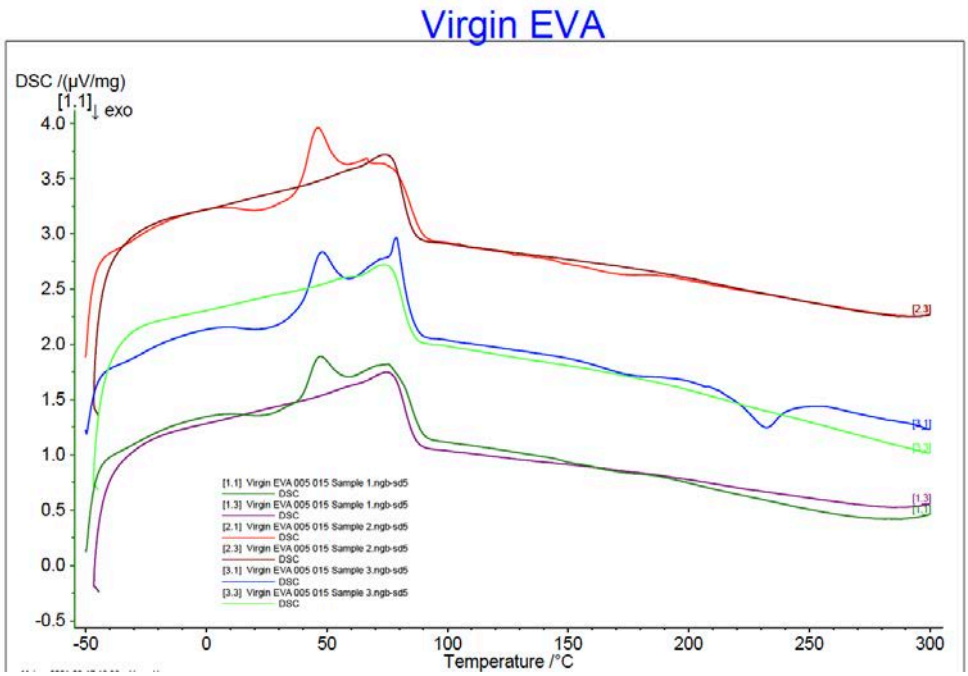

Figure 55: DSC Testing for Virgin EVA-005-015.

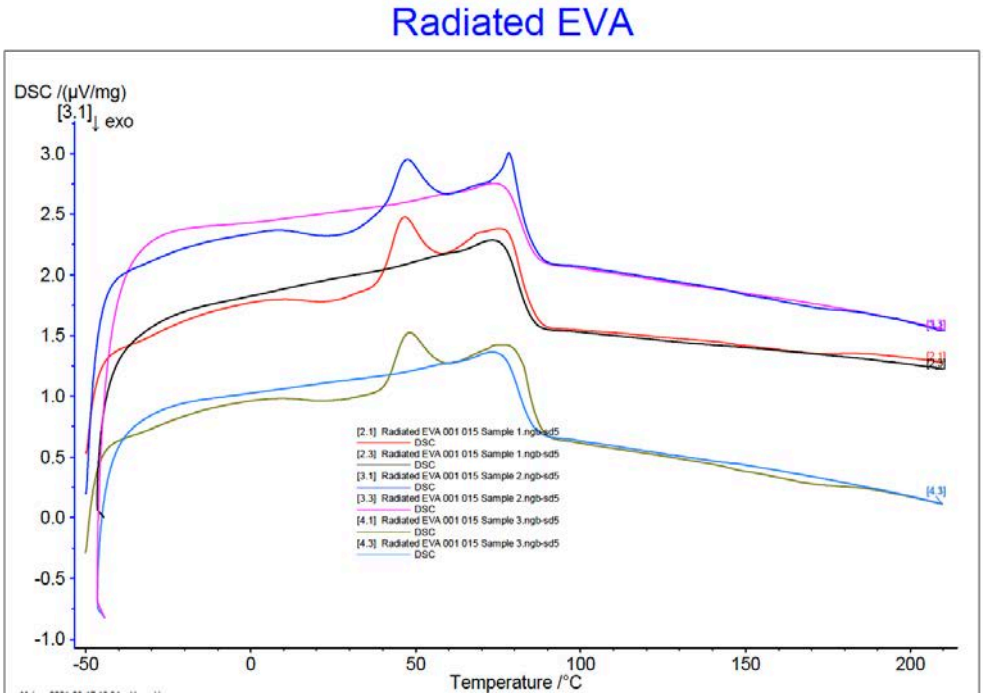

Figure 56: DSC Testing for radiated EVA-001-015.

Transition temperatures for radiated PVB tended to trend upward following radiation treatment. Other materials texted were less clear on the results. The results

provided were not shared with full data and have limits on the amount of usable data that can be obtained from them.

7. Optimal Neutron Dose for EVA Interlayer Polymer

Following multiple successful treatments, it became a matter of testing efficiency to do evaluations on optimal neutron dosage. These evaluations could reduce irradiation timeframes and produce final products that exhibit maximum material behavior changes. Samples were irradiated at at low neutron flux for a varying amount of time, and were then tested with the static tensile testing process for comparison. Results were expected to show either an increasing trend of tensile capacity, or an increase followed by a decrease or leveling off in tensile capacity increases. Test specimen can be seen in Figure 57.

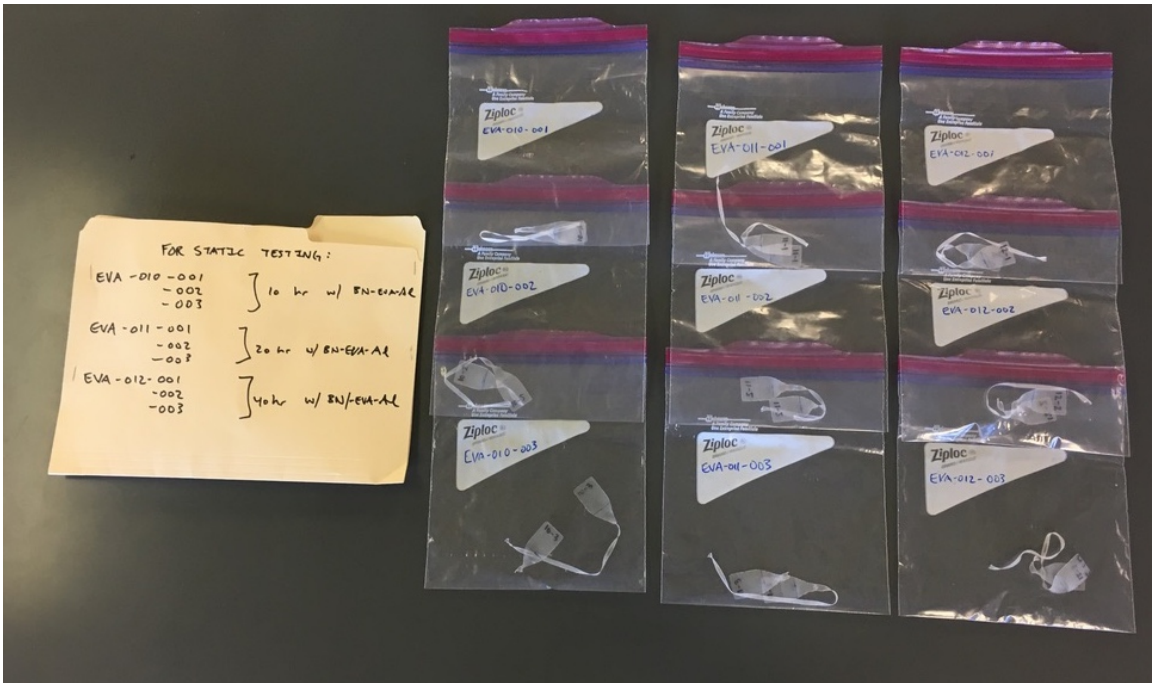

Figure 57: Static tensile tested specimens for dose effects on interlayer materials.

7.1. Experimental Setup

Samples that were irradiated at the same 8.4x108 N/cm2/sec neutron flux for varying time durations were tested with the static tensile testing process for comparison. This evaluation will provide insight to the effects of progressively larger doses of neutron radiation. Samples included irradiation durations of 0-, 10-, 40-, and 100-hours for comparison.

7.2. Analysis

Three individual test coupons were made for tensile evaluation regarding each irradiation, and the average of the three tensile tests are provided. These samples were tested with the quasi-static tensile test, and were compared to the untreated control sample, as well as being compared to each other.

7.3. Results

Results from the study can be seen in Figure 58. The sample legend indicates the total duration of irradiation for treated samples as 10, 40, and 100 hours.

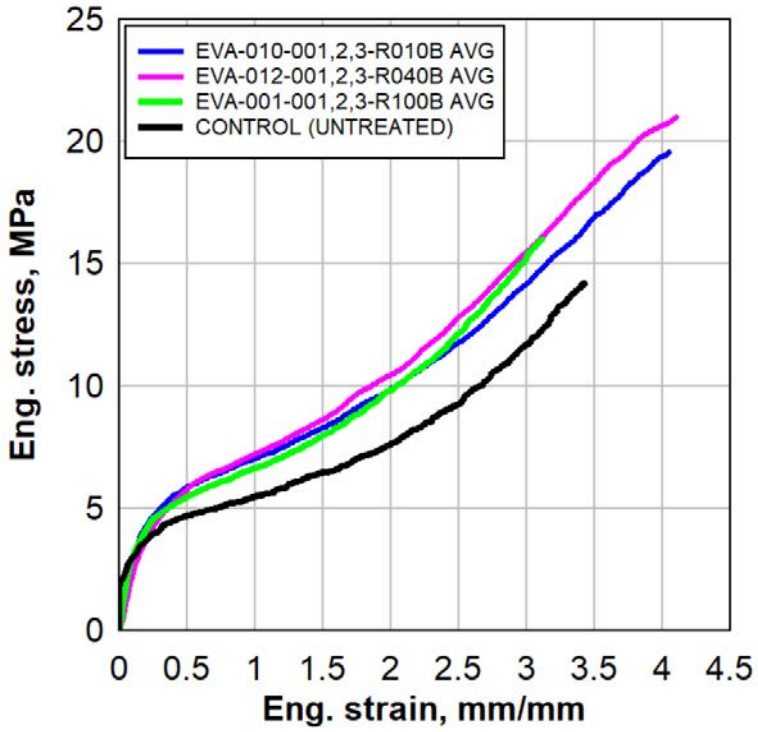

Figure 58: Dose effects of EVA with surface treatment.

As seen in Figure 58, all radiated specimen exhibited higher stiffness compared to the control specimen. There was significant stiffness behavior change at even the lowest 10-hour irradiation, specimen EVA-010. The 40-hour irradiation, specimen EVA-012, showed slightly higher stiffness than the 10-hour irradiation. As the duration reached the 100-hour length, it appears there may even be some degradation. This may be indicative of damage due to overtreatment. It could be that the most effective treatment dose may be closer to the 40-hour duration, and that there is still a high level of efficiency at only the 10-hour dose.

With this information, future testing could take place at the lower range of total neutron dosage in order to save time and be more efficient overall. It had not been

previously understood that longer durations could in fact cause degradation, but the evidence from this testing indicates that longer durations may pose a negative result.

8. Conclusions and Recommendations

The initial research effort has taken a theoretical process and applied it through commercially available polymers, custom polymers, and then through a surface treatment technique. There have been successful results that show material behaviour changes indicative of the cross-linking methods theorized, and further described below. Applications and recommendations for further research are also provided in order to develop a path forward for the technique development, and application to laminated glass window systems.

8.1. Conclusions

In this research, it has been shown that the use of the boron neutron capture reaction can improve the material characteristics of a polymer. Specifically, a surface treatment of the polymer EVA was described, where the boron is exterior to the polymer and the energetic alpha and recoiling lithium ion are allowed to interact primarily with the first 10 microns of the material. This interaction increases the material's Toughness, or in other words, its ability to absorb energy per volume. This characteristic is of particular value in application to laminated glass systems designed to protect from blast or impact, with spalling glass resulting.

Polymer treatment through the boron-neutron-capture radiation treatment has produced polymer interlayers with potential increased resilience towards blast threats. The research to date has evaluated treated polymers in accordance with theoretical research and shown that hardening and increased elasticity of the material can be initiated through treatment, thus indicating cross-linking behavior (James E. Mark, 2005).

Furthermore, applications according to theoretical work has shown that lower neutron flux rates are required, in contrast with the theoretical work. The early work evaluated bulk borated polymer treatment at lower neutron flux rates and lower exposure durations than theorized work, yet showed that the flux rates and exposure time were considerably higher than the material properties could withstand. Alternative approaches were found to produce more desirable material property changes.

The research has developed methods beyond radiation of boron doped polymers, through surface treatment, and applied them to polymer interlayers typically used in window systems. These results showed distinct changes in the material behavior, particularly with the EVA interlayer material, utilizing multiple material characterization methods to fully understand and verify the behavior change. The harder surface may assist in the cutting of the interlayer surface by glass shards, overall Toughness of the polymer material is increased allowing for higher energy absorption, and overall improvement of window performance in blast conditions is expected. The treatment technique can further be applied to window interlayer products to determine optimal material characteristics for blast conditions.

Polymer treatment through the boron-neutron-capture radiation treatment has produced polymer interlayers with increased resilience towards blast threats. The research to date has evaluated commercially available polymers in accordance with theoretical research, and shown that hardening of the material can be initiated, indicating cross-linking behaviour. The research developed additional methods through surface treatment, and applied them to polymer interlayers typically used in window systems. These results showed improved material behavior particularly with EVA interlayer

material, and additional in-depth material characterization was performed to fully understand the behavior changes. The technique can further be applied to window systems to determine optimal material characteristics for blast conditions.

8.2. Recommendations and Applications

There are several areas of study that could be further pursued in the near term. These include additional work into blast and ballistic protection, electrical conductivy changes in the material, numerical modeling of hardening applications on interlayer material, patterned hardening studies, material treatment with borated glass, and advanced manufacturing techniques for the material treatment.

8.2.1. Blast and Ballistic Protection

Application of interlayer material for blast and ballistic protection has been closely outlined in early sections of this work. However, it should be noted that in field testing of laminated glass window systems that have been treated according to methods outlined in this research effort, have not yet taken place. Following proven manufacturing techniques and thorough numerical modeling; small scale and full scale testing could proceed to confirm the benefits of the interlayer treatment.

8.2.2. Electrical and Radio Frequency Effects

Samples were tested for changes in electrical conductivity. This evaluation utilized a multimeter to test for conductivity at varying widths. Preliminary results from electrical conductivity did not show any change in conductivity. Future testing could utilize more sensitive instrumentation to determine any change.

Radio Frequency blocking could be further reviewed with the treated material to deterimine any level of shielding that the treatment may provide beyond the level of effect that untreated material already provides. This could be of benefit to secure facilities, and has not been seen reviewed in other studies.

8.2.3. Numerical Modeling

Initial numerical models of 150mm discs were developed with varying polymer layers, as seen in Figure 59. The finite element model was developed using ANSYS software. This model is for a polycarbonate disk with a layer of borated polymer. For initial modeling, assumptions were made for the stiffness and strength of the borated polymer. The objective of this model was to investigate the effect of the outer layer stiffening of the total stiffness of the disc. It was assumed, roughly, that the stiffness and strength of borated polymer are higher than that of the polycarbonate layer by about 10 to 50%. Under the quasi-static testing condition, it was found that a 0.1 mm borated polymer layer can decrease the maximum deflection of the plate by about 3%.

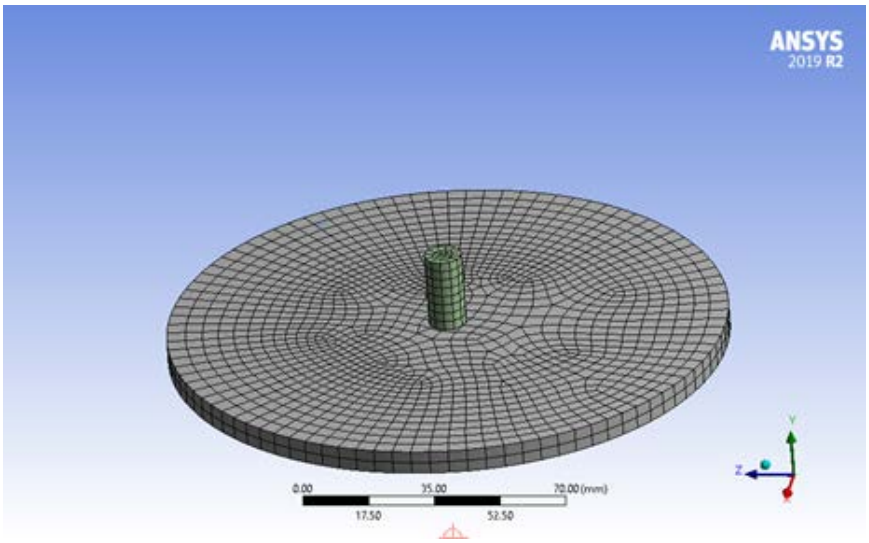

Figure 59: Modeled disc with penetrator.

8.2.4. Patterned Hardening

Another pursuit could be patterned hardening, whereas the interlayer material is treated such that it does not have uniform hardness, but rather would be treated with particular patterns. This patterning could theoretically alter shockwave propagation from ballistic impacts by disrupting the wave propagation. Numerical modeling of patterned hardening could help to validate its effectiveness and to determine optimal patterns. Further field testing could verify the models.

8.2.5. Applications using Pyrex Glass

Pyrex the brand name for a borosilicate glass with low thermal expansion. Commonly used in cookware, this product has many applications beyond including use in telecscopes. Pyrex has a composition that is approximately 4% naturally occurring boron, making the material a good candidate for use in surface treatment of polymer interlayer materials. Laminated glass window systems could be assembled with one glass surface made up of Pyrex sheet glass, and the window system could be treated according to processes described previously.

Approximate calculations show that total neutron flux can be adjusted in order to obtain similar treatment results as those found conducted in Section 6. As the boron nitride plate had been composed of roughly 40% boron and the Pyrex glass is composed of roughly 4% boron, then an increase of ten times the total flux should meet expectations.

8.2.6. Manufacturing

To treat bulk interlayer material, treatment could be facilitated by constructing an appropriate facility for neutron radiation treatment. The treatment facility could be used to irradiate long sheets of material that will be used for industrial purposes. The material can be pre-positioned on a spool outside the neutron treatment area, and then rolled through the neutron treatment area through an automated control process, and then pass to a final containment area for storage. A rough schematic of the processing facility can be seen in Figure 60.

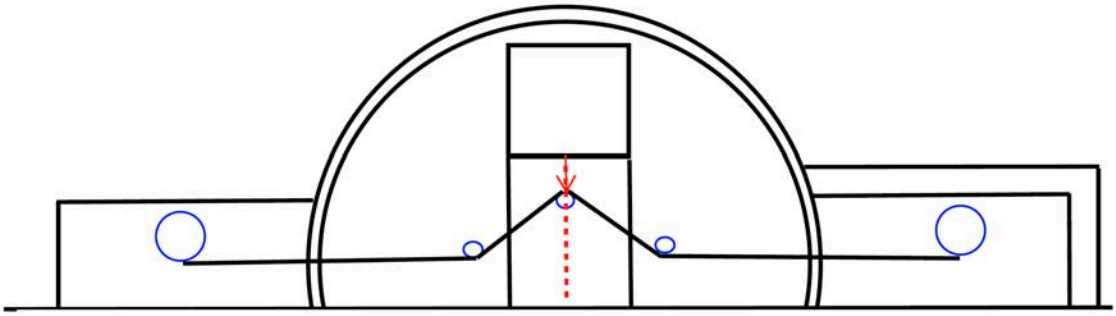

Figure 60: Facility cross section showing pre-positioning area on the left, neutron treatment area in the middle, and the storage area on the right.

The facility could utilize boron-nitride rollers that, once bombarded with neutrons, will emit an energetic alpha and lithium particle of approximately 2.5 - 4.0 MeV (United States of America Patent No. US5942156, 1999). These particles are to surface treat the sheeted material as it passes through the bombardment region.

The facility could also utilize a commercially available neutron source. These neutron sources rely on deuterium-deuterium reactions to produce a fusion reaction that

will emit neutrons. A diagram of the reaction can be seen in Figure 61, where the manufacturer displays their process (Phoenix, 2020).

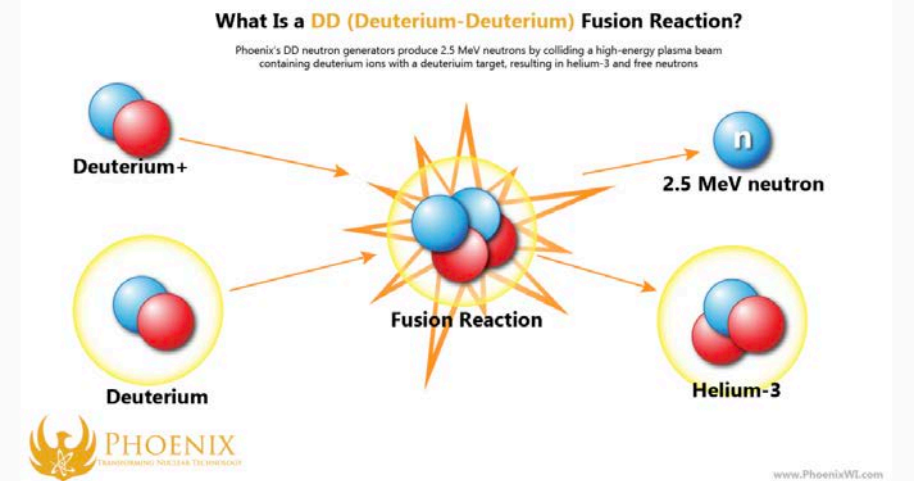

Figure 61: Deuterium-deuterium reaction for producing neutrons (Phoenix, 2020).

There are several safety hazards that must be resolved to ensure the facility can produce the treated material without causing harm to workers. The first item is the neutron source equipment. This equipment will contain isotopes of deuterium and tritium that can be harmful if ingested. The neutron beam produced by the equipment will need to be contained as this radiation is highly penetrating due to its uncharged state. The second item is the treated material. The material is not expected to be radioactive prior to treatment, so the pre-positioning area requires no radiation protection. Once the material passes through the processing point, there is potential for short term activity in the material. Activity could include low MeV Gamma emissions with less than 1 μCi Activity. This material is then stored in the post-processing area following treatment.

The neutron source contains deuterium and tritium. This equipment is expected to be self-contained, as purchased from the manufacturer, and all requirements are to be

set forth by the manufacturer. This will prevent any of the base material from being ingested. The neutron beam will be directed towards the ground, eliminating the majority of risks from neutrons passing outside the facility. Regardless of the beam direction, additional containment steps are to be taken in order to ensure that neutrons are contained within the facility. The facility's shape is spherical to minimize the surface area required to be shielded. The outer shell of this half-sphere is to be made from a borax infused concrete mixture. This provides both strength and contributes to shielding through a high-neutron capture cross-section material that surrounds the facility.

The pre-processing area is not expected to hold radioactive material, and therefore requires minimal shielding. The post-processing area is expected to hold material with low activity Alpha, Beta, and Gamma emissions. For this reason, this area will have lead-lined walls inside of a concrete wall.

Personnel will be required to have training regarding the proper handling of radioactive material. This will include proper use of Personal Protective Equipment (PPE), and a fundamentals of radiation effects review. Radiation dose monitoring systems will be required while in the facility. All personnel should closely follow the ALARA (As Low As Reasonably Acheivable) principles with respect to radiation exposure. Personnel will be required to use proper PPE when handling radioactive material. For this specific process, gloves will be the primary PPE for handling the treated material.

Radiation dose monitoring will include a dose metering badge, and a dose ring to be worn on the working hand. Monitoring badges will be evaluated monthly to determine any hazards that workers may have been exposed to. Staff must fleece themselves with a

GM (Geiger-Muller) counter before entering and leaving the facility. This check must be completed on their hands and feet. Following this action, a gamma radiation detector portal must be used at the point of exit to do a final evaluation.

Portions of the process will have an interlock system to prevent accidental human irradiation from the neutron beam. For this reason, individuals must log in and out of the irradiation area to ensure that there are no personnel left inside the area prior to processing. Once personnel are confirmed clear, both by log-in/out and by visual inspection, then the doors to the facility are set in a locked position while the neutron beam is activated. This will prevent direct exposure to the neutron irradiation by implementation of process controls.

Following the processing procedure, the material is stored in the protected post-processing storage facility. This material must be inspected with a GM counter to determine if there is activity from the process.

Waste depositories must be labeled to separate radioactive waste from normal waste. All radioactive wastes must be properly disposed of as outlined in the Radiation Safety Manual (MU Radiation Safety Committee, 2011).

Regular inspections will aid in the safety of the facility. These will be completed as required. Outside audits of the facility will also ensure a redundant safety inspection process is completed without bias.

This new facility will enable ongoing neutron irradiations that can be done without the need for a fission reactor. There are specific safety measures taken with regard to the facility, the personnel and the processes in place. The separate structures that are built for the separate steps in the process will assist in keeping radiated material

from exposing the workers in the facility and keep contamination from leaving the facility. The personnel's PPE, badges, and training will help keep them safe on a daily basis. The process itself will have measures built into each step to keep any unexpected radiation exposure from occurring. Overall, following these guidelines, as well as those found in the Radiation Safety Manual, the facility should safely produce the material required for industrial partners.

8.2.7. Additional Testing

Additional testing could be completed with the interlayer material in order to produce clear redundant results using static and dynamic tensile test methods. These additional tests could take advantage of the radiation optimatizations. Furthermore, treatment of both faces of the polymer interlayers could be conducted in order to increase strength beyond current testing on single face treatment.

Testing the real life environmental effects, such as water immersion and temperature variations, can help understand behavior changes experienced from the treatment technique (Dean, 2021). This will also help understand additional effects of solar radiation on the treated material.

Further cross-linking behaviour could be anaylzed by utilizing ASTM D2765 or ASTM F2214 to quantify cross-linking behavior. These methods use a solvent to swell the material and measure that degree of swelling to determine the overall cross-linking.

9. Bibliography

ASTM D2240-15. (2021). *Standard Test Method for Rubber Property - Durometer Hardness.* West Conshohocken, PA: ASTM International.

ASTM D638-10. (2010). *Standard Test Method for Tensile Properties of Plastics.* West Conshohocken, PA: ASTM International.

ASTM E18-20. (2020). *Standard Test Methods for Rockwell Hardness of Metallic Materials.* West Conshohocken, PA: ASTM International.

ASTM E384-17. (2017). *Standard Test Method for Microindentation Hardness of Materials.* West Conshohocken, PA: ASTM International.

Baum, E., Ernesti, Knox, Miller, & Watson. (2010). *Nuclides and Isotopes: Chart of the Nuclides.* Bechtel Marine Propulsion Corporation.

Bennison, S. J., Sloan, J. G., Kristunas, D. F., & Buehler, P. J. (2005). Laminated Glass for Blast Mitigation: Role of Interlayer Properties. *Glass Processing Days* .

Bennison, S. J., Smith, C. A., Anderson, C. C., & Sloan, J. (2003). Expanding Bomb Blast Performance of Architectural Glass. *Glass Processing Days.*

Biolzi, L., Cattaneo, S., Orlando, M., Piscitelli, L. R., & Spinelli, P. (2020). Constitutive Relationships of Different Interlayer Materials for Laminated Glass. *Composite Structures, 244*.

Biolzi, L., Cattaneo, S., Orlando, M., Piscitelli, L., & Spinelli, P. (2018). Post-Failure Behavior of Laminated Glass Beams Using Different Interlayers. *Composite Structures*.

Brockman, Nigg, D. W., & Hawthorne, M. F. (2013). Computational Characterization and Experimental Validation of the Thermal Neutron Source for Neutron Capture Therapy Research at the University of Missouri. *International Conference on Mathematics and Computational Methods Applied to Nuclear Science & Engineering.* Sun Valley, Idaho, USA.

Brockman, Nigg, D., Hawthorne, M., & McKibben, C. (2009). Spectral Performance of a Composite Single-Crystal Filtered Thermal Neutron Beam for BNCT Research at the University of Missouri. *Applied Radiation and Isotopes, 67*, 222-225.

Brockman, Nigg, D., Hawthorne, M., Lee, M., & McKibben, C. (2009). Characterization of a Boron Neutron Capture Therapy Beam Line at the University of Missouri Research Reactor. *Journal of Radioanalytical and Nuclear Chemistry, 282*, 157-160.

Calcagno, L., Compagnini, G., & Foti, G. (1992). Structural Modification of Polymer Films by Ion Irradiation. *Nuclear Instruments and Methods in Physics Research B65*, 413-422.

Centelles, X., Martin, M., Sole, A., Castro, J. R., & Cabeza, L. F. (2020). Tensile Test on Interlayer Materials for Laminated Glass Under Diverse Ageing Conditions and Strain Rates. *Construction and Building Materials, 243*.

Dean, B. (2021). *Effect of Water Absorption and Outdoor Weathering on Emerging Polymer Interlayers.* University of Missouri - Columbia, MS Thesis.

Ed Vitz, J. W.-R. (2022, April 3). *Chemical Education Digital Library.* Retrieved from LibreTexts: chem.libretexts.org

El-Shami, M. M., Norville, S., & Ibrahim, Y. E. (2012). Stress Analysis of Laminated Glass with Different Interlayer Materials. *Alexandria Engineering Journal, 51*(1), 61-67.

Hidallana-Gamage, H. D., Thambiratnam, D., & Perera, N. (2015). Influence of Interlayer Properties on the Blast Performance of Laminated Glass Panels. *Construction and Building Materials*.

Hooper, P. (2011). *Blast Performance of Silicone-Bonded Laminated Glass.* Imperial College London.

Hooper, P., Blackman, B., & Dear, J. (2011). The Mechanical Behaviour of Poly(vinyl butyral) at Different Strain Magnitudes and Strain Rates. *Journal of Material Science, 47*, 3564-3576.

Iwasaki, R., Sato, C., Latailladeand, J., & Philippe, V. (2007). Experimental Study on the Interface Fracture Toughness of PVB Glass at High Strain Rates. *International Journal of Crashworthiness, 12*, 2930298.

James E. Mark, B. E. (2005). *Science And Technology of Rubber.*

Knight, J. (2020). *Experimental Evaluation of Laminated Glass Interlayer Polymers at Various Strain Rates and Temperatures.* Columbia, MO: University of Missouri - Columbia.

Larcher, M., Solomos, G., Casadei, F., & Gebbeken, N. (2012). Experimental and Numerical Investigations of Laminated Glass Subjected to Blast Loading. *International Journal of Impact Engineering, 39*(1), 42-50.

Lee, E., & Lewis, M. (2011). Improved Surface Properties of Polymer Materials by Multiple Ion Beam Treatment. *Journal of Materials Research, 6*(3), 610-628.

Lee, E., Rao, G., Lewis, M., & Mansur, L. (1993). Ion Beam Application for Improved Polymer Surface Properties. *Nuclear Instruments and Methods in Physics Research B74*, 326-330.

Liu, J.-C., Yang, S.-G., Yang, Y., Fang, Q., Rong, C., & Gan, J.-P. (2020). Experimental Study of the Dynamic Response of PVB Laminated Glass Under Vented Explosion Loads of Methane-Air Mixtures. *International Journal of Impact Engineering, 143*.

Lopez-Aenlle, M., Noriega, A., & Pelayo, F. (2019). Mechanical Characterization of Polyvinil Butyral from Static and Modal Tests on Laminated Glass Beams. *Composites Part B: Engineering, 169*, 9-18.

Martin, M., Centelles, X., Sole, A., Barreneche, C., Fernandez, A., & Cabeza, L. (2020). Polymeric Interlayer Materials for Laminated Glass. *Construction and Building Materials, 230*.

MicroChem. (n.d.). *SU-8 2000, Permanent Epoxy Negative Photoresist, Processing Guidelines.* Newton, MA: MicroChem.

Morison, C. (2010). *The Resistance of Laminated Glass to Blast Pressure Loading and the Coefficients for Single Degree of Freedom Analysis of Laminated Glass (PhD Thesis).* Cranfield University.

MU Radiation Safety Committee. (2011). *Radiation Safety Manual, Fifth Edition.* Columbia, Missouri: The Curators of the University of Missouri.

Nawar, M., Salim, H., Lusk, B., & Kiger, S. (2015). Modeling and Shock Tube Testing of Architectural Glazing Systems for Blast Resistance. *Journal of Structural Engineering, 141*(7).

Norville, H. S., & Conrath, E. J. (2001). Considerations for Blast-Resistant Glazing Design. *Journal of Architectural Engineering, 7*(3).

Norville, H. S., Harvill, N., Conrath, E. J., Shariat, S., & Mallonee, S. (1999). Glass-Related Injuries in Oklahoma City Bombing. *Journal of Performance of Constructed Facilities, 13*(2).

Osnes, K., Holmen, J. K., Hopperstad, O. S., & Borvik, T. (2019). Fracture and Fragmentation of Blast-Loaded Laminated Glass: An Experimental and Numerical Study. *International Journal of Impact Engineering, 132*.

Phoenix. (2020, 12 15). *D-T Neutron Generators*. Retrieved from https://phoenixwi.com/neutron-generators/d-t-neutron-generator-deuterium-tritium/

Rej, D. J., & Wrobleski, D. A. (1999). *United States of America Patent No. US5942156.*

Rej, D. J., Pickrell, M. M., & Wrobleski, D. A. (1996). Neutron-Capture-Induced Radiation Treatment of Polymeric Materials. *Applied Physics Letters*, Letter 68.

Roff, W., & Scott, J. (1971). *Fibres, Films, Plastics and Rubbers - A Handbook of Common Polymer.* Butterworth-Heinermann.

Samieian, M., Cormie, D., Smith, D., Wholey, W., Blackman, B., Dear, J., & Hooper, P. (2019). On the Bonding Between Glass and PVB in Laminated Glass. *Engineering Fracture Mechanics, 214*, 504-519.

W.C. Oliver, G. P. (1992). An Improved Technique for Determining Hardness and Elastic Modulus Using Load and Displacement Sensing Indentation Experiments. *Journal of Materials Research*.

Zhang, X., Hao, H., & Wang, Z. (2015). Experimental Study of Laminated Glass Window Responses Under Impulsive and Blast Loading. *International Journal of Impact Engineering, 788*, 1-19.

Zhang, X., Liu, H., Maharaj, C., Zheng, M., Mohagheghian, I., Zhang, G., . . . Dear, J. P. (2020). Impact Response of Laminated Glass with varying Interlayer Materials. *International Journal of Impact Engineering, 139*.

Zhao, C., Yang, J., Wang, X., & Azim, I. (2019). Experimental Investigation into the Post-Breakage Performance of Pre-Cracked Laminated Glass Plates. *Construction and Building Materials, 224*, 996-1006.

10. Appendices

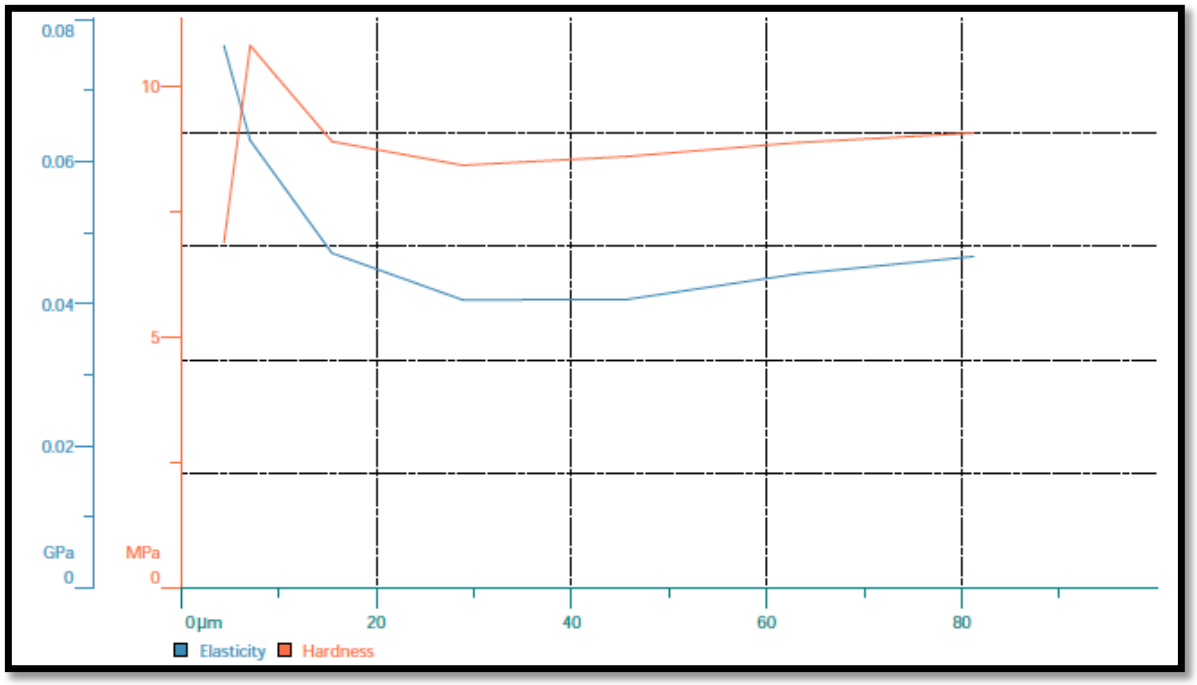

Figure 62: Raw Graph Data from Anton Paar showing Hardness and Elasticity, EVA-001-004, Treated Face.

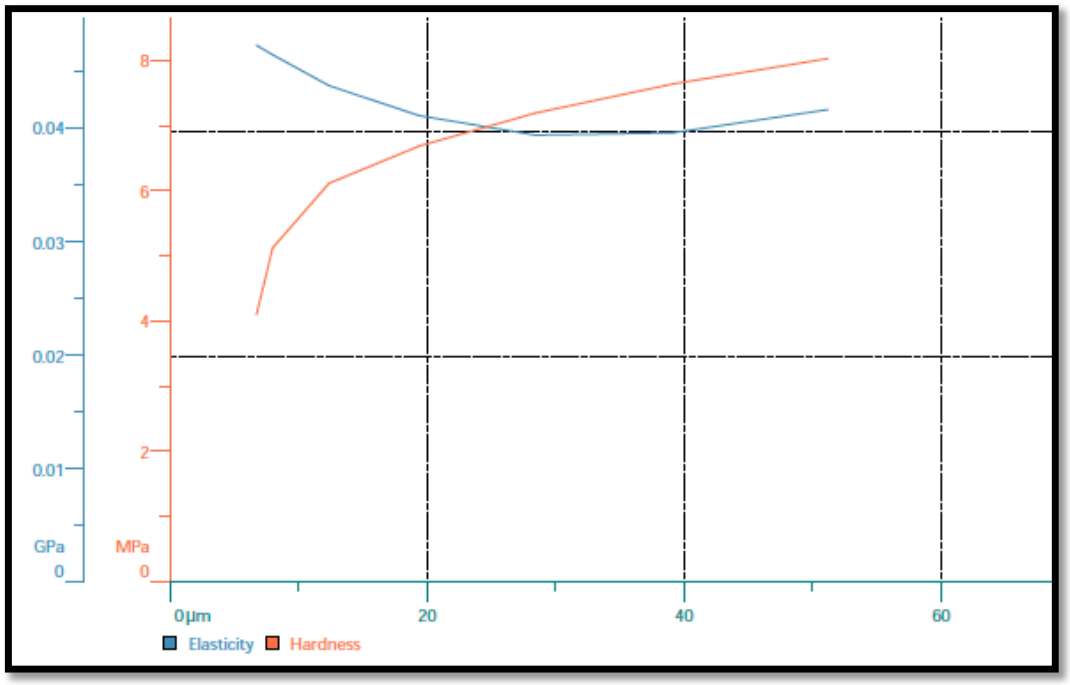

Figure 63: Raw Graph Data from Anton Paar showing Hardness and Elasticity, EVA-001-004, Untreated Face.

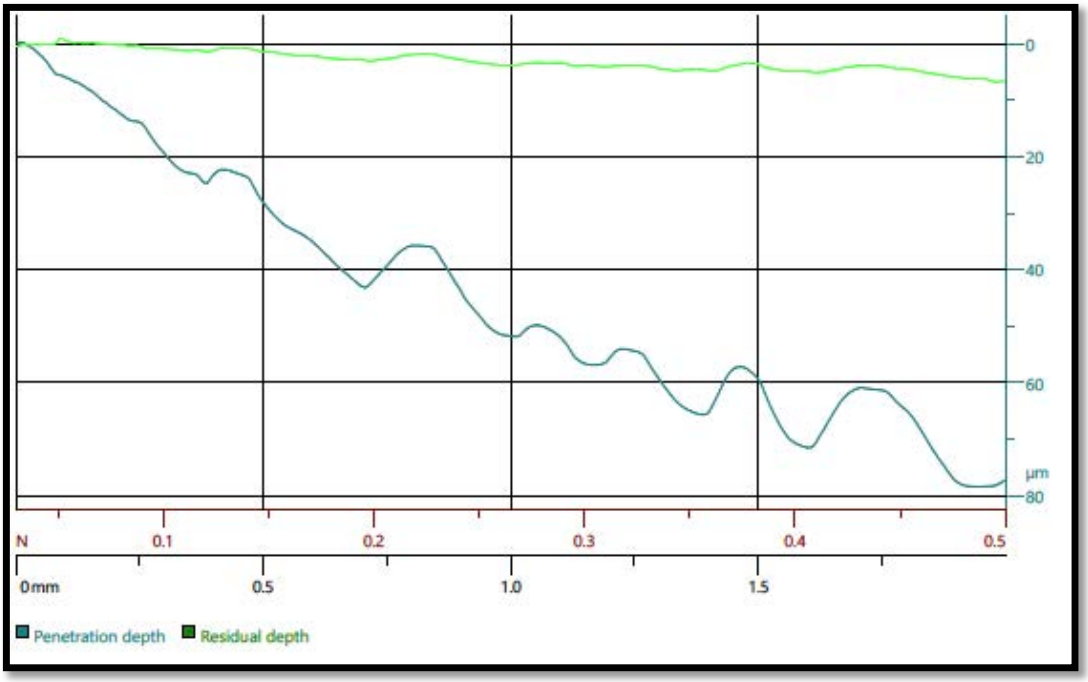

Figure 64: Scratch #1, 4mm/min, Raw Graph Data from Anton Paar showing Penetration Depth vs Force/Distance, EVA-014-001, Treated Face.

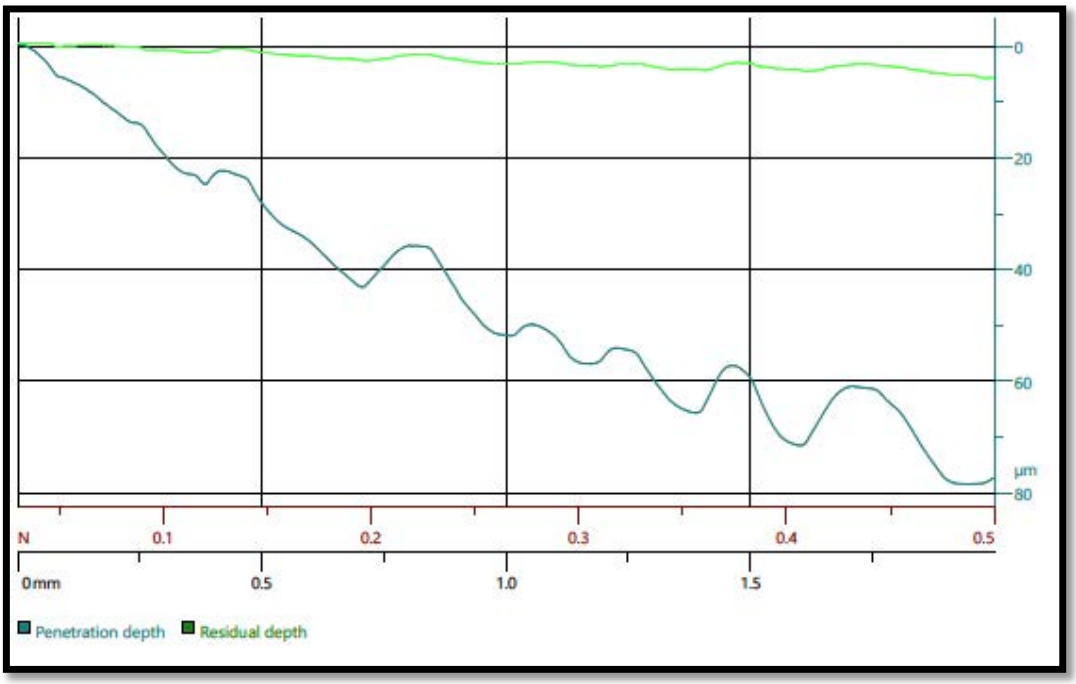

Figure 65: Scratch #2, 4mm/min, Raw Graph Data from Anton Paar showing Penetration Depth vs Force/Distance, EVA-014-001, Treated Face.

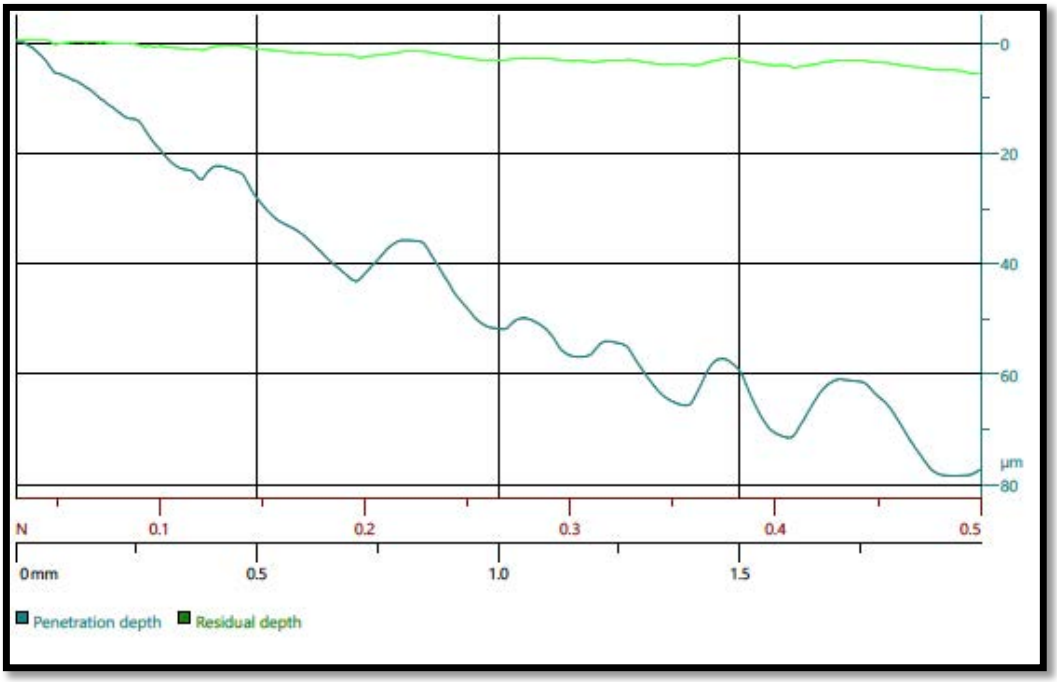

Figure 66: Scratch #3, 4mm/min,Raw Graph Data from Anton Paar showing Penetration Depth vs Force/Distance, EVA-014-001, Treated Face.

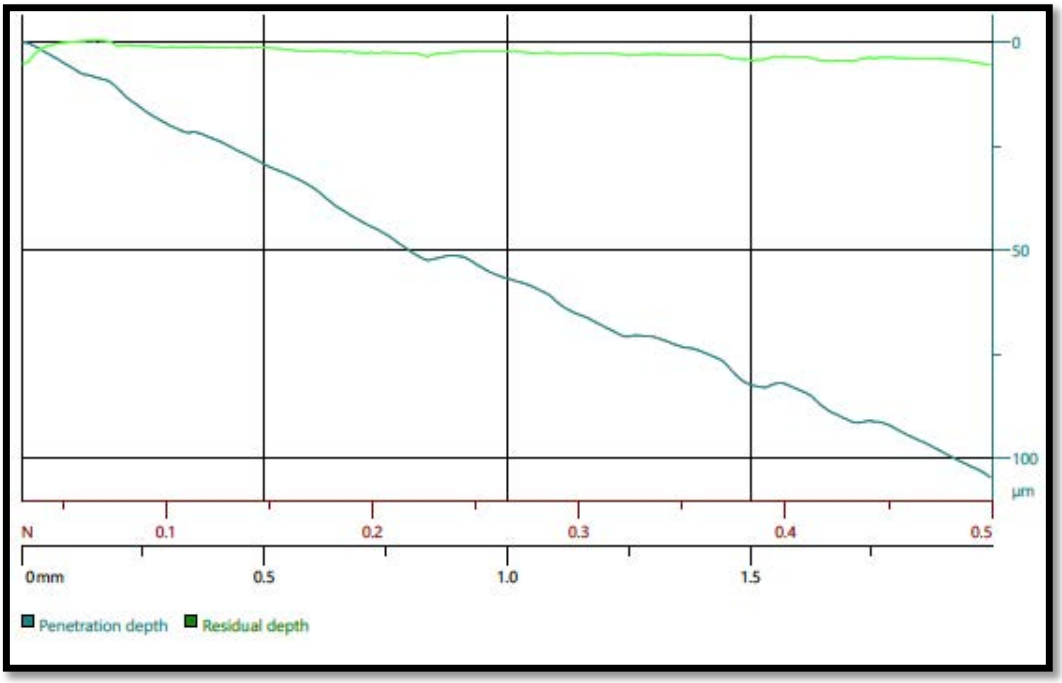

Figure 67: Scratch #1, 4mm/min,Raw Graph Data from Anton Paar showing Penetration Depth vs Force/Distance, EVA-014-001, Untreated Face.

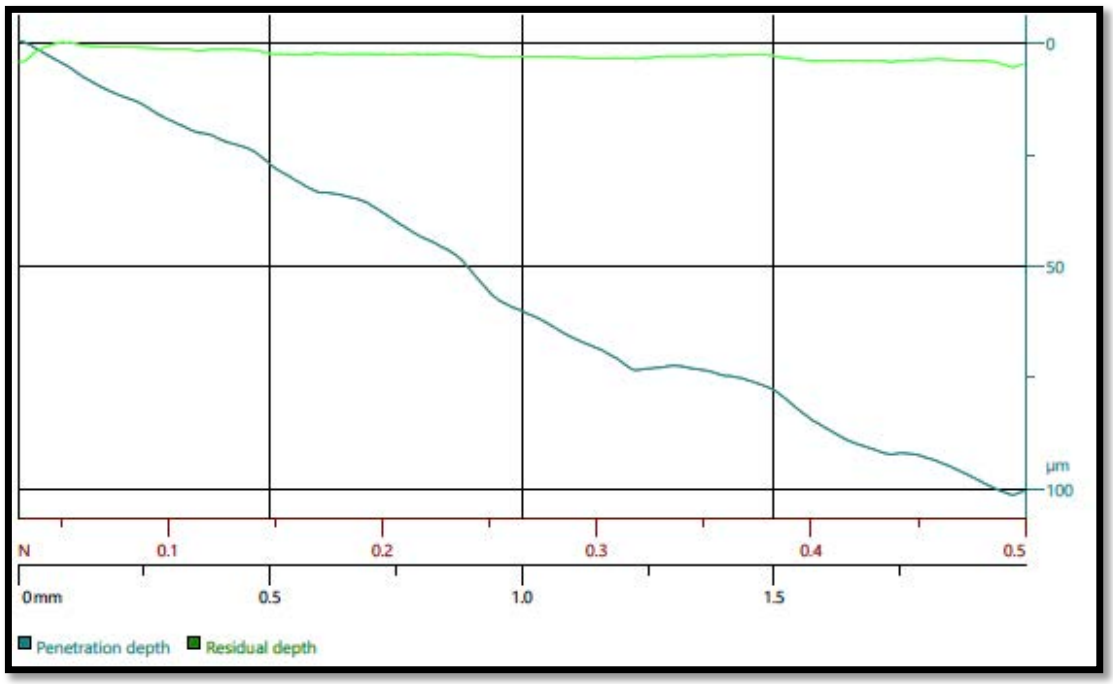

Figure 68: Scratch #2, 4mm/min,Raw Graph Data from Anton Paar showing Penetration Depth vs Force/Distance, EVA-014-001, Untreated Face.

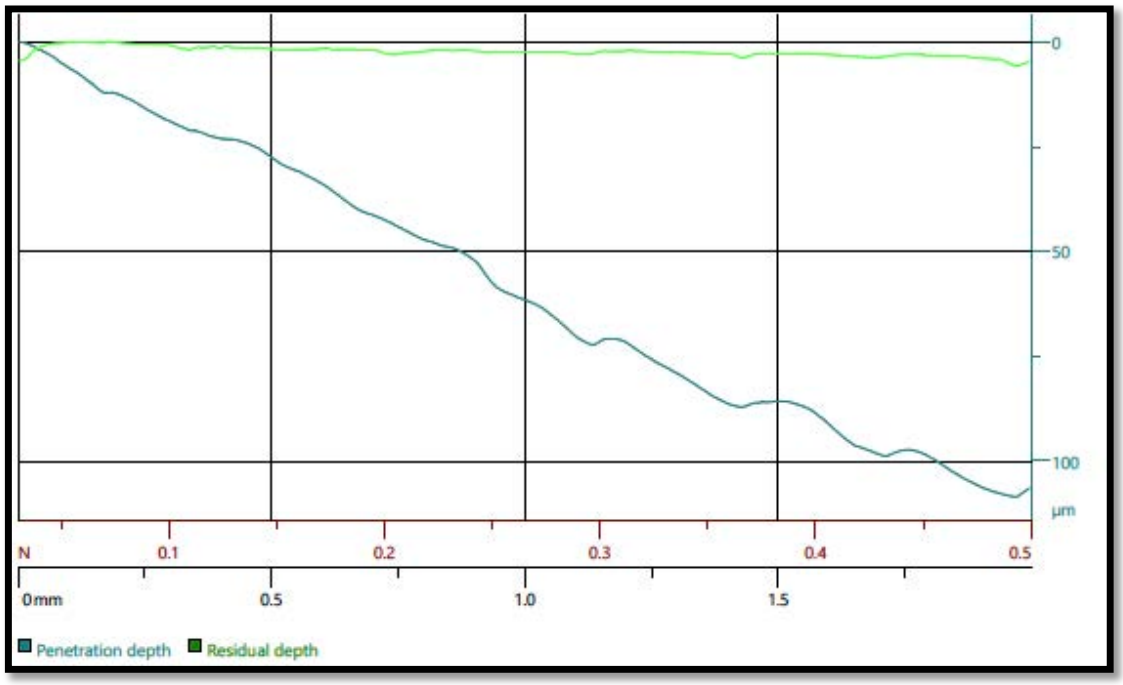

Figure 69: Scratch #3, 4mm/min,Raw Graph Data from Anton Paar showing Penetration Depth vs Force/Distance, EVA-014-001, Untreated Face.

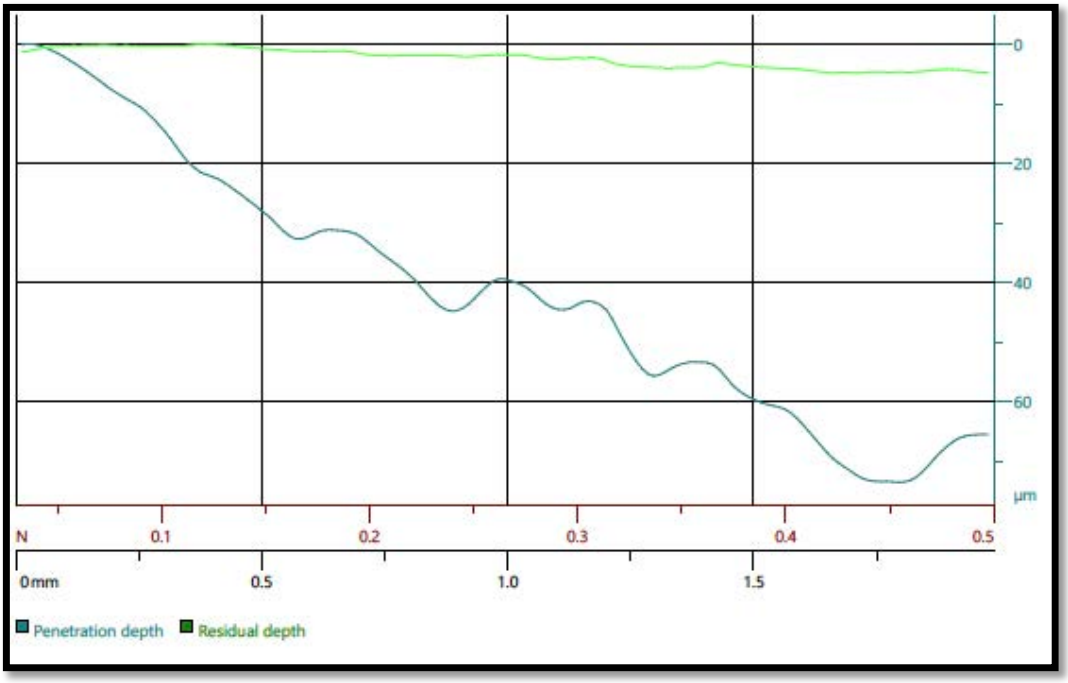

Figure 70: Scratch #1, 20mm/min,Raw Graph Data from Anton Paar showing Penetration Depth vs Force/Distance, EVA-014-001, Treated Face.

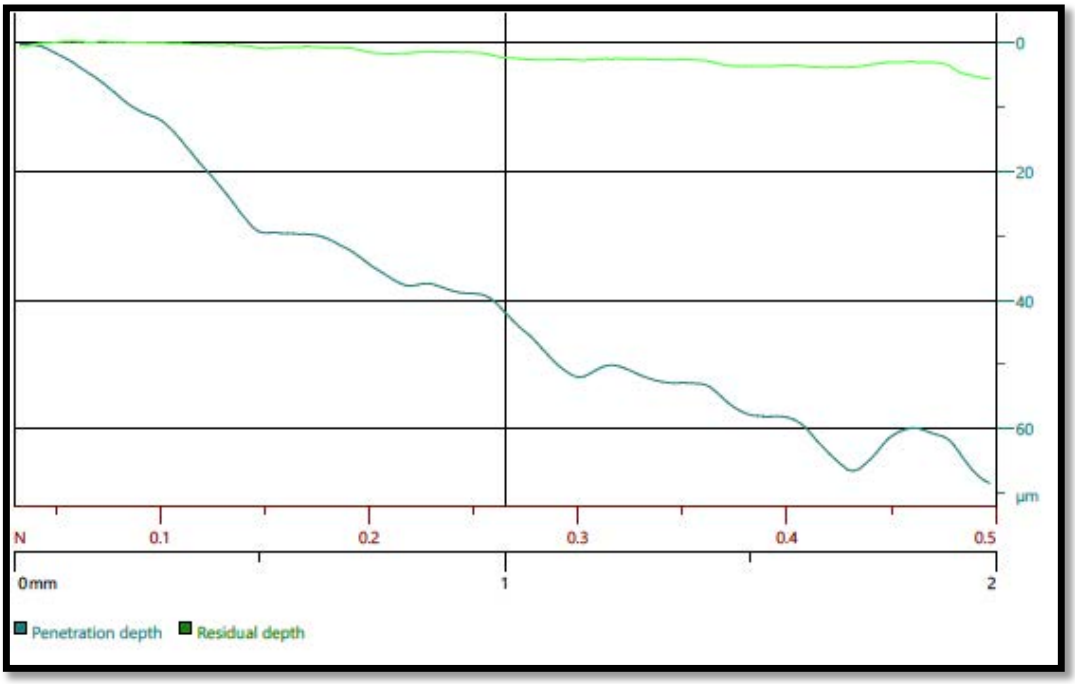

Figure 71: Scratch #2, 20mm/min,Raw Graph Data from Anton Paar showing Penetration Depth vs Force/Distance, EVA-014-001, Treated Face.

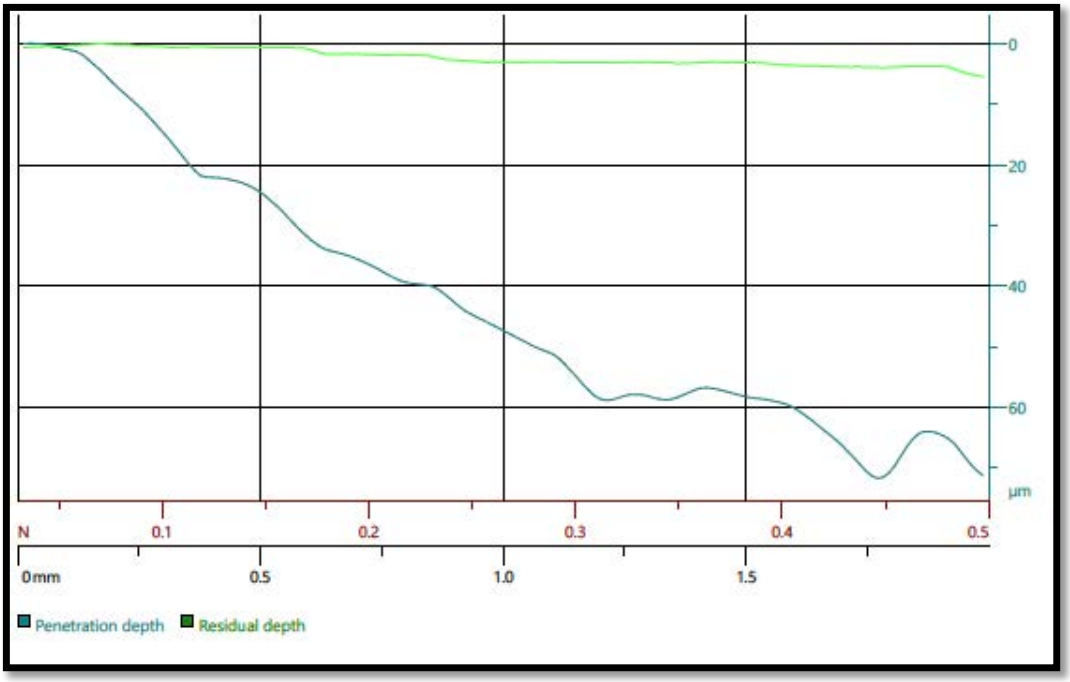

Figure 72: Scratch #3, 20mm/min,Raw Graph Data from Anton Paar showing Penetration Depth vs Force/Distance, EVA-014-001, Treated Face.

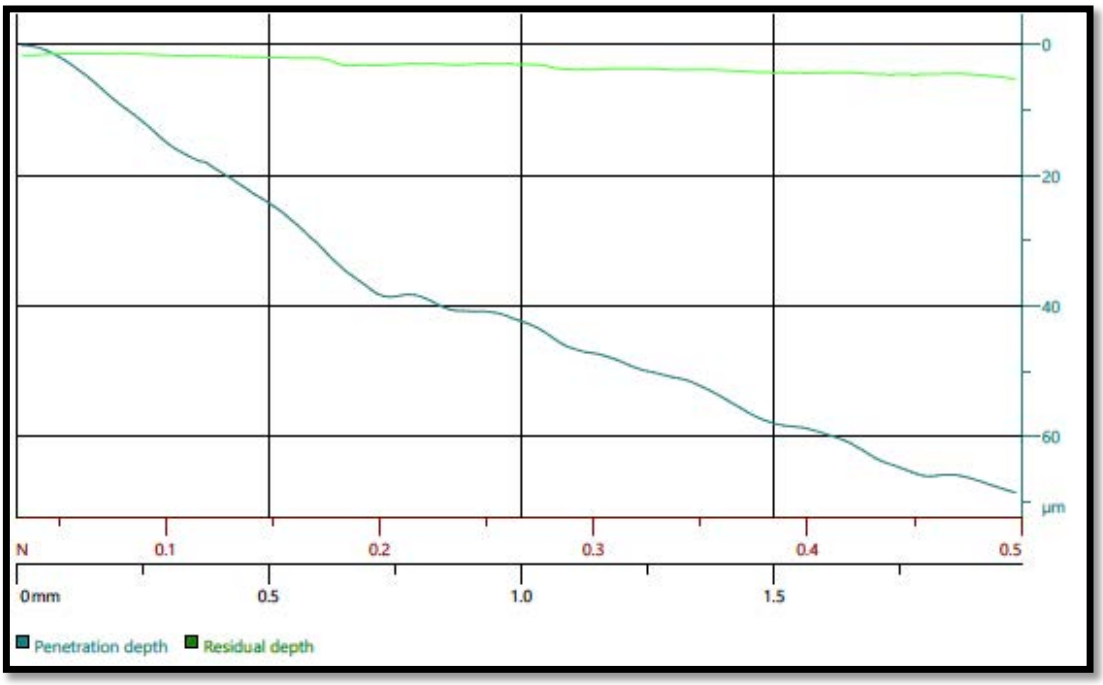

Figure 73: Scratch #1, 20mm/min,Raw Graph Data from Anton Paar showing Penetration Depth vs Force/Distance, EVA-014-001, Untreated Face.

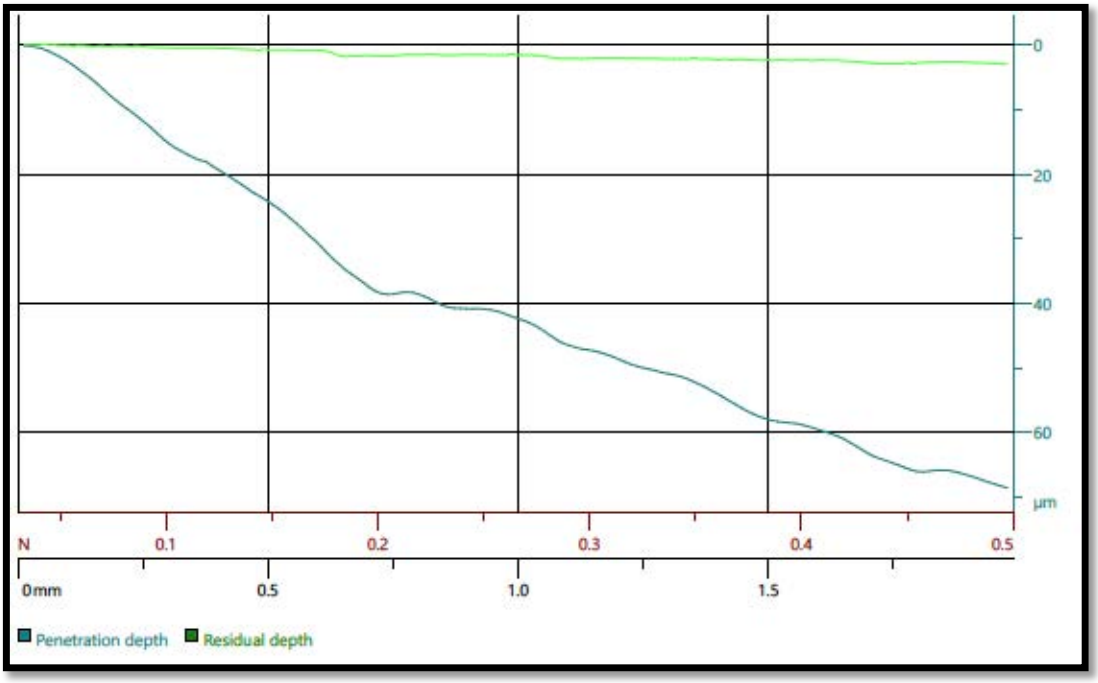

Figure 74: Scratch #2, 20mm/min,Raw Graph Data from Anton Paar showing Penetration Depth vs Force/Distance, EVA-014-001, Untreated Face.

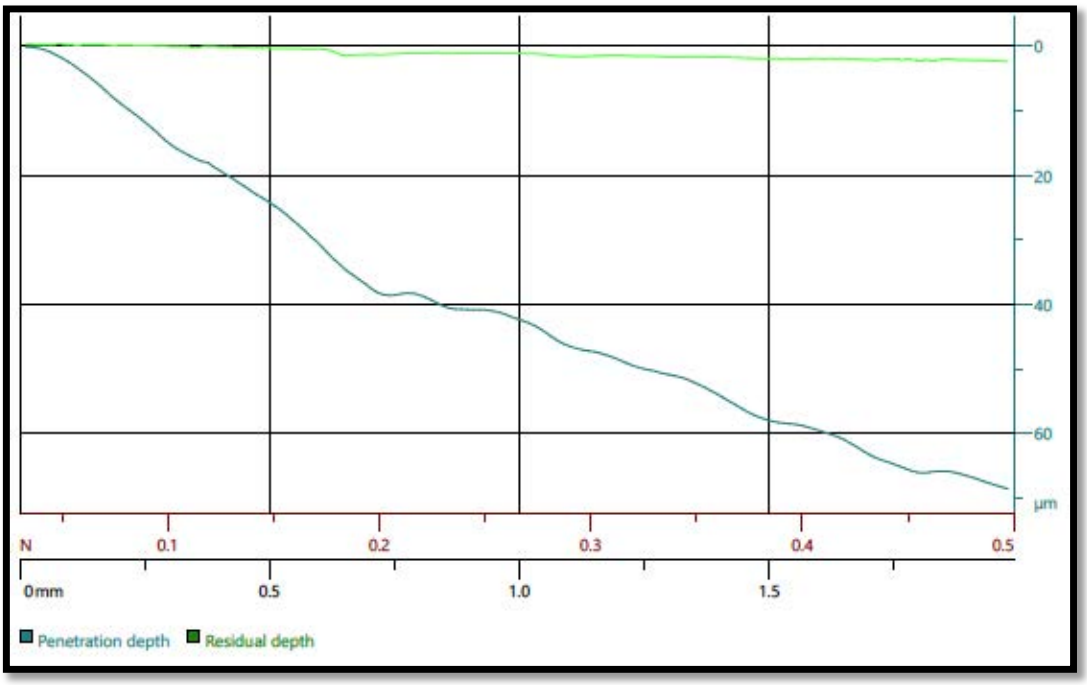

Figure 75: Scratch #3, 20mm/min,Raw Graph Data from Anton Paar showing Penetration Depth vs Force/Distance, EVA-014-001, Untreated Face.

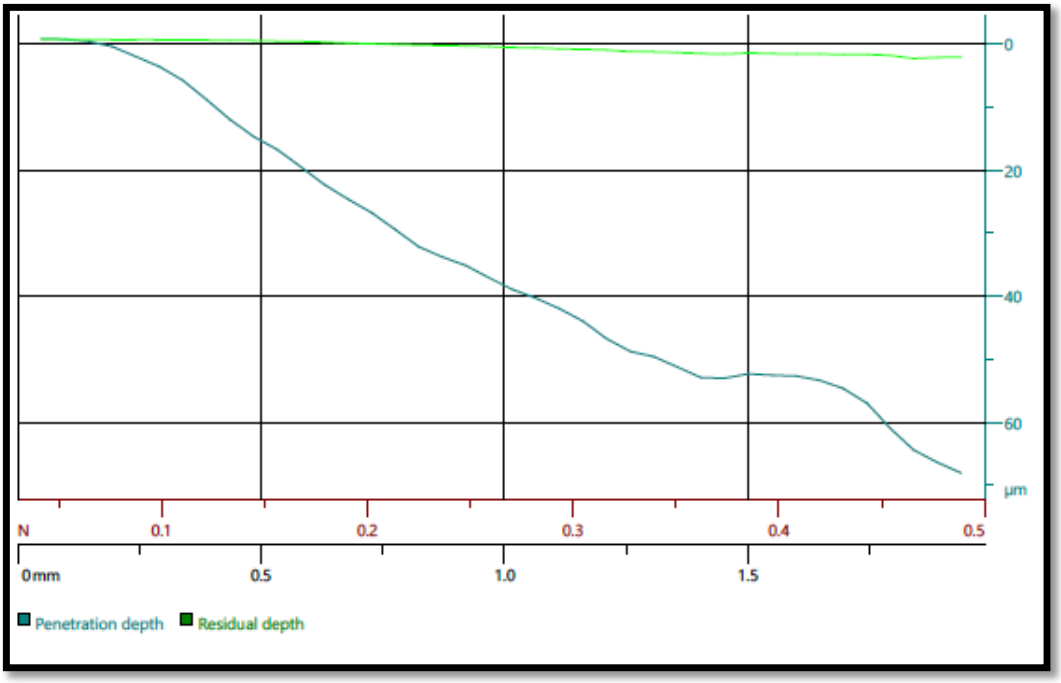

Figure 76: Scratch #1, 85mm/min,Raw Graph Data from Anton Paar showing Penetration Depth vs Force/Distance, EVA-014-001, Treated Face.

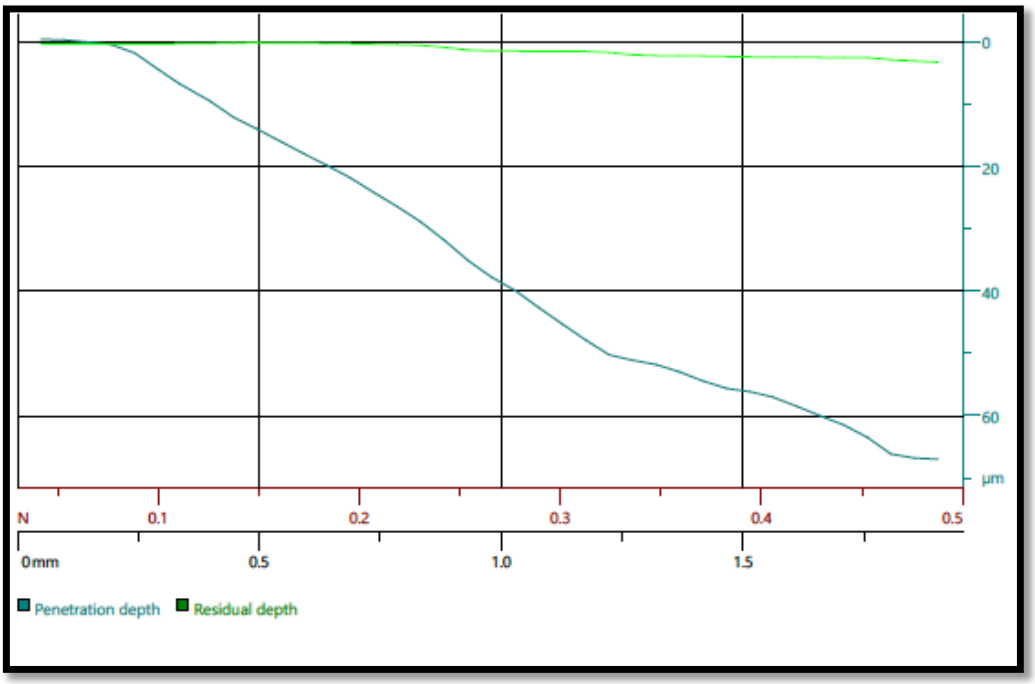

Figure 77: Scratch #2, 85mm/min,Raw Graph Data from Anton Paar showing Penetration Depth vs Force/Distance, EVA-014-001, Treated Face.

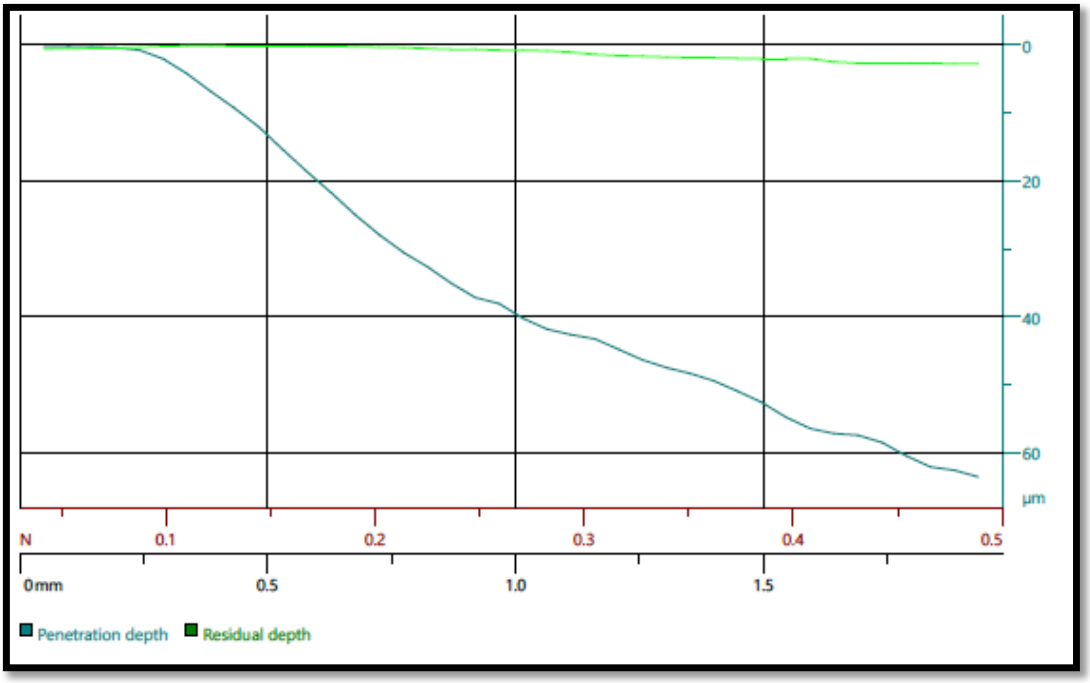

Figure 78: Scratch #3, 85mm/min,Raw Graph Data from Anton Paar showing Penetration Depth vs Force/Distance, EVA-014-001, Treated Face.

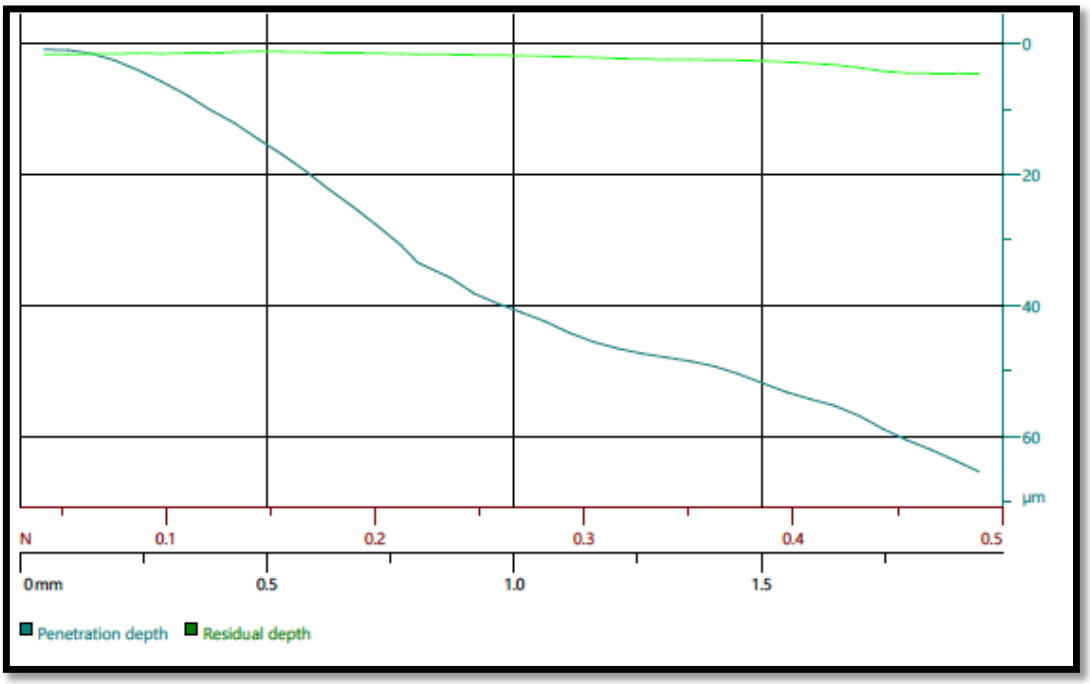

Figure 79: Scratch #1, 85mm/min,Raw Graph Data from Anton Paar showing Penetration Depth vs Force/Distance, EVA-014-001, Untreated Face.

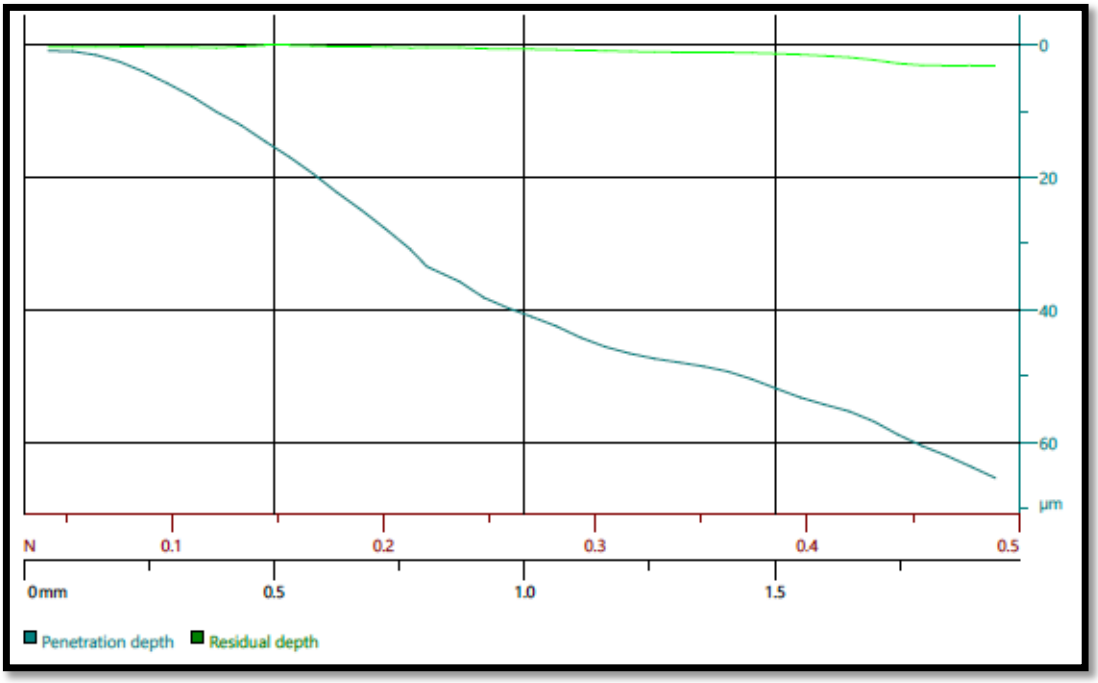

Figure 80: Scratch #2, 85mm/min,Raw Graph Data from Anton Paar showing Penetration Depth vs Force/Distance, EVA-014-001, Untreated Face.

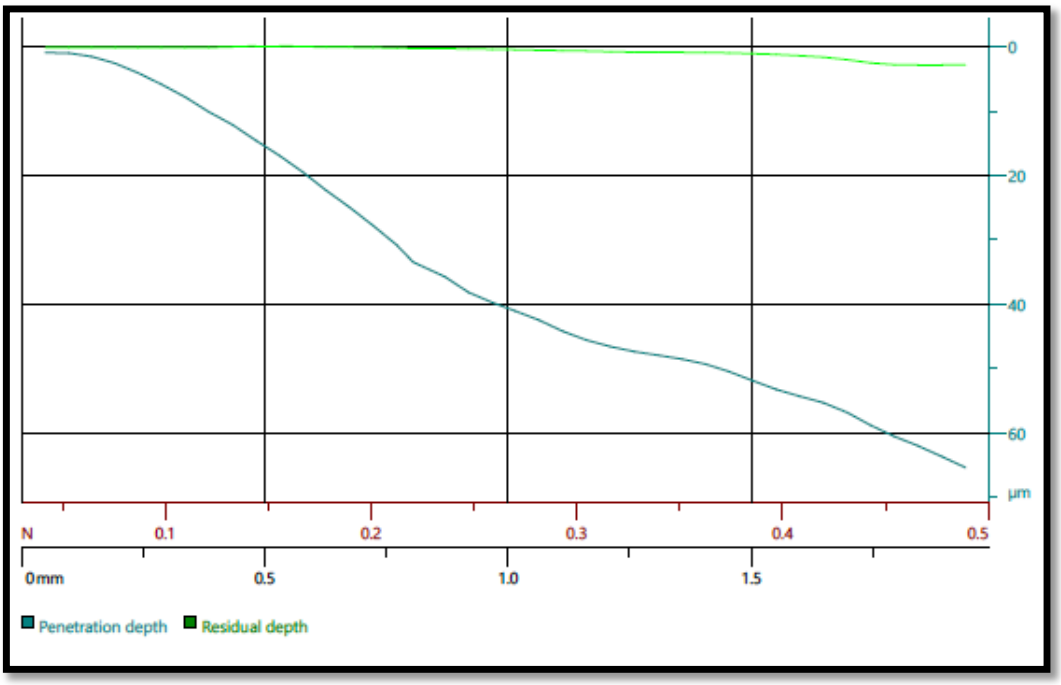

Figure 81: Scratch #3, 85mm/min,Raw Graph Data from Anton Paar showing Penetration Depth vs Force/Distance, EVA-014-001, Untreated Face.

VITA

Joseph Caleb Philipps began his career path while working residential construction jobs with his father in Dover, Missouri. He pursued related studies at the University of Missouri – Columbia, where he sought a B.S. Degree in Civil Engineering. During this time he began work in research related to "Post-Event Condition Assessment of Structures" as well as other non-destructive evaluation techniques. This work flowed into the pursuit of a M.S. Degree in Civil Engineering where he completed a thesis titled "Sensor Characterization for Long-Term Remote Monitoring of Bridge Piers." This provided significant exposure to civil infrastructure, electronics, and related instrumentation.

Following his initial University experience, he spent the next decade in the engineering and construction industry. The majority of this time was with Burns & McDonnell, where he worked several years in Structural Design and then later Site/Project Management with Electric Transmission Line and Substation Construction. He later worked at Renewable Energy Systems (RES) Americas, developing sustainable electrical energy through the construction of wind turbine infrastructure. He also worked in Federal government as a Foreign Service Construction Engineer with the US Department of State, where he managed design and construction of Embassies and Consulates throughout the world.

He returned to research to the University of Missouri – Columbia to pursue a PhD in Civil Engineering, focusing on "Blast Resistant Windows and Structures" and "Radiation Treatment of Polymers." This effort will aid his future endeavors to develop his own research objectives in infrastructure development.